Archives of Computational Methods in Engineering
https://doi.org/10.1007/s11831-022-09757-0

REVIEW ARTICLE

On the Modeling of Biomechanical Systems for Human Movement Analysis: A Narrative Review

Ivo Roupa[1,3] · Mariana Rodrigues da Silva[2] · Filipe Marques[2] · Sérgio B. Gonçalves[1] · Paulo Flores[2] · Miguel Tavares da Silva[1]

Received: 20 December 2021 / Accepted: 18 April 2022

Abstract
The rising importance of movement analysis led to the development of more complex biomechanical models to describe in detail the human motion patterns. The models scaled from simplistic two-dimensional to three-dimensional representations of body including detailed joint, muscle, tendon, and ligament models. Different computational methodologies have been proposed to extend traditional kinematic and dynamic analysis to include not only the evaluation of muscle forces but also the action of the central nervous system. Hence, a large number of models varying in complexity and target application are available in literature. This narrative review aims to provide an overview of the modeling of biomechanical systems used for the analysis of human movement within the framework of multibody dynamics, for those enrolled in engineering, clinical, rehabilitation and sports applications. The review includes detailed and generic models, as well as the main methodologies applied to model muscle activation and contraction dynamics. Numerous skeletal, musculoskeletal and neuromusculoskeletal models with variable degrees of complexity, accuracy and computational efficiency were identified. An important remark is that the most suitable model depends on the study objectives, detail level of the depicted anatomical structures, target population or performed motion. Summarizing, biomechanical systems have evolved remarkably during the last decades. Such advances allowed to gain a deep knowledge on how the human nervous system controls the movement during different activities, which has been used not only to optimize motor performance but also to develop solutions that allow impaired people to regain motor function in cases of disability, among other applications.

1 Introduction

The study of the human movement has been an object of interest since classical Antiquity. However, the first quantitative studies regarding human locomotion only appeared in the 1880s with the pioneer works of Marey et al. [1]. They allowed to progressively change the study of human motion from a qualitative to a quantitative science.

Nowadays, detailed analyses of the mechanics of the human neuromuscular system can be easily performed in a non-invasive approach using biomechanical models with variable degrees of complexity. These models are mathematical representations of a given biological system and can be established with different numerical approaches, such as multibody systems (MBS) methodologies [2–5] or the finite elements method (FEM) [6–8].

Multibody dynamics methodologies are numerical methods used to model and analyze multibody systems in a systematic and efficient way. To that purpose, these methods require the definition of a set of parameters that completely define the topology of the model under analysis. Such parameters, commonly referred as generalized coordinates, can be obtained using different multibody formulations [9–12]. These formulations enable the inverse and forward dynamic analysis of large and complex systems [13], such as full body biomechanical models containing several muscular actuators and a high number of degrees of freedom (DoF),

✉ Ivo Roupa
ivo.roupa@tecnico.ulisboa.pt

✉ Miguel Tavares da Silva
miguelsilva@tecnico.ulisboa.pt

1 IDMEC, Instituto Superior Técnico, Universidade de Lisboa, Av. Rovisco Pais, 1, 1049-001 Lisbon, Portugal

2 CMEMS-UMinho, Departmento de Engenharia Mecânica, Universidade do Minho, Campus de Azurém, 4804-533 Guimarães, Portugal

3 IDMEC IST Alameda, Avenida Rovisco Pais, No 1, Edifício Mecânica II, Room 1.11, 1049-001 Lisbon, Portugal

Published online: 14 May 2022

which is fundamental when studying the dynamics of human movement.

In the beginning, multibody dynamics was used in simple systems composed of rigid bodies and ideal joints. However, due to the numerous advances in these numerical methods, nowadays they provide an efficient and accurate solution to analyze and simulate the behavior of very complex systems, with a high number of degrees of freedom or linearly and nonlinearly elastic multibody systems with non-ideal joints [14]. Moreover, such efficiency allows the use of multibody dynamics even in real-time applications [15, 16].

The FEM is a computational technique that enables the spatial and temporal discretization of continuum models into a finite number of non-overlapping elements [17]. Such elements, have a simple geometry and are usually designated as finite elements or elements. This method allows to replace the differential equations that govern complex dynamic systems with algebraic equations for each element [18, 19]. Since the model is composed by many elements, the number of algebraic equations that describe the model becomes very large. Moreover, this method is time consuming and requires a high level of information on the system, such as, the type and number of the elements of the mesh (a set of points and cells connected to form a network), and the materials properties (density, young's modulus, Poisson ratio) [20].

The FEM provides the system's state of stress and deformation (local effects), producing more accurate results and allowing more versatile investigations than the MBS methodologies. Hence, FE models are applied in cases in which localized structural deformations or soft tissues need to be described and analyzed in detail such in the study of bone remodeling [21, 22], to address the performance of joint implants [6, 23], to perform articular cartilage tissue engineering [24], or to estimate muscle forces [25]. Although widely used in the field of biomechanics, FEM are out of the scope of this work. Consequently, only biomechanical models develop or used within the framework of multibody system dynamics will be included.

Due to their simplifying premises, MBS methodologies allow the study of forces and/or displacements at a lower number of body points (global effects) when compared with a typical FE mesh. Within the scope of biomechanics, multibody dynamics are widely applied in areas such as, sports, clinical, rehabilitation or ergonomics to enhance human performance [26, 27], to improve prosthesis design [28], to identify asymmetries between limbs after injuries [26] or to characterize the loads associated with repetitive movements [29]. Despite these differences, both methods have been successfully applied in injury prevention [30, 31], equipment design improvement [32] or movement techniques' optimization [33–35].

According to Ezati et al. [36], biomechanical models can be classified into skeletal (SK), musculoskeletal (MSK) or neuromusculoskeletal (NMSK) models. This distinction is based on the number and type of anatomical structures constituting each model. For each of these three classifications, there are numerous examples of planar [37–39] and spatial models [40–42]. Planar models represent a restricted number of DoF of the system and only allow a simple motion analysis limited to the frontal and, more commonly, sagittal planes. These models are typically less complex and require less data to be implemented when compared with spatial biomechanical models, which makes them a suitable solution to use in motion simulation or in the educational context [39, 43].

On the other hand, three-dimensional modeling allows for a more realistic definition of the motion of the anatomical segments, as well as the forces produced. The complexity and accuracy of those models are usually achieved through an increase of the computational burden. There are biomechanical models which refer to the full body [44–46], and others which target a more detailed anatomical structure, including models of the upper body [47–51], lower body [52–54], upper limb [55] or single segment models, such as the foot [56–59].

Skeletal models are the least complex biomechanical models since they only include segments and their interconnecting joints. When performing SK modeling under the framework of MBS methodologies, the segments are usually defined as rigid bodies. Thus, the dimensions of each segment are kept constant and the relative position of all its points does not change during the analysis, which means that only the DoFs associated with full body translations and rotations are considered. However, in biomechanical models, the no-deformation requirement is not completely fulfilled during experimental data acquisition since, due to the displacement of the human skin with respect to the bones, the relative position of the markers at specific bony landmarks varies. This phenomenon, usually referred to as soft tissue artifact (STA) or skin motion artifact, can lead to an unrealistic motion of the model joints and inconsistencies during the dynamic analysis [60].

The STA occurs due to inertial effects of the body segments (e.g., wobbling of the muscle and skin apparatus in relation to the skeletal system), skin deformation and sliding, gravity and muscle contraction [61] and is task- and subject-dependent, which makes standard filtering techniques ineffective [62–64]. To address this issue, several methods that minimize the errors associated to the experimental acquisition of anatomical points have been proposed, being the optimization-based methods the most common approach [65]. Despite the several methodologies employed to deal with STA, the segments are usually defined as rigid bodies in the framework of the modelling of biomechanical system using MBS methodologies.

An important issue that results from the rigid body assumption is that this approach does not allow to measure bone strain, which is fundamental in bone remodeling [66]. To overcome this issue, Nazer et al. [66] proposed the use of flexible multibody dynamics. Regardless the adopted approach (flexible or rigid), model segments represent human anatomical segments, therefore it is fundamental that their inertial parameters are similar to those measured in the human segments to ensure the accuracy of the dynamic outputs produced by the biomechanical model [67–70].

The selection of the joints' topology defines the complexity of the biomechanical model, as well as its total number of DoFs. In planar biomechanical models, all kinematic pairs are usually modeled as ideal hinge joints [71], although other mechanical models have been used [3, 72, 73]. In turn, the spatial models can also include joints with out-of-plane motion, such as ball and socket, condyloid, gliding, saddle, hinge, and pivot joints, which are represented by their equivalent mechanical model, that is, spherical, plane, universal, hinge and pivot joint kinematic constraints [74], respectively. Literature review also allowed to identify examples of spatial model in which non-ideal joints have been successfully used [75]. An important point is that the modelling approach will greatly influence the dynamic response of the multibody system [76, 77].

Depending on the characteristics of each joint model, different procedures are used to correctly calculate its center or axis of rotation [78]. These processes allow to obtain the orientation of the local reference frame of each segment, which compromises the accuracy of the results from kinematic and kinetic analyses [61, 79].

Despite their simplicity, SK models provide kinematic and dynamic outputs of the movement, including segments orientation, angular displacements, intersegmental forces and/or moments using a non-invasive approach, however, the intersegmental loads have no physical meaning because SK models disregard muscle forces. These outputs are very important to increase the knowledge about how different individuals find unique solutions to the demands of a sports or exercise task, under the various constraints of that task, the environment and their own organism [80].

In contrast to SK models, which only comprise the modeling of the anatomical segments and joints, MSK models also include muscles. Muscle contraction plays a fundamental role in joint motion. Initially, the muscle receives an electric signal from the nervous system that will result in an action potential and produce a fiber muscle contraction. The force produced during muscle contraction is transmitted to the bones through tendons which will produce joint motion [81, 82] The functional unit that produces joint motion consists of the muscle fibers (muscle without its tendinous attachments) and its respective tendon, that is, the muscle–tendon unit (MTU) [81].

Consequently, MSK modeling involves selecting the most appropriate muscle model and the most accurate method for muscle parameters' scaling, defining each muscle path and solving the muscle redundancy problem with a suitable optimization technique.

Amongst the developed mathematical models of human skeletal muscles, the biophysical and the phenomenological models are the most used in the context of biomechanics. Biophysical or Huxley muscle models are physiologically based and describe the muscle contraction mechanism with great accuracy. The force produced by each cross-bridge between miosin and actin filaments is calculated and the sum of all those contributions provides the total muscle force [83]. From a mathematical perspective, a set of complex partial differential equations represents the physics of these models, which results in a high computational cost and limits their application within the framework of MBS formulations [84, 85]. In contrast, phenomenological or Hill type models are simplified physical models used to describe the force-producing properties of the skeletal muscle when subjected to imposed patterns of lengthening and shortening [86]. They are widely used in MSK modeling due to their simplicity, low computational cost, large experimental data set regarding specific model parameters and accurate predictions of muscle force [87–90].

Hill type models require a set of parameters to provide force estimations, such as (i) optimal fiber length—length at which the maximum active force is generated; (ii) tendon slack length—length at which the tendon starts resisting to stretch; (iii) muscle pennation angle—angle measured between the muscle fibers and tendon; (iv) maximal isometric muscle force—estimated with the physiologic cross-sectional area (PCSA) [87] or obtained from available databases [91] and (v) state of the system—length and contraction velocity of the muscle fibers. Some of these parameters can be directly measured via ultrasound or magnetic resonance imaging (MRI) [92], while others require an indirect estimation from MRI [93], surface electromyography (sEMG) [94], and experimental measurements in cadaveric specimens [95]. According to Ackland et al. [96] and Xiao et al. [97], researchers should use these procedures to obtain subject-specific parameters of the individual under analysis. The use of generic muscle parameters is inappropriate due to the high sensitivity of MSK models' force production to these parameters [98–102]. However, the construction of subject-specific models is often impractical, as it can be too expensive and extremely time consuming. The most common approach consists of applying generic MSK models based on data available in the literature, and scaling them to the subject under analysis [103]. According to Winby et al. [104], scaling should be performed using anthropometric and functional data of the subject of interest, that is, bone dimensions and moment-generating characteristics [105,

106], respectively. Moreover, the muscle parameters can also be tuned considering the EMG data and optimization techniques [107].

Every human muscle connects to the bones by means of tendons, spans one or several joints and bypasses several anatomical structures. From a computational point of view, each muscle is defined as a line that passes through a set of points, called via points. These are defined with respect to the anatomical segment crossed by the muscle and define the muscle path and its line of action. The detailed description of the via points of each human muscle is available on anthropometric tables, such as the one presented in Yamaguchi [108] or Carbone et al. [109]. In particular, the last one presents a detailed description of the lower limb muscle apparatus.

The accurate definition of the muscle path and line of action of each muscle plays a key role on the estimation of muscle forces and joint torques. The simplest model to address this issue uses a straight line between the muscle origin and the insertion to represent the muscle path [110]. However, for most muscles, as they may pass through bones or other tissues, this model represents an inaccurate muscle path. To overcome this limitation and accurately represent muscle paths, Garner et al. [110] proposed a method in which the muscle path is defined by several via points that wrap around anatomical structures. However, in some cases this method is not anatomically accurate since not all anatomical structures can be represented by such simple solids. To address this issue, several approaches such those presented by Gao et al. [111], Stavness et al. [112], Scholz et al. [113] or Hammer et al. [114] are available.

The number of muscles of the human body largely surpasses its number of DoFs [81], which means that, in average, each DoF is controlled by more than one muscle. This muscle redundancy allows the human central nervous system (CNS) to have infinite possibilities of muscle actuation to perform any motion. In case of injury, muscle redundancy allows the subject to still perform a given task by recruiting different muscles, which can be less efficient, but it provides a temporary alternative until recovering full functionality. From a mathematical point of view, muscle redundancy means that the number of unknown variables (musculo-tendon forces, muscle activation, or neural control) surpasses the number of independent equations of motion (body's DoFs), which results in an indeterminate system with an infinite number of possible solutions. To solve this problem, optimization techniques [108] are applied to find the combination of musculo-tendon forces that minimizes a particular cost function, which is a mathematical formula used to calculate a particular parameter, such as the sum of musculo-tendon forces. Although several cost functions have been proposed [115, 116], the determination of muscle force distribution remains one of the most fundamental problems in biomechanics.

Briefly, MSK models estimate the body's kinematics, intersegmental forces, joint moments, and also muscle forces. Although they mimic complex MSK systems [117], they disregard muscle excitation contraction (EC) coupling dynamics, which is also referred as activation contraction dynamics, and only deal with the muscle contraction dynamics. This is a significant drawback, since EC dynamics, is the process that relates the neural signal that arrives at a motor neuron and the muscle activation level. Therefore, MSK models neglect the process that inhibits the instantaneous activation or relaxation of the muscle, also known as electromechanical delay, and produce a physiological inaccurate instantaneous muscle force [36].

Neuromusculoskeletal models overcome the limitations of MSK models since they include a full representation of the excitation–contraction coupling (ECC) dynamics of the muscle. Briefly, these models comprise three main components: (i) "neuro", which includes the ECC dynamics, (ii) "musculo", which represents the muscle activation dynamics, and (iii) "skeletal", which relates to the skeletal dynamics.

These models not only provide kinematic and joint moments outcomes of human movement, but also allow to obtain muscle forces and the EC dynamics, which make them suitable to identify the relationship between the neurophysiological and muscle levels [118]. Consequently, NMSK models play a role on: (i) the understanding of impaired and unimpaired limbs movements control, (ii) the study of the response of impaired muscles to functional electrical stimulation, (iii) the design of exoskeletons controlled by myoelectric activity; (iv) the comprehension of the physical mechanisms of muscle contraction in the analysis of neuromuscular control [119–122].

The major issue associated with NMSK models is the modeling of the EC coupling dynamics. The EC dynamics encompasses the process by which the electric neural control signal is converted into the activation signal input of the muscle–tendon model, and it is modeled by a first order differential equation [87]. Since this system is time dependent NMSK models require the use of dynamic or windowing optimization techniques with a high computational cost.

Shortly, SK, MSK or NMSK modeling requires a deep understanding of numerous topics and it lacks in the literature a single work describing and reviewing them in detail. The main goal of the present study is to provide an overview of the most relevant topics related to the modeling of the components of SK, MSK and NMSK systems within the framework of MBS formulation [2] for those, not only with an engineering background, but also for those enrolled in the fields of clinical, rehabilitation, or sports sciences. Application cases of each model type and its main features

are also under the scope of this work. To that purpose, the methodology of narrative reviews will be used.

The remaining of this paper is organized as follows. In Sect. 2, the research methods used to obtain the records that supports the main findings of this manuscript are presented. Detailed analysis and discussion of the modeling issues related to the main components of SK, MSK or NMSK are presented in Sects. 3 to 5, respectively. Finally, the concluding remarks of this study are provided in Sect. 6.

2 Methods

In the following subsections, an explanation of the methodology carried out to choose the studies to be included in this review is provided. The definition of the search strategy is described, followed by the selection process of the studies. This section ends with the results obtained from the application of the referred methodology.

2.1 Search Strategy

Published studies were identified using Web of Science, SCOPUS and MEDLINE/PUBMED electronic databases, since these contain the large majority of works presenting or applying biomechanical models in the context of human movement analysis. The search was performed by two independent researchers, restricted to studies published until April 30, 2021, and included the following keywords: skeletal models, inertial parameters, joints model, musculoskeletal models, muscle models, muscle path, muscle scaling, tendon models, EC coupling, biomechanical cost functions, neuromusculoskeletal models, which were combined using AND/OR/NOT Boolean operators.

2.2 Study Selection

After duplicate removal, the titles and abstracts of relevant articles resulting from database search were screened by two independent researchers. As inclusion criteria, studies that addressed (i) the development and/or use of skeletal, musculoskeletal or neuromusculoskeletal biomechanical models for the analysis of human movement, (ii) modeling of segments, joints, MTU, ligaments and ECC, were selected during the screening process.

When the title or abstract did not clearly indicate whether an article should be included, then the complete article was obtained, and its full text was carefully reviewed. At this stage, articles, conference articles or proceedings and books that were not written in the English language or that contained models developed within the framework of the Finite Element Method (FEM) were excluded. After the application of these eligibility criteria, articles, conference proceedings and books that included skeletal, musculoskeletal or neuromusculoskeletal models of the human body were selected for inclusion in the review. Finally, additional references for this review were obtained by analyzing the bibliographic references of the selected articles.

2.3 Results

A large number of works were initially identified by applying the methodology presented in the previous subsections. Consequently, a word count was not performed during these stages. After the removal of duplicated and non-eligible works, 388 publications were considered relevant to be included in this review. It is important to note that these publications, which are compiled on Tables 1, 2, 3, 4, 5 and 6, were selected according to their historical relevance or innovative approach in the area of the development of biomechanical models and movement analysis.

The included models/methodologies were divided into three major groups according to the anatomical/physiological structures they represent: (i) Skeletal Models (SK), which present the tools to properly define the body segments (anthropometry and inertial parameters) and anatomical joints; (ii) Musculoskeletal Models (MSK), that explore the computational models for depicting the muscle, tendon and ligament active and passive behavior; and Neuromusculoskeletal Models (NMSK), which describe the muscle activation dynamics. Additionally, a subdivision was considered for the elements that compose these models. For the SK models, a sub-division in methods used for segment and joint modelling was performed. In a similar way, the MSK models were sub-divided into seven sections, addressing the modelling of the musculotendon unit (MTU) and ligaments, computational models for representation of the MTU and ligaments, methodologies for scaling and defining the muscle path and finally strategies for solving the muscle redundancy problem. Finally, the NMSK were sub-divided into models for describing the excitation contraction coupling and the computational methodologies required for describing this behavior. A section of application cases presenting different models and discussing their major issues is also presented at the end of each section.

3 Skeletal Models

The human musculoskeletal system is composed of the skeleton, muscles, ligaments, tendons, joints, cartilage, and other connective tissues. However, the SK models usually only include the representation of the skeleton and the joints.

From a mechanical point of view, the skeleton plays a fundamental role in supporting the body and protecting the internal organs. Together with the joints and muscles, the

Table 1 List of datasets containing body segment inertial parameters

Population	Author	Year	Population characteristics		Sample size	BSIPs	Body segments
			Gender	Age			
Infants	Schneider and Zernicke [164]	1992	M & F	0.04 to 0.5 Years	114	Segment mass, CoM location, and transverse moments of inertia	12—Upper arms, forearms, hands, thighs, shanks, and feet
	Sun and Jensen [165]	1994	–	2 to 9 Months	27	Segment inertia	16—Head/neck, upper trunk, lower trunk, combined trunk, upper arms, forearms, hands, thighs, shanks, and feet
	Jensen [166]	1989	M	4 to 20 Years	12	Segment mass, radius to the mass center and radius of gyration	16—Head/neck, upper trunk, lower trunk, combined trunk, upper arms, forearms, hands, thighs, shanks, and feet
Toddlers and Children	Yokoi et al. [167]	1986	M & F	5 to 15 Years	184	Segment mass, location of the center of gravity (X, Y, Z), and radii of gyration about the center of gravity (kX, kY, kZ)	16—Head/neck, upper trunk, lower trunk, combined trunk, upper arms, forearms, hands, thighs, shanks, and feet
	Jensen et al. [168]	1988	M	4 to 20 Years	12	Segment moments and products of inertia about the segment mass centroid, and principal moments and axes	15—Head, upper trunk, lower trunk, upper arms, forearms, hands, thighs, shanks, and feet
	Chester and Jensen [169]	2005	M & F	28 to 55 Weeks	10	Segment mass	13—Head/neck (combined), upper trunk, lower trunk, arms, forearms/hands (combined), thighs, shanks, and feet
	Bauer et al. [159]	2007	F	9.6 ± 0.9 Years	10	Segment mass, radius to the CoM, and radius of gyration	2—Thigh and shank
	Van Dam et al. [170]	2009	M & F	15 to 36 Months	100	Segment mass, CoM location, and three principal moments of inertia	15—Head, thorax, pelvis, upper arms, forearms, hands, thighs, shanks, and feet
Adolescents	Ackland et al. [171]	1988	M	*	13	Segment mass, CoM, and mass moment of inertia	6—Legs, thighs, lower trunk, and upper trunk
	Durkin [172]	2003	M & F	19 to + 55 Years	11	Segment mass, CoM and radius of gyration in the frontal plane	5—Forearms, hand, thigh, shank, foot
Adults	Dempster [136]	1955	M	68.5 Years (Mean)	3	Segment mass, radius to the CoM, and radius of gyration	13—Head, upper arms, forearms, hands, thighs, shanks, and feet
	Clauser et al. [139]	1969	M	49.3 Years (Mean)	13	Segment CoM	14—Head, trunk, upper arms, forearms, hands, thighs, shanks, and feet
	Chandler et al. [173]	1975	M	54.3 Years (Mean)	6	Segment weight and CoM location	14—Head, torso, Upper arms, forearms, hands, thighs, shanks, feet
	McConville et at [174]	1980	M	27.5 ± 5.6 Years	31	Segment volume, center of volume, and principal moments of inertia	17—Head, neck, thorax, abdomen, pelvis, upper arms, forearms, hands, thighs, shanks, and feet
	Young et al. [152]	1983	F	21 to 45 Years	46	Segment mass, moments of inertia, and center of volume,	17—Head, neck, thorax, abdomen, pelvis, upper arms, forearms, hands, thighs, shanks, and feet

Table 1 (continued)

Population	Author	Year	Population characteristics		Sample size	BSIPs	Body segments
			Gender	Age			
	Hinrichs † [175]	1985	M	–	6	Segment moments of inertia from Chandler (1975)	14—Head, torso, upper arms, forearms, hands, thighs, shanks, and feet
	Hinrichs †† [176]	1988	M	–	6	Segment CoM from Chandler (1975)	9—Trunk, upper arms, forearms, thighs, and shanks
	Mungiole and Martin [157]	1990	M	25.6 ± 3.4 Years	12	Segment mass, CoM location, and moment of inertia	1—Shank
	Zatsiorsky et al. [138]	1990	M & F	M: 24 Years F: 19 Years	115	Relative body segment mass, CoM position, and radii of gyration	14—Head, trunk, upper arms, forearms, hands, thighs, shanks, and foot
	Pearsall et al. [177]	1994	M & F	40.5 ± 14.4 Years	4	Segment mass, CoM location, and moments of inertia	3—Thorax, abdomen, and pelvis
	deLeva††† [137]	1996	–	M: 24 Years F: 19 Years	–	Segment relative body segment mass, CoM position, and radii of gyration	16—Head, upper trunk, middle trunk, lower trunk, upper arms, forearms, hands, thighs, shanks, feet
	Kingma et al. [178]	1996	M & F	M: 23 ± 4.8 Years F: 26.2 ± 10.0 Years	10	Relative body segment mass, CoM position, and radii of gyration	15—Head, trunk, pelvis, upper arms, forearms, hands, thighs, shanks, and feet
	Cheng et al. [179]	2000	M	26.0 ± 4.0 Years	8	Segment relative mass, CoM (%), and moments of inertia	14—Head/neck, trunk, upper arms, forearms, hands, thighs, legs, and feet
	Pavol et al. [180]	2002	M & F	M: 73.2 ± 4.4 Years F: 70.3 ± 4.8 Years	79	Segment mass and CoM location	14—Head, pelvis, upper arms, forearms, hands, thighs, legs, and feet
	Ganley and Powers [181]	2004	M & F	23 to 50 Years	20	Segment mass, CoM, and moment of inertia	3—Thighs, legs, and feet
	Nikolova and Toshev [182]	2007	M & F	30 to 40 Years	5290	Segment mass, volume, location of the CoM and moments of inertia	16—Head/Neck, upper torso, middle torso, lower torso, upper arms, lower arms, hands, thighs, legs, and feet
	Dumas et al. †††† [69]	2007	M & F	27.5 ± 5.6 Years	77	Segment mass, principal moments of inertia, CoM location, and the orientation of the principal axes of inertia	17—Head, neck, thorax, abdomen, pelvis, upper arms, forearms, hands, thighs, legs and feet
	Challis et al. [183]	2012	M & F	M: 27.2 ± 6.8 Years F: 26.2 ± 5.7 Years	3982	Segment relative mass, CoM %, radius of Gyration	3— Thighs, Legs, Feet
	Muri et al. [184]	2008	M	20 to 79 year	66	Segment Mass %, CoM (%), Transverse and Longitudinal Moment of Inertia	8—Thighs, legs, upper arms, and forearm
Elderly	Clarys and Marfell Jones [185]	1986	M & F	M: 54.0 Years (Mean) F: 79.9 Years (Mean)	6	Segment mass	14—Head, trunk, upper arms, forearms, hands thighs, legs, and feet

Table 1 (continued)

Population	Author	Year	Population characteristics		Sample size	BSIPs	Body segments
			Gender	Age			
	Jensen and Fletcher. [186]	1994	M & F	M: 69.5 Years (Mean) F: 67.4 Years (Mean)	19	Segment volume, CoM position, and principal moments of inertia	16—Head/neck, upper trunk, lower trunk, combined trunk, upper arms, forearms, hands, thighs, legs, and feet
	Ho Hoang and Mombaur [187]	2015	M & F	IG: 82.3 ± 6.6 Years CG: 82.9 ± 7.0 Years	147	Segment relative body segment mass, CoM position, and radii of gyration	14—Head, trunk, upper arms, forearms, hands, thighs, shanks, and feet

M male, *F* female, *IG* Intervention Group, *CG* Control Group, – non available

*Stage two of Tanner's (1962) five-stage pubescent rating

†Based on the original work of Clauser

††Based on the original work of Chandler

†††Based on the original work of Zatsiorsky

††††Based on the original work of McConvile

skeleton contributes to enable the human motion, since it allows to increase the mechanical advantage of the musculoskeletal system (i.e., the ratio of the force that performs work to the applied force). On the other hand, the joints promote or constrain the relative movements between segments, which define the number and type of DoFs, as well as their admissible range of angular motion.

The modeling approaches of both segments and joints affect the accuracy of the kinematic and dynamic outcomes, and the most relevant issues associated with it, consist of (i) defining the type of segment model and its respective inertial and geometrical parameters, and (ii) selecting the joint model and the method to estimate its respective joint axis or center of rotation. Having this in mind, in the following sections these issues are comprehensively addressed/reviewed.

3.1 Segments

Within the framework of MBS methodologies, the bodies to be modeled can be treated as rigid or flexible. The flexible multibody systems are composed of both rigid and flexible bodies [14], and they are commonly used in areas where those bodies experience deformations with a magnitude comparable to their global space motion such as such flexible robots, precision machinery, road vehicles and aerospace systems [123]. The flexible multibody approach is rarely employed in the modeling of biomechanical systems for the analysis of human motion since its computational cost is very high for dynamic analysis of the entire system [124]. In rigid multibody dynamics, all bodies are considered to be rigid, which means that the bodies do not bend, stretch, or compress. For a detailed explanation of the physics behind rigid multibody systems, many textbooks and research papers are available [9, 125–129].

Body segment inertial parameters (BSIPs) comprise the mass, position of the center of mass, and moments and products of inertia of the segments of the human body. These parameters, excluding the products of inertia, are the ones with the greatest sensitivity when performing an inverse dynamic analysis [70]. The segment's inertia and position of the center of mass are typically obtained from databases available in literature and computed as percentages of the subject's body mass and segment's length, respectively. In contrast, other parameters, such as the subjects' mass and height or the segments length, can be directly measured. Due to differences between the anthropometric characteristics of the subject under analysis and those used to create the generic database it is necessary to adjusts these quantities to a specific subject. This procedure, is commonly known as scaling,

In the field of biomechanics applied to human motion, BSIPs are essential for the study of intersegmental moments, angular momentum, mechanical work and whole body

Table 2 Predictive methods used to estimate the shoulder and hip joint centers

Author	Year	Joint
Andriacchi et al. [244]	1980	Hip
Bell et al. [245]	1989	
Davis et al. [237]	1991	
Seidel et al. [246]	1995	
Shea et al. [247]	1997	
Harrington et al. [239]	2007	
Hunt et al. [248]	2008	
Weinhandl and Connor [249]	2010	
Hara et al. [238]	2016	
Meskers et al. [240]	1997	Shoulder
Campbell et al. [250]	2009	

dynamic stability [68, 130]. These parameters vary through the lifespan of the human subjects due to alterations in the size and shape of the body segments. These alterations are caused by: (i) rapid changes in growth during infancy, (ii) obesity or pathological issues, and (iii) aging conditions in old age, such as bone and muscle mass decrease or adiposity increase, among others [131]. Furthermore, BSIPs can also change during muscle contraction, due to the changes in mass distribution, as reported by Pain and Challis [132].

According to Cizgin et al. [133], BSIPs can be estimated with different methods, namely: (i) Statistical models; (ii) Geometrical models; (iii) Dynamic parameter estimation methods or (iv) Medical imaging-based technologies.

The most used techniques to estimate BSIPs are based on statistical models, namely anthropometric tables and the regression equations [68], usually based on the subjects' body mass and segment's lengths of cadaver samples. These equations are developed based on samples with different sizes and anthropometric characteristics, which, together with the differences in tissue composition and morphology between the cadaver samples and a given human subject, can lead to errors on the parameters estimation [134]. Although several authors developed specific equations for particular populations, the most used regression equations [135–139] are inappropriate to atypical populations as children, elderlies, obese, individuals with prostheses, amongst others [68]. Despite providing accurate estimations for the segments' mass and center of mass location (within 10% error), the regression equations are unreliable in estimating the remaining inertia parameters since, these errors may vary between 10 and 40% [140–142]. Table 1 presents a list of anthropometric datasets available in literature to estimate BSIPs for several populations, such as infants, children, adolescents, and adults. Moreover, for each method, the sample gender and the respective segments are also presented.

An alternative approach to obtain such parameters is using geometric models of the human body [140]. Their most relevant advantages are: (i) detailed modeling of the shape and density of a segment; (ii) no assumptions on segmental symmetry; (iii) accurate modeling of male and female subjects with different body morphology, (iv) valid for children, pregnant or obese subjects; and (v) adjustable densities of specific parts of some segments. Nevertheless, direct anthropometric measurements are required to scale the model and reduce overall error of the analysis, which is their main drawback [140].

To reduce the time spent with these measurements, Clarkson et al. [143] proposed a method to obtain the body's volumes based on three dimensional (3D) scanning using four depth sensors and random sample consensus optimization to identify and exclude outliers in the sample. Peyer et al. [144] suggested a low-cost body scanner that reconstructs the surface of a 3D object from multiple uncalibrated two

Table 3 Functional methods to estimate the shoulder and hip joint center

Transformation techniques			Sphere fitting		
Method		Joint	Method		Joint
Centre Transformation Technique (CTT)	[256, 259]	Hip & Shoulder	Algebraic Sphere Fit Method (ASF)	[247, 260, 261]	Hip & Shoulder
Holzreiter Approach (HR)	[262]		Bias Compensated Algebraic Sphere Fit Method (bcASF)	[263]	
Helical Pivot Technique (HPT)	[264]		Geometric Sphere Fit method (GSF)	[256, 265]	
Minimal Amplitude Point (MAP)	[266]		Incomplete Algebraic Sphere Fit Method (iASF)	[263, 267]	
Monte Carlo Pivoting (MCP)	[268]				
Revised Functional Method (RFM)	[269]				
Symmetric Centre Of Rotation Estimation (SCoRE)	[253]				
Schwartz Transformation Technique (STT)	[270]				

Table 4 Examples of marker set protocols used for SK modelling

Category	Author	Year	Model name	N. Segments	Segments	N. Markers
Ankle	Nair [294]	2010	–	1	Ankle	3
Fullbody	Vicon [208]	2002	Plug-In-Gait	15	Head, Thorax, Upper Arm, Forearm, Hand, Pelvis, Thigh, Leg, Foot	39
	Rabuffetti [44]	2004	–	16	Upper Arm, Forearm, Pelvis, Thigh, Shank and Foot	33
	Begon [279]	2008	–	14	Upper limbs, Shoulder girdle, Torso-Head, Pelvis, Thighs, Shank-Foot	16
	Guilbert [16]	2019		25	Head, Thorax, Upper Arm, Forearm, Hand, Pelvis, Thigh, Leg, Foot, All vertebrae	70
LowerBody	Kadaba [52]	1990	Helen Hayes	7	Pelvis, Thigh, Shank, Foot	7
	Benedetti [295]	1998	–	7	Pelvis, Thigh, Shank, Foot	43
	Frigo [278]	1998	–	7	Pelvis, Thigh, Shank, Foot	15
	Nadeau [54]	2003	–	8	Foot, Legs, Thighs, Pelvis, Trunk	25
	Leardini [280]	2007	–	7	Pelvis, Thigh, Shank, Foot	26
	Donati et al. [296]	2008		3	Pelvis, Thigh, Shank	16
	Duffell [281]	2014	–	7	Pelvis, Thigh, Shank, Foot	36
LowerBody + TrunkUpperArm	Krosshaug [297]	2005	–	21	Head, Neck, Collar, Chest, Upper Arm, Forearm, Hand, Abdomen, Pelvis, Thigh, Shank, Rearfoot, Forefoot	33
Shoulder	Jackson [284]	2012	–	4	Thorax, Clavicle, Scapula, Humerus	35
	Haering [285]	2014	–	4	Thorax, Clavicle, Scapula, Humerus	45
Spine	Hidalgo [230]	2012	–	6	Upper and Lower thoracic spine, Total lumbar spine, Shoulder segment	9
Thorax	Kiernan [283]	2014	Central Remedial Clinic Thorax Model	1	Thorax	3
	Armand [282]	2014	–	1	Thorax	27
Trapezio Metacarpal	Cerveri [298]	2008	–	1	Trapezio-Metacarpal Joint	9
UpperBody	Schmidt [299]	1999	–	6	Upper Arm, Forearm, Hand	11
	Lloyd [300]	2000	–	6	Upper Arm, Forearm, Hand	13
	Hingtgen [47]	2006	–	5	Trunk, Upper Arm, Forearm	14
	Sybelle [49]	2006	–	9	Thorax, Clavicle, Upper Arm, Fore-arm, Hand	17
	vanAndel [301]	2008	–	8	Thorax, Acromion, Lateral Upper Arm, Forearm, Hand	LED
	Rettig [48]	2009	–	7	Thorax, Clavicles, Upper-arms, Forearms	14
	Fohanno [302]	2013	–	5	Thorax, Shoulder, Arm, Forearm, Hand	29
Wrist + Hand	Metcalf [287]	2008	–	8	Wrist, Metacarpal Arch, Fingers, Thumb	26

Table 4 (continued)

Category	Author	Year	Model name	N. Segments	Segments	N. Markers
Multi Segment Foot Models	Arampatzis et al. [303]	2000	–	7	Tibia and Fíbula, Talus, Calcaneus, Navicular, Cuneiforms, Metatarsals I, II and III, Cuboid and Metatarsals IV and V, Phalanges I, II and III, Phalanges IV and V	18
	MacWilliams et al. [289]	2003	Kinfoot	9	Hallux, Medial Lateral toes, Medial and lateral forefoot, Calcaneus, Cuboid, Talus / Navicular / Cuneiforme, Tibia/Fíbula	19
	Hwang et al. [288]	2004	–	10	Hallux, Medial and Lateral toes, Medial and Lateral forefoot, Calcaneus, Cuboid, Talus, Tibia/Fibula	16
	Davis et al. [218]	2006	Shriners Hospital for Children	3	Shank, Forefoot and Hindfoot	12
	Kitaoka et al. [304]	2006	–	3	Shank, Hindfoot, Midfoot, Forefoot	11
	Pohl et al. [305]	2006	–	3	Shank, Rearfoot, Forefoot	14
	Simon et al. [290]	2006	Heidelberg Foot Measurement	10	Tibia, Navicular, Medial Arch, Lateral Arch, Hindfoot, Midfoot, Forefoot, Hallux, Metatarsal I, Metatarsal V	17
	Jenkyn and Nicol [306]	2007	–	6	Thigh, Shank, Hindfoot, Midfoot, Medial forefoot, Lateral forefoot	24
	Leardini et al. [53]	2007	Rizzoli Foot Model (RFM)	5	Foot overall, Shank, Calcaneus, Midfoot, Metatarsus	20
	Rao et al. [307]	2007	–	4	Shank, Calcaneus, Forefoot, First Metatarsal	12
	Cobb et al. [308]	2009	Cobb foot model	4	Shank, Rearfoot, Calcaneonavicular, Medial forefoot, First metatarsophalangeal complex	33
	Sawacha et al. [309]	2009	Padua foot model	4	Shank, Hindfoot, Midfoot, Forefoot	13
	Hyslop et al. [310]	2010	–	6	Shank, Single Foot, Rearfoot, Midfoot, 1st Metatarsal, Lateral Forefoot, Hallux	28
	Tulchin et al. [311]	2010	–	3	Shank, Hindfoot, Forefoot	8
	Bruening et al. [312]	2012	–	4	Shank, Hindfoot, Forefoot, Hallux, Foot	16
	De Mits et al. [56]	2012	Ghent foot model	6	Shank, Hindfoot, Midfoot, Medial forefoot, Lateral forefoot, Hallux	–
	Saraswat et al. [57]	2012	modified SHCG (mSHCG)	4	Shank, Hindfoot, Forefoot, Hallux	14
	Bishop et al. [313]	2013	–	4	Shank, Heel, Midfoot, Toe box	25
	Chard et al. [314]	2013	–	5	Shank, Rearfoot, Forefoot, First Metatarsal, Hallux	14
	Nester et al. [315]	2014	Salford foot model	6	Shank, Calcaneus, Midfoot, Lateral Forefoot, Medial Forefoot, Hallux	20
	Seo et al. [58]	2014	–	5	Hallux, Hindfoot, Forefoot, Medial forefoot, Lateral forefoot	15
	Malaquias et al. [59]	2015	–	5	Shank, Fibula, Rearfoot, Midfoot, Toes	17
	Oosterwaal, et al. [219]	2016	Glasgow–Maastricht foot model	26	All feet bones	31

– Non available

Table 5 Musculoskeletal models

Model Name	Author	Year	Anatomical Segments	Type	Model	Software
GaitFullBody	de Zee et al. [232]	2007	Lumbar Spine	3D	Generic	AnyBody
Thoraco-Lumbar Spine	Ignasiak et al. [226]	2015	Thoraco-Lumbar Spine	3D	Generic	
GaitFullBody	Peng et al. [74]	2017	Full Body	3D	Specific	
GaitFullBody	Skals et al. [392]	2017	Full Body	3D	Generic	
GaitFullBody	Eltoukhy et al. [316]	2017	Full Body	3D	Specific	
GaitFullBody	Bassani et al. [227]	2017	Full Body + Lumbar Spine (L4–L5)	3D	Generic	
GaitFullBody	Kuai et al. [228]	2017	Full Body + Lumbar spine model (L2–L3–L4)	3D	Generic	
–	Malaquias et al. [213]	2016	Foot—Leg	3D	Generic	Custom
	Quental et al. [198]	2016	Upper Limb	3D	Generic	
–	Wesseling et al. [102]	2017	Full Body (Hip Specific)	3D	Specific	
Lisbon Lower Extremity Model (LLEM)	Quental et al. [23]	2019	Lower Body	3D	Generic	
	Ma'touq et al. [418]	2019	Hand	3D	Generic	
–	Millard et al. [39]	2019	Full Body	2D	Generic	
	Dumas et al. [43]	2019	Lower Body	2D	Generic	
–	Holzbaur et al. [417]	2005	Upper Limb + Hand	3D	Generic	OpenSim
–	Hamner et al. [414]	2010	Full Body	3D	Generic	
–	Arnold et al. [212]	2010	Lower Limb	3D	Generic	
Delf Shoulder Elbow Model	Nikooyan et al. [412]	2011	Shoulder + Elbow	3D	Specific	
–	Dorn et al. [413]	2012	Full Body	3D	Generic	
–	Christophy et al. [415]	2012	Full Body + Lumbar Spine	3D	Generic	
–	Martelli et al. [419]	2015	Full Body (Hip Specific)	3D	Specific	
–	Raabe and Chaudari [229]	2016	Full Body + lumbar spine	3D	Generic	
London Lower Limb Model	Moissenet et al. [437]	2017	Lower Limb	3D	Generic	
	Lai et al. [448]	2017	Lower Limb	3D	–	
–	Catelli et al. [436]	2019	Full Body	3D	Generic	
–	Kim and Kipp [416]	2019	Fullbody + Multi segment foot	3D	Generic	

Table 6 Neuromusculoskeletal models

Author	Year	Category	Type	Approach
Jonkers et al. [475]	2002	Lower Limbs	3D	Forward dynamics
Hase et al. [469]	2002	Fullbody	3D	
Buchanan et al. [356]	2004	Shoulder + Elbow	3D	
Koo and Mak [468]	2005	Elbow	3D	
Seth and Pandy [480]	2007	Trunk + LowerLimb	2D	
Doheny et al. [471]	2007	Elbow	3D	
Ghafari et al. [481]	2009	Lower Limbs	3D	
Kim et al. [473]	2011	Fullbody	3D	
Thangal et al. [476]	2013	Fullbody	2D	
Wang et al. [474]	2014	Ankle	3D	
Buongiorno et al. [482]	2018	Shoulder + Elbow	3D	
Rahmati et al. [479]	2018	Fullbody	3D	
Allouch et al. [483]	2015	Finger	3D	Inverse dynamics
Hoang et al. [368]	2019	Lower Limbs	3D	
Quental et al. [75]	2018	Shoulder	3D	
Stienen et al. [484]	2007	Spine	3D	Neural network

dimensional (2D) images taken from different positions without any assumptions of the body's geometry. Sheets et al. [145] approach uses a laser scanner and an automated pose and shape registration algorithm to segment the body surface, and identifies the joint center positions to define the body's geometry and volume.

Dynamic parameter estimation methods, also referred to as identification techniques, are based on the linear relation between the inverse dynamics of a system and the inertial properties of its segments [146–150]. This approach requires the implementation of a dynamic model of the human body, kinematic and kinetic data (e.g., ground reaction forces, contact forces on segments, among others) of the movement to analyze, and the application of optimization tools to minimize the difference between the computational and experimental results for the distal extremity kinetics. This approach has been originally applied by Vaughan et al. [150] in the analysis of three different planar movements, namely running, long jumping and kicking. Fregly et al. [149] extended this method, later referred to as Residual Reduction Algorithm (RRA), to the 3D analysis of human gait.

More recently, Venture et al. [151] presented a methodology to estimate the standard inertial parameters on real-time, which produced similar results for the limbs when compared with the data from Young et al. anthropometric database [152]. However, this methodology leads to physically incorrect estimation of some parameters, such as negative segment's masses or non-positive definite inertia matrix. To address this problem and eliminate the referred physical inconsistencies, Jovic et al. [153] used the hierarchical quadratic programming optimization technique [154], which also estimates the BSIPs of limbs with different masses. This is a significant advantage when compared to methods based on anthropometric databases, which assume that left and right sides of the human body are fully symmetric [150]. Hansen et al. [155] proposed a novel method that presents smaller errors in the estimation of the BSIP parameters when compared to the approach proposed by Dumas et al. [69].

Medical imaging technologies include MRI [156–159], computed tomography (CT) [160] and gamma-mass scanning [161–163], which allow to obtain accurate measures of the internal structures of the human body, such as the tissue composition, providing a rigorous estimation of subject-specific parameters. However, they are time consuming and expensive, which limits their application in large-scale clinical studies.

In summary, BSIPs are key parameters during the dynamic analysis of human motion [68]. An important step to obtain accurate BSIPs is the scaling of these parameters obtained from generic databases to the subject under analysis. Usually, this procedure is performed based on subject's anthropometric characteristics such as, weight, height, segments length, and gender.

Although, the BSIPs obtained from regression equations are more accurate for healthy older Caucasian males than for females, children, or pathological subjects [68], they are commonly used for all populations due to their expediency. The major problems associated with the computation of the BSIP include: (i) the difficulty to obtain subject-specific parameters; (ii) the lack of parameters for specific populations such as child, elderly, obese or pathological; (iii) the matching between the segment definition used for the BSIP assessment with the biomechanical model construction; and (iv) the differences in the estimation of BSIP when using wobbling or rigid mass models.

Regarding the estimation of subject-specific BSIPs, the approaches addressed before, namely the geometrical, dynamic parameter estimation and the medical image-based methods can be applied. However, Robert et al. [147] showed that the estimation of these parameters, when using the parameter estimation methods, is very sensitive to the quality of the experimental data.

3.2 Joints

Human joints are complex structures composed of several tissues, such as cartilage, synovial membrane, ligaments, bursas, or synovial fluid, which interact with each other and create internal loads that are transmitted to adjacent tissues and anatomical structures. Joints play a fundamental role in the relative angular movement of the segments since they promote or constrain rotation about different DoFs. The combination of the DoF of multiple joints leads to a condition, designated DoF problem [188]. From a motor control perspective, it means that humans can choose between different solutions to perform a desired motor task without compromising its efficacy.

Despite their complexity, each human joint can be approximated by a mechanical model with similar functional capabilities. The selection of the appropriate joint model of the biomechanical model is of great importance to attain valid and reliable kinematic and dynamic outcomes. For this purpose, mechanical joint models with variable degrees of complexity have been developed, which can be classified into ideal or perfect and non-ideal or imperfect joint models.

The ideal models neglect clearance, local deformations, polycentric effects, wear, and lubrication effects. Most skeletal models present ideal joints, such as: (i) ball and socket joint (three DoFs) to model the neck, the hip and shoulder joint [189]; (ii) universal joint (two DoFs) to model the elbow and the wrist [189]; and (iii) the hinge joint (one DoF) to model the knee and ankle joint [190, 191].

These approaches consider that joint rotations are not coupled and, therefore, can be modeled as "open-loop" systems. However, several joints, such as the shoulder [4, 192], the elbow and radio-ulnar [193], the knee [194, 195] or the

ankle [196, 197] have a complex behavior, which requires more sophisticated modeling assumptions. In those cases, the joint rotations or the movement of the body segments are coupled and "closed-loop" systems should be used [192]. Those systems have been successfully implemented both for the modelling of lower and the upper limb joints as anatomy-based constraints (e.g., isometric ligaments, sphere-on-plane contacts), which mimic the physiological behavior of the joints [192–194, 196–198]. To couple the joint translations and rotations, planar four-bar-linkage mechanisms [199–201], spatial parallel mechanisms [195, 202], 5-rigid-link parallel mechanism with rigid surface contact and isometric ligaments [203], 6-link parallel mechanism [203], or mechanisms incorporating articulating spheres constrained by rigid ligaments [204] have been used for both the lower and the upper limbs.

On the other hand, imperfect joint models have been used when more realistic outcomes of joint internal loads are required. These models involve several challenging aspects, such as computing the contact-impact forces due to collisions between the bodies or the hydrodynamic forces owing to the lubrication effect [205]. One example of this approach is the work presented by Quental et al. [198] in which the shoulder was modeled as an imperfect joint with clearance. More complex and detailed joint models include the subject-specific joint models in which the geometry of the articulating surfaces is obtained using MRI or CT images. The elbow model developed by Terzini et al. [206], composed of the humerus, the ulna, the radius, the ligament complexes and the intraosseous membrane, or the knee model developed by Dzialo et al. [207], with a moving tibiofemoral axis, are representative of such complex models.

The selection of the correct procedure to estimate the joint center or axes of rotation is crucial to define the anatomical reference frame of the segments, and it varies substantially according to the selected joint. If the joint coordinates are incorrectly computed, the results obtained during the kinematic and dynamic analyses will be affected due to incorrect segment orientations [61, 79]. For the ankle, knee, elbow and wrist joints, the most popular approaches are: (i) the midpoint between two anatomical landmarks, or (ii) a combination of markers and anthropometric measures [208].

More complex knee joint models have been proposed, which include the tibio-femoral and patello-femoral joints, as the overall knee movement results from the coupled motion between these two joints [209, 210]. Rajagopal et al. [209] applied the method proposed by Walker et al. [211] to couple the tibia rotation and translation with the knee flexion angle. Moreover, the kinematic behavior of the patello-femoral joint is computed using the knee flexion angle and the method proposed by Arnold et al. [212]. On its turn, Favier et al. [210] presented a knee model in which the patello-femoral joint is modelled as a hinge/revolute joint. Other models present mathematical approaches to estimate the effective moment arms of the quadriceps muscles taking into account the polycentrism of the knee joint and the lever and spacer action of the patella. These can predict with more accuracy the effective moment arms from the knee instantaneous positions, namely the flexion angle, and anthropometric parameters related to the patella [73].

Regarding the ankle, more complex models, including those presented by Rajagopal et al. [209] and Malaquias et al. [59, 213], can be found in literature. In both studies, the talocrural and subtalar joints are independently modelled as a revolute joints, considering the non-intersecting lines-of-action of the two joints [214]. In particular, to eliminate the dynamic issues pointed out by Anderson and Pandy 1999 [215], namely the increase of the integration time as the result of the small mass of the talus segment, Malaquias et al. [59] presented an ankle model, in which this segment is modelled as a massless link. This way, the kinematic action of the talus is modelled resorting only to kinematic constraints, avoiding the explicit definition of the segment.

Different foot models, with different complexity levels, can be found in literature [216, 217]. They vary from simplistic models, in which the foot is represented only by one [5] or two segments [218], to complex representations of the foot that considers all foot bones and joints [219].

Many approaches have been used to model the human trunk, varying with the objectives of the study. The simpler ones consider that the upper body (trunk, upper limbs, neck and head) is defined as a single rigid body, usually referred to as HAT model (Head–Arms–Trunk) [220–222]. More complex models divide the trunk into thorax and abdomen [223, 224] or into other specific segments, such as the cervical [225], thoracic [226], or lumbar spine [210, 227–229]. Even more detailed models represent the upper and lower thoracic and lumbar spine [230]; the thoracolumbar spine, including each individual vertebrae, ribs, and sternum [231]; or all the vertebrae [16, 232, 233]. To define the instantaneous center of rotation of the lumbar vertebrae, Pearcy and Bogduk [234] used the Reuleaux technique [235], while Bruno et al. 2015 [231] considered the geometric center of the intervertebral disk as the center of rotation of the intervertebral joint models. Although these methods enable the computation of the intervertebral joints for each pair of vertebrae, it is important to note that the spine is largely affected by STA, and, therefore, the coordinates of the markers placed in each vertebrae must be used with caution [210]. To overcome this problem, White et al. proposed that the movement of specific parts of the spine, such as the lumbar spine, could be estimated as a linear function of the overall movement of the spine [236].

The shoulder and hip joints require more complex procedures than just a midpoint between two landmarks since the anatomical landmarks do not allow for a direct definition

of their center of rotation. To overcome this limitation, researchers use regression methods based on anthropometric measures [237–240]. These methods yield non negligible errors due to skin movement artifacts [241, 242]. Additional errors may arise from the selection of inaccurate anthropometric predictors for the regression equations [243]. Table 2 lists several predictive methods used to compute the hip and shoulder joint location.

Despite their advantages, they neglect the variability of the anatomical structures due to diseases, such as cerebral palsy, which leads to musculoskeletal deformities, or maturation, since regression methods are usually developed based on healthy people [239]. In this sense, functional methods have been used to estimate the hip and shoulder joint centers [251], which tend to provide more accurate results than the regression methods [78, 251, 252]. Using these methodologies, geometric or optimization methods are applied to the kinematic data (i.e., markers coordinates) of the segment of interest during multi-plane movements, collected during a short period of time [78]. Sphere fitting approaches and transformation techniques are examples of existing procedures within functional methods. In the former, a sphere is fitted to a set of identified coordinates belonging to a particular anatomical segment, while in the latter, a local coordinate system is defined for each time frame using the markers on each segment. Finally, all local systems are transformed into a common reference system that enables the estimation of the time-independent joint parameters [253].

Recent studies showed that the duration of the trial used to acquire the kinematic data of the segment of interest, the range of motion of the segment [78, 254], the subject's gender [254], the algorithm used to compute the center or axis of rotation and the location of the retro-reflective markers affect the estimation of the results [255]. Despite their accuracy, even in restricted ranges of motion [256], these methodologies may be difficult to apply in pathological subjects with neuromuscular deficits [257, 258]. In such cases, Miller and Kaufman [257] propose that the regression methods should be used instead. Table 3 presents several functional methods that may be used to determine the shoulder and hip joint centers.

In summary, the methods presented in Tables 2 and 3 enable the computation of the shoulder and hip joint centers in a non-invasive approach. However, according to Sangeux et al. [271] and Lempereur et al. [272], the geometric sphere fit method and the algorithm proposed by Gamage and Lasenby [261] are the most accurate methods to compute the hip and shoulder joint center, respectively. The results presented by Sangeux et al. [271] are based on the comparison of several functional methods with the results obtained when using a new imaging system with low dose radiation, designated EOS to estimate the hip joint center. In the shoulder joint, Lempereur et al. [272] compared the results of different algorithms with those obtained when using used a magnetic resonance scanner.

To conclude, several studies showed that the functional methods are more accurate than the predictive methods to compute the shoulder and hip joint centers [252]. However, the predictive method suggested by the ISB [273] is the most accurate to determine the sternoclavicular and the acromioclavicular joint center [274], while the regression method proposed by Rab et al. [275] should be used for the glenohumeral joint [274]. Likewise, Fiorentino et al. [276] demonstrated that the combination of predictive techniques based on skin markers and dual fluoroscopy leads to more accurate results in the estimation of the hip joint center.

3.3 Application Cases and Discussion

There are numerous SK models available in the scientific literature. The Conventional Gait Model (CGM) developed in the 80s was one of the first biomechanical models used to compute 3D joint angles and moments using an inverse dynamics approach [277]. At that, another biomechanical model, later known as the Helen Hayes model, and very similar to the CGM, was presented by Kadaba et al. [52]. These two models are a milestone in the history of biomechanical models, and precursors for a great number of models with different degrees of complexity developed since then (Table 4).

The first SK models had a limited number of segments, since the cameras used could only acquire a reduced number of markers per anatomical segment. Thus, only the main anatomical segments, such as the pelvis, the thigh, the shank and the foot, were represented [52, 278]. Over time, SK models became more complex, more anatomical structures were represented and modeled with more detail [48, 49, 208, 279–281]. The thorax models of Hidalgo et al. [230], Armand et al. [282] and Kiernan et al. [283], the shoulder models of Jackson et al. [284] and Haering et al. [285] or the wrist models of Cerveri et al. [286] and Metcalf et al. [287] are some illustrative examples of this increased complexity. The most representative examples include the multi-segment foot models presented by Hwang et al. [288], MacWilliams et al. [289], Simon et al. [290], and Oosterwaal et al. [219], which divide the foot in 10, 10, 11 and 26 segments, respectively. The technological advancements led to this enhancement in models' complexity, since more cameras and with higher resolution were used, which increased the number of retro-reflective markers per segment.

The increasing number of SK models and their lack of standardization in the presentation of kinematic data and in the definition of local reference frames led to the publication of two manuscripts, regarding the upper limb and the lower limb, by the International Society of Biomechanics to create guidelines for modeling and reporting procedures of

SK models between results from different research groups [273, 291]. These guidelines include the anatomical landmarks and planes used to define the local reference frames of each body segment are presented allowing for a standardization of the motion data between the different laboratories or research groups. Despite these standards and guidelines, the identification of the anatomical landmarks depends strongly on the user's experience, knowledge, and expertise, which may lead to significant variations in the kinematic outcomes across subjects [292].

When applied to the analysis of human movement, SK models require experimental data that describe the motion in study. Traditionally, acquisition systems based on markers have been used, since these are considered the gold standard in the area of motion analysis [293]. The set of markers, commonly referred to as marker set protocols, are located at relevant points or anatomical landmarks of the body, which allow to depict the position and orientation of each model segment. The main issue during the selection of a specific marker set protocol is the relation between the parameters of the biomechanical model and the information provided by it. Some methods, such as those used to predict joint centers or BSIPs, require alternative points of interest that the chosen protocol does not consider. Hence, adaptations to the original marker set should be implemented or a different one should be selected to allow for the acquisition and computation of the model parameters (e.g., segment lengths, rotation axis, reference frames, among others).

Skeletal models have been applied successfully in populations with distinct characteristics, such as athletes [48, 279], healthy [281, 283, 301] and pathological [47, 278], in different age groups, namely children, young adults, adults, and elderly [46, 48, 230, 278] and for different tasks, including walking, running, jumping, functional tasks, among others.

Regarding the motion acquisition systems, although optical systems based on retro-reflective markers are considered the gold standard method, other technologies, such as inertial motion units, light emitting diodes (LEDs), or depth sensors, have been successfully employed [293, 316–318].

Nowadays, researchers can develop subject-specific SK models using registration techniques [319], which align two or more images of a specific anatomical structure captured at different times and multiple view-points. This allows to obtain accurate parameters regarding the morphology of the subject under analysis [320], which strongly influences force and moment predictions. The main limitation is the need of medical images, in particular MRI, which increases the cost of the analysis.

In summary, SK models have been widely used in populations with different age, gender, and health conditions. Amongst these studies the anatomical segments, usually treated as rigid bodies are simplified representations of the human body, being the most common the following segments: head, thorax, upper arm, forearm, hand, pelvis, thigh, leg, and foot.

In turn, the multisegment foot, ankle, shoulder, spine, thorax or trapezio metacarpal models indicated in Table 4 represent the detailed modeling of a specific anatomical structure. Several techniques, such as retro-reflective markers, clusters of retro-reflective markers, markerless systems, or LEDS can be used to obtain the experimental data. Regarding the definition of the joint's axis or center of rotation and the inertial parameters, several approaches are available and must be selected according to the characteristics of the subject under analysis. Thus, although limited to kinematic and some dynamic outcomes, the SK models are crucial in musculoskeletal modeling since they provide the bone-fixed coordinate systems in which the musculotendon attachment points, via points, and obstacles are expressed.

4 Musculoskeletal Models

Musculoskeletal models try to mimic complex MSK systems composed of bones, muscles, tendons, ligaments, and other connective tissues that altogether provide function and structure [117]. In contrast to SK models, in which only kinematics, intersegmental forces, and joint moments are computed [321], MSK models also provide muscle forces and activations. For that purpose, MSK models include muscle representations which require the scaling of the model parameters, a computational method to compute the muscle paths and an optimization technique to solve the muscle redundancy problem. MSK models neglect muscle EC coupling dynamics and only deal with the muscle contraction dynamics. Finally, MSK models with ligaments also require the computation of the ligament's paths. A detailed explanation of these topics, their working principles, advantages, and limitations is given in the following sections.

4.1 MusculoTendon Unit (MTU)

Muscles are soft tissues composed of fibrous elastic and excitable tissue that can contract and extend and play a fundamental role in human mobility, stability, posture, respiration, digestion, vision, among others. There are three types of muscles in the human body: skeletal muscle, smooth muscle, and cardiac muscle. However, the skeletal muscle is the only one that can be voluntarily controlled by the electrical impulses transmitted by nerves [322]. They are attached to the bones by means of tendons, and span one or several joints, producing pulling forces that can generate movement. The force exerted depends on the type of muscle fiber [323], neural control [324], muscle physiological cross-sectional area [325], muscle fiber arrangement [326], joint angle displacement and velocity [326], body size [326], and

the force–velocity and force–length relationships [327, 328]. Amongst these factors, the ones commonly used in MTU computational models are the neural control, the muscle cross-sectional area, the muscle fiber arrangement, and the force–velocity and force–length relationships. The neural control will influence the level of muscle activation which is directly related to the muscle maximal force [323]. According to Fukunaga et al. [82] the ability of a muscle to produce force is directly related to its physiological cross-sectional area and muscle specific tension. The muscle architecture (i.e., muscle fiber orientation with respect to the line of action of the muscle force, also referred as pennation angle) is also an important topic since during muscle contraction, the fiber muscle rotates which changes the fraction of force directed along the muscle's line of action.

Figure 1 depicts the relations between normalized muscle force (ratio between muscle force and maximal isometric muscle force) and normalized fiber length (ratio between actual muscle fiber length and muscle fiber length at rest), and normalized muscle force and normalized fiber elongation velocity (ratio between actual muscle shortening velocity and muscle fiber maximum shortening velocity).

The muscle force vs. fiber length relation includes two components, the active and passive force. The active force results from the number of cross-bridges between the actin and myosin filaments, and it achieves its maximum value when the muscle is at rest since there is the largest interaction between the actin and myosin filaments [87]. This part of the force–length relation plot is the so-called plateau region. For higher lengths, the muscle stretches, and the filaments tend to stray, which decreases the opportunities to form cross-bridges. In turn, for lower lengths, the muscle becomes compressed, which increases the lateral distance between filaments and also decreases the number of cross-bridges. On the other hand, the passive force, caused by the elastic elements of the muscle fiber, is null when the muscle length is lower than the resting length. For higher lengths, it increases exponentially as depicted in Fig. 1a [87].

The rate at which the muscle changes length, for an activated muscle, also affects the force produced. This relation was initially described by Hill [328] and it is illustrated in Fig. 1b. The muscle lengthening corresponds to an eccentric contraction in which a higher force is observed, while the muscle shortening corresponds to a concentric contraction in which a lower force is produced. In fact, a maximum force level is attained at a given lengthening velocity after which the force no longer increases. In addition, any force produced during a concentric contraction is lower than that produced during an isometric contraction, that is, when the rate of change of muscle fiber length is zero. Thus, the force production capacity is inversely related to its contraction velocity.

Tendons are viscoelastic structures composed of strong flexible but inelastic fibrous collagen tissue (60–85%) and non-collagenous extracellular matrix components, such as cartilage oligomeric matrix protein, elastin, proteoglycans, and inorganic components. Tendons withstand tension, however, in contrast to muscles, they are unable to contract. They connect the muscle to the bone, transmit and modulate the forces from muscle contraction to the skeletal system to promote movement or provide additional stability [329], dissipate energy in abrupt movements and store and transfer energy [330].

The mechanical properties of the tendon depend on the collagen fiber diameter and orientation [331]. When stretched, tendons exhibit a typical "soft tissue" behavior with a stress–strain curve consisting of three distinct regions: the toe region which starts with a very low stiffness that progressively increases; the linear region with constant stiffness; and the yield or failure region in which the tendon stretches beyond its physiological limit.

Additionally, tendons hold viscoelastic properties, such as creep (increasing deformation under constant load), stress relaxation (decreasing tendency for the material to return to its original shape when unloaded), and hysteresis (energy dissipation during a loading and unloading cycle).

The main factors that affect the mechanical forces on tendons are: (i) the type of muscle force produced (passive or active), (ii) the type of movement (flexion–extension, adduction–adduction), (iii) the level of muscle contraction, (iv) the tendon's relative size (the greater the cross-sectional area of a muscle, the higher force it can produce and the larger stress its tendon undergoes), (v) the type of activities performed, and (vi) the rate and frequency of loading [331]. These properties, allow to describe the tendon behavior using a differential equation that relates tendon stiffness and strain rate.

4.2 MTU Computational Models

Muscle activity helps to understand how forces are generated during a particular movement. The direct measurement of muscle forces requires the use of invasive methodologies, since subjects must undergo a surgical procedure for the implantation of transducers [332], which limits and makes this approach often impractical [333]. Thus, surface electromyography appears as a non-invasive alternative to measure muscle activity, which has some inherent shortcomings, since it does not quantify the muscle force and, in some cases, the crosstalk phenomenon occurs, i.e., the recorded activity results from the simultaneous contribution of different muscles.

Computational MSK models consist of a non-invasive solution to these limitations, and they have been used to: (i) analyze the performance of athletes [334], (ii) study the function of single muscles [120, 321], (iii) study the

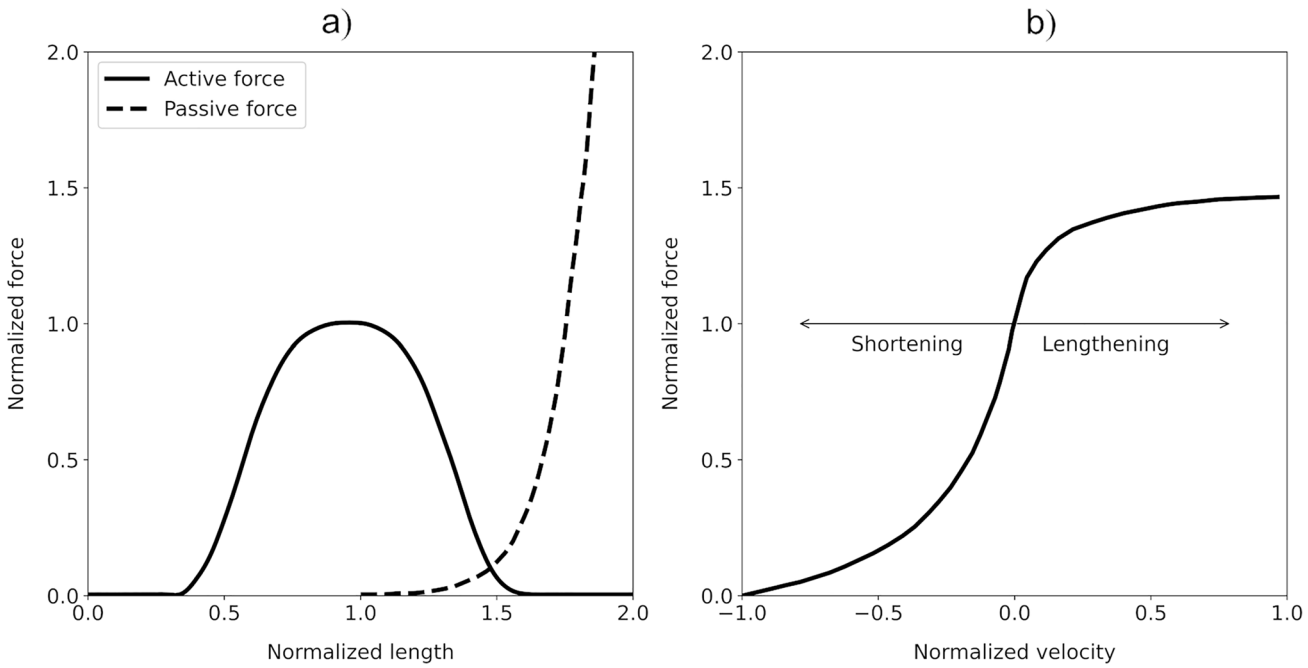

Fig. 1 **a** Force–length relation plot. **b** Velocity relation plot

influence of tendon properties [335], (iv) predict forces in crash-test studies and, (v) study the movement induced by a set of muscle forces or activations, just to name a few examples.

Distinct computational muscle models describing the mechanical behavior of skeletal [328], smooth [336] and cardiac [337] muscle are available in the literature. However, since only skeletal muscle is directly involved in human movement the models that address the modeling of smooth and cardiac muscle are out of scope of the present work.

Biophysical models are represented by a set of complex partial differential equations, which allows to describe the muscle contraction mechanism with accuracy and results in high computational cost that limits their application within the framework of MBS formulations [84, 85]. In turn, phenomenological or Hill-based lumped-parameter models describe the force-producing properties of skeletal muscle [86] with more simplicity and lower computational cost. Several mechanical muscle models have been proposed to study the muscle contraction dynamics [108, 338], namely, the Maxwell, Voight, Kelvin and the Hill Model [108] (see Fig. 2).

In the Maxwell, Voight and Kelvin models, the behavior of the skeletal muscle tissue is described by means of passive elements, such as spring and damping elements as represented in Fig. 2. The difference between these models lies on the different arrangements of those elements. Since these models are not currently used in the context of human movement analysis, they will not be addressed in detail. For more information regarding these models, the interested reader can consult the work of Yamaguchi [108]. The Hill model [328] has an additional force generator element to simulate the tension produced by the contractile proteins, actin and myosin. The passive and active elements can accurately represent the contractile properties of the muscle tissue and the elasticity of the muscle fibers and tendon. Furthermore, in contrast with the Kelvin model, in which the passive elements have a linear response, the Hill model typically uses nonlinear springs to represent both parallel and series spring elements.

In Hill muscle model, the modeling of the MTU requires some simplifications, including the assumption that MTU actuators are extensible, frictionless, and massless strings. All muscle fibers are assumed to be straight, parallel, of equal length, and coplanar. Moreover, the cross-sectional area and height of the fibers are assumed to be constant and the pennation angle varies in order to maintain muscle height. The muscle force production is directly related to the force developed by a single representative fiber and a function of each muscle activation, length and velocity of contraction, each of which modulates force production independently [339, 340].

Several Hill-type models [328], ranging from simple [341] to very complex models [42, 87, 342, 343], can be found in the literature. Figure 3a illustrates a simple Hill-type model in which only a contractile element is considered, and the tendon is treated as infinitely stiff and aligned with the muscle fibers. This model oversimplifies the MTU

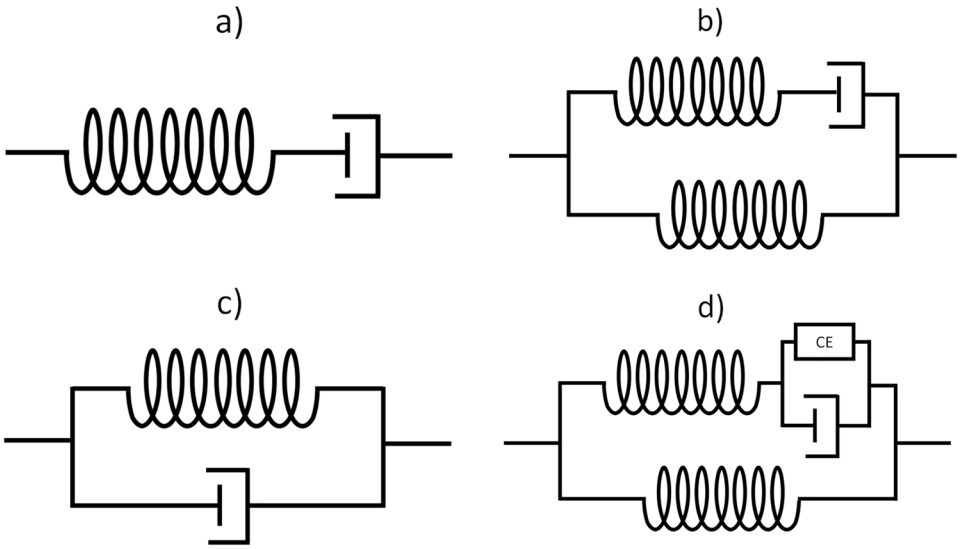

Fig. 2 Schematic representation of muscle models (tendon not included). **a** Maxwell model. **b** Kelvin model. **c** Voight model. **d** Hill model (CE Contractile Element)

behavior and its ability to produce force. Figure 3b shows a slightly more complex and more physiologically accurate MTU model since also takes into account the pennation angle which changes the amount of force transmitted from the muscle fibers to the tendon and, consequently, to the bone. The model presented in Fig. 3c neglects the pennation angle but includes the passive element, which considers the force–length relationships. Figure 3d illustrates a MTU model that covers all features of the previous model but also includes the pennation angle. Finally, Fig. 3e–f depicts a model in which the tendon is treated as an elastic element, which provides a response closer to the real function of the MTU.

Although an elastic tendon model suggests a more realistic behavior [340], according to Millard et al. [339] in cases where the muscle has a short tendon, the stiff tendon model attains similar results that those obtained with an elastic tendon model. Thus, the stiff model assumption performs well for those cases where the tendon does not stretch enough to affect the normalized length of the contractile element [339]. Regarding the accuracy and efficiency of different MTU models, considering both rigid (Fig. 5d) and elastic tendons (Fig. 5e), Millard et al. concluded that both models produced similar MTU forces when the tendon slack length is lower than the muscle optimal length, but the rigid tendon model could run simulations from 2 to 54 times faster than the elastic model [339].

In addition, Pereira et al. [344] presented a muscle model that allowed to efficiently compute redundant muscle forces in the presence of muscle fatigue, and Guo et al. [345] addressed the mass distribution of the skeletal muscle during motion. Although fatigue and muscle mass wobbling play a key role in human motor control [344] and MSK dynamics [346, 347], these topics are not usually considered in most of the existing MSK models, which leads to non-negligible errors. Both models allow to obtain more realistic outputs, which turns out to be their great advantage.

4.3 MTU Scaling

The musculotendon unit models described in the previous section require the quantification of a set of parameters, namely (i) optimal fiber length, (ii) tendon slack length, (iii) muscle pennation angle, and (iv) maximal isometric force [87]. Some of these parameters can be directly measured via ultrasound [348–350] or MR imaging [92]. However, some others, such as the optimal muscle length or tendon slack, are difficult to measure [104].

Several authors consider that the use of generic muscle model parameters is inappropriate due to the high sensitivity of MSK models to them [98–101]. The use of subject-specific parameters of the individual under analysis is the most appropriate modeling procedure [102] since the parameters have great influence on muscle force production [96, 97]. However, the construction of subject-specific models is an expensive and time-consuming procedure which makes it usually unfeasible. Therefore, most researchers apply generic MSK models, based on datasets available in the literature, which are scaled to the subject under analysis [103]. The most used datasets are those presented by Yamaguchi [108], Horsman et al. [351] and Carbone et al. [109], in which the data was collected from a single cadaver, or by Delp [352], Ward et al. [353], Handsfield et al. [354] and Rajagopal et al. [209], in which several subjects were used.

According to Winby et al. [104], the optimal muscle fiber length and tendon slack length greatly affect the capacity of a MTU to generate force. The scale of these two parameters should be performed using anthropometric and functional data of the subject of interest. Anthropometric scaling adjusts MTU lengths and moment arms using

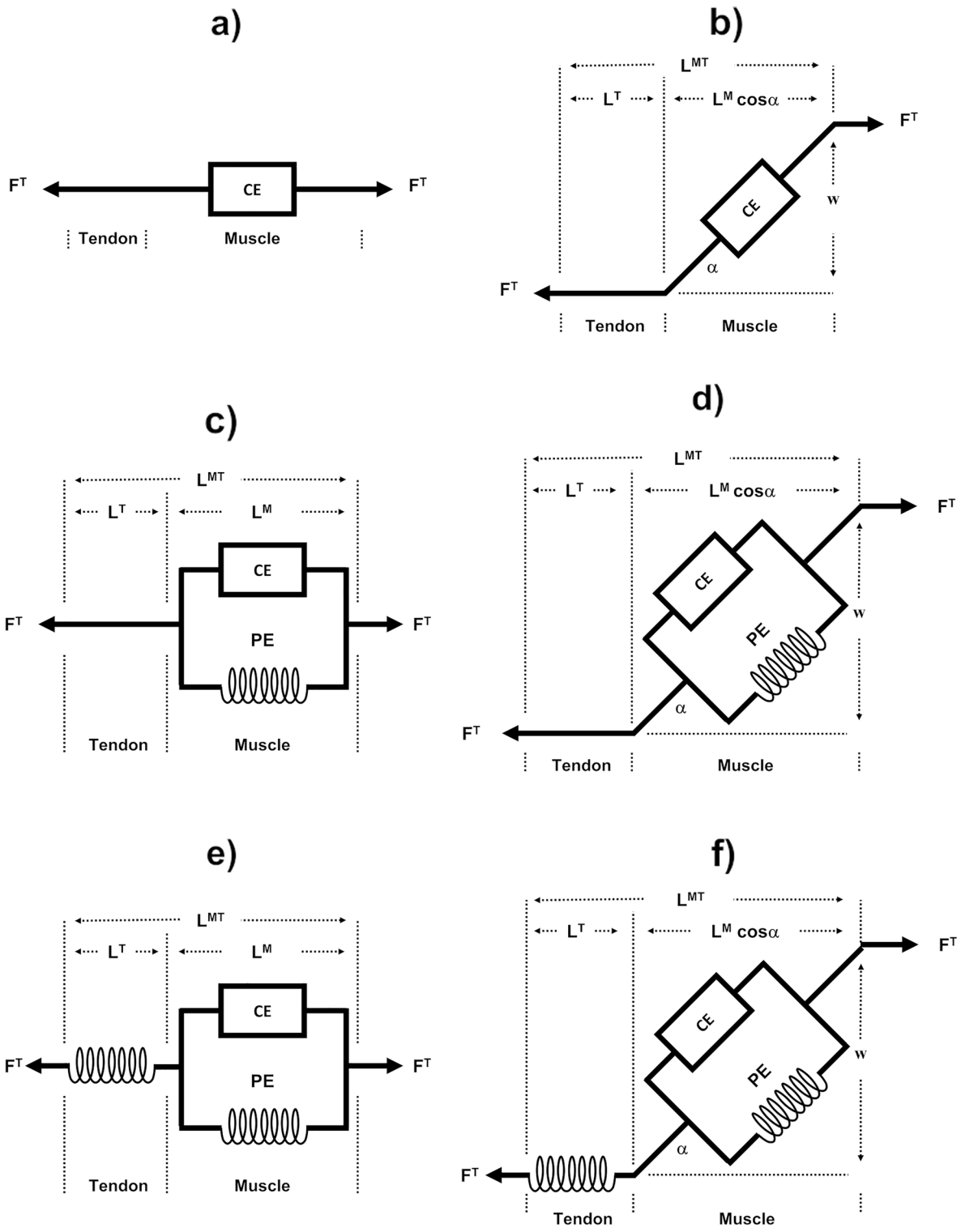

Fig. 3 Representation of MTU models: **a** Simple model; **b** Simple model with pennation angle; **c** Force–length-velocity; **d** Force–length-velocity with pennation; **e** Force–length-velocity with elastic tendon; **f** Force–length-velocity with elastic tendon and pennation angle. (*CE* contractile element; *PE* passive element; F^T tendon force; L^{MT} muscle–tendon length; L^T tendon length; L^M muscle length; *a* pennation angle)

the anthropometric parameters of the subject under analysis, while functional scaling reflects each subject's specific moment-generating characteristics [105, 106].

Regarding anthropometric scaling, different techniques can be used, namely, linear scaling [355], scaling by maintaining a constant tendon slack length throughout the range of joint motion [356], and scaling by maintaining muscle operating range throughout the range of joint motion [103, 104, 357]. In the first and most used method, a linear anthropometric scaling of the optimal muscle fiber length and tendon slack length is performed based on subject's bone dimensions [355, 358].

The second method was originally proposed by Manal and Buchanan [359]. Herein, the MTU length was computed at three different postures. Afterwards, the normalized muscle length was adjusted to minimize the difference between the subsequent tendon slack length computed in each posture. Since the normalized muscle force can be estimated through the interpolation of the normalized fiber length on the force–length curve, the tendon slack length can be computed based on the muscle's optimal fiber length, musculotendon lengths measured and the pennation angle. This method allows to estimate subject-specific tendon slack lengths for an individual muscle, rather than estimating architectural parameters for all muscles within a group.

Finally, in the scaling method that maintains the muscle operating range throughout the range of joint motion, the normalized muscle length between the scaled and unscaled model is preserved for different joint postures. Moreover, the relation between the normalized maximum force and joint angle was also preserved since normalized muscle force is the only determinant of muscle force during a maximum isometric contraction [104].

In view of the above methods, when performing musculotendon unit parameters scaling, the most appropriate is the one that maintains the muscle force-generating characteristics during a maximal contraction [104].

Bujalski et al. [90] grouped MTU parameters according to their influence on the muscle force output. The parameters that present more influence in muscle force production capacity are the maximum isometric force, the pennation angle, the optimal fiber length, the tendon slack length, the tendon reference strain, and the tendon shape factor, respectively. In contrast, the force enhancement during eccentric contraction, the curvature constant in the force–velocity curve, the maximum contraction velocity or the shape at the extremities of the active contractile element exhibit small impact on the capacity of muscle to produce force.

4.4 MTU Path

The definition of the muscles path is fundamental for the dynamic analysis of MSK systems, since the muscle length and its rate of change affect the computation of muscle forces, moment arms, and the resulting body and joint loads [113]. The first and simplest muscle path model is the straight-line model, in which the muscle path is represented by a straight line between the centroids of both the muscle origin and insertion [110]. Since the MTU may wrap around several bones or other tissues, and form curved paths, the straight-line model is often inadequate. To overcome this limitation, the centroid-line model [360, 361] represents the muscle path as a line that passes through the locus of cross sectional centroids of the muscle [110], which are difficult to obtain for every joint configuration and make the application of this model challenging. Methods that consider several via points (i.e., several points along a muscle path whose positions are constrained by the presence of another anatomical structure) along the segment have also been presented [108, 352], but they are only valid for simple hinge joints [110]. For joints with more than one DoF, the muscle can slide over the anatomical surfaces and lead to an incorrect computation of muscle lengths and muscle moment arm discontinuities.

Considering these limitations, Garner and Pandy [110] proposed a new method, designated Obstacle-Set Method, in which each muscle is modelled as a frictionless elastic rubber band that wraps around anatomic structures. The muscle is considered as a series of straight-line and curved-line segments that pass through several via points, which may be fixed or not to bones. This approach defines two types of via points: fixed via points that remain fixed in a bone reference frame, and obstacle via points that are not fixed in any reference frame but are constrained to move on the surface of an underlying obstacle.

In this approach, straight lines connect adjacent via points, while curved lines define the muscle path around the surface of anatomical structures, which are represented by regular-shaped rigid bodies, including a single-sphere, a single cylinder, a double cylinder, and a sphere-capped cylinder [110]. All these methods require the definition of the radii of geometric elements (spheres and cylinders), the position and orientation of the fixed reference frame on those elements and the position of two bounding-fixed via points with respect to the bone reference frame. An example of the application of the single sphere obstacle-set is to define the path of the biceps brachii muscle [110]. The single cylinder obstacle-set can be used to obtain the path of uniarticular muscles, while the double cylinder obstacle-set is a suitable option to model the path of biarticular muscles and it differs from two simple cylinders since, in the double cylinder, no bounding fixed via points exist between the two cylinders [110]. Additionally, the double cylinder obstacle-set enforces both cylinders not touching each other where the muscle path interacts with each cylinder. Finally, the sphere-capped cylinder allows to obtain the muscle path of long muscles that span joints with more than one DoF [110].

Although the Obstacle-Set method allows the automatic generation of muscle wrapping around anatomical structures, it only considers simple geometries, which is not always anatomically accurate. Later, Gao et al. [111] proposed an alternative method to generate muscle wrapping over surfaces with arbitrary shape, while maintaining a high numerical efficiency. This method can be applied to all muscles and it only requires data regarding muscle origin and insertion and the geometry of the bones that interact with the muscle. To simplify the computations, the bones are treated as a stack of cross sections, and the muscle paths as a set of connected lines passing through the cross sections where muscle and bone interaction occurred [111].

More recently, Stavness et al. [112] proposed a method in which the total muscle path is composed of geodesic segments wrapping around each surface and joined by straight-line segments. The proposed algorithm computes the shortest path across multiple implicit surfaces, which define the anatomical structures, using an iterative procedure in which the positions of the origin points of the geodesic segments are adjusted to ensure the two geodesic segments on each surface connect collinearly and the adjacent straight-line segments are tangent to the surface in the connection points. Although this method is generic and provides accurate results, it is computationally slow [112].

Afterwards, the Natural Geodesic Variation technique has been proposed to improve the accuracy and computational efficiency of the calculation of MTU's shortest path across an arbitrary number of general smooth wrapping surfaces [113]. This method uses a single geodesic segment per surface, therefore, it only considers the constraints for the shortest path at the transitions between the geodesic and straight-line segments.

4.5 Muscle Redundancy Problem

Human joints are spanned by a large number of muscles, which allows to perform a specific movement with different combinations of muscle actuation without compromising its goal. According to Bernstein [188], "It is clear that the basic difficulties for co-ordination consist precisely in the extreme abundance of degrees of freedom, with which the [nervous] center is not at first in a position to deal". This issue is commonly known as muscle redundancy and means that there is not a unique solution for a specific motor task [188].

In case of injury, muscle redundancy allows the subject to perform a given task by recruiting different sets of muscles, which is less efficient but provides a temporary alternative until recovering full functionality. In addition, muscle redundancy also allows for having muscles optimized to perform different combined movements (e.g. flexion + rotation) or muscles which, when active, act immediately at the level of two joints (biarticular muscles).

From a mathematical perspective, the number of unknown variables, i.e., musculo-tendon forces, muscle activation, or neural control surpasses the number of dynamic equations, equal to the DoFs of the system, which results in an undetermined problem with an infinite number of possible solutions. Optimization techniques are often applied [108] to find the combination of musculo-tendon forces that minimizes a particular cost function. It should be noted that musculo-tendon forces, commonly used in the MSK models, do not distinguish the forces produced by the muscle and the forces produced by the tendon at the MTUs. The definition of the cost function is a critical step [37], which, in some cases, becomes easy when the performance criterion is clear, as in a vertical jump, in which the goal is to maximize the vertical displacement of the body's center of mass during the flight phase [215]. However, the cost function becomes hard to define when there is no clear criterion, as in walking. A wide variety of cost functions with different physiological criteria can be found in the literature, namely mechanical energy, dynamic effort, jerk, stability, or maximum absolute joint torque, muscle activations, volume-scaled activations, forces, stresses, metabolic energy, and joint contact forces [362]. The most commonly used consider the muscle stress-endurance relationship to minimize muscle stress, while maximizing muscle endurance [115, 363], or consider the muscles' energy consumption mechanisms, the cross bridges detachment and the calcium re-uptake, to minimize the energy expenditure [364]. However, these cost functions are not suitable for tasks in which the goal is to maximize its performance [365].

Generally, performance criteria based on principles of energy minimization, such as the metabolic energy, mechanical energy and dynamic effort, tend to present better results [37, 366]. However, Ackerman et al. showed that the use of only energy-related cost functions does not always lead to natural and realistic movements. While simulating the gait movement, these authors showed that this type of functions do not allow to obtain the typical knee flexion pattern that occurs during the stance phase [37]. To improve the realism of the simulation, several authors consider the use of tracking control approaches, which can be included in the objective function or as an optimization constraint to minimize [367]. More recently, several authors addressed the inclusion of joint reaction forces in the cost function to obtain more physiological musculo-tendon forces and joint contact forces [41, 362, 368]. Moissenet et al. [41] showed that their inclusion resulted in contact force patterns similar to those observed in vivo and in a more physiological loading pattern during the stance phase. However, the authors also refer that the tuning of the optimization weights has a strong influence on the obtained muscle–tendon forces.

The selection of the optimization technique and the definition of the design variables and constraints [369, 370] is

a fundamental issue, and static and dynamic optimization routines are the most used. In static optimization, the optimization problem is solved independently for each time frame, the set of muscle forces that balances the joint moments is found while also satisfying the selected cost function [115, 371, 372]. However, this method only takes into consideration instantaneous criteria, which does not mimic the decisions of the CNS and leads to non-physiological on–off switching of muscle forces. Despite these limitations, this approach is very robust and computationally efficient. In dynamic optimization, the time history of the simulation along with the muscle contraction and EC coupling dynamics are used to find muscle forces [36], which leads to more accurate physiological results. Moreover, such optimization techniques also allow to define time-integral cost functions or time-dependent functions. The dynamic optimization can also address questions for which no experimental data exist, such as, deep muscles forces using non-invasive approaches.

In general terms, dynamic optimization problems can be stated from three different perspectives: forward dynamics optimization, inverse dynamics optimization and predictive dynamics. In forward dynamic problems, the variables to optimize are the forces, joint torques, muscle forces or muscle excitations. This type of methods has the advantage of the movement be directly obtained from the integration of the equations of motion and from the initial state of the system. On its turn, these methods tend to be computationally expensive and require accurate boundary values to stabilize the system. Inverse dynamic-based problems optimize variables related with the kinematic of the system (e.g., position, angular joint position, among others). This type of problem does not require the integration of the equations of motion and accurate boundary values, being consequently more efficient than the previous methods. However, this type of analysis requires experimental data and the forces are not directly obtained from the optimization. Predictive dynamic problems optimize simultaneously the kinematics and dynamics of the system. This way, the optimized positions, torques and forces of the biomechanical system are obtained directly from the simulation. Predicative methods present also other computational advantages. Since the equations of motion are treated as equality constraints, this type of methods does not require their explicit integration, as well as no boundary information is needed to achieve the optimal solution. In contrast, this method leads to large optimization problems with a large number of design variables, requiring specific optimization algorithms [373].

Predictive methods can be further divided into semi-predictive or fully predictive methods [374]. The former requires tracking the error between the optimization outputs and experimental data. For that purpose, the differences between the simulated and experimental data (e.g., the position of a given point/joint at a specific time instant) are included in the optimization process as a cost function to minimize. Other approaches consider alternative algorithms, such as the proportional-integral-derivative control or the computed torque control to track the experimental data. Although these methods enable the computation of realistic joint torques and muscle forces [375], they are limited to the study of human motion with experimental measurements and cannot be used when the conditions (environment, goal, execution speed, amongst others) in which the task is performed change [36]. In contrast, fully predictive methods do not require experimental data, which make them suitable to study movements in which the data is missing or to test tasks with varying conditions [376].

In addition to the methods addressed before, other approaches can be found on literature. These include variations to the inverse and forward dynamics methods, mixed approaches, implicit methods, neural networks, among others. The interest reader is referred to the works of Ezati et al. and Xiang et al. for more information on this topic [36, 373].

From a computational point of view, dynamic optimizations have a high computational cost, since they require to simulate the entire movement for each possible solution and a more detailed MSK model [377]. To address this issue, the optimization problem, and in particular the predictive methods, can be stated in terms of an optimal control problem, which can be solved using indirect or direct methods [378]. To solve an optimal control problem, four key elements are required: (i) the state equations of the dynamical system, (ii) the controls that influence the behavior of the system; (iii) the constraints and (iv) a performance criterion [379].

In the context of biomechanics, direct methods, which include the direct shooting and direct collocation methods, tend to be preferable, since they do not require the solution of a boundary-value problem. Amongst them, the direct collocation method is the most commonly used, since it avoids the integration of equations of motion, as these are included in the optimization as equality constraints that must be fulfilled. This procedure enables to decrease significantly the computational costs when compared with direct shooting methods [380].

However, both forward dynamic and predictive approaches require the inclusion of models to depict the interaction between the body and the surrounding environment (e.g., foot–ground [381–383], leg-orthosis [384–386], hand-assistive device contact [387–389], among others), since contact forces play a key role in muscle, ligament, and joint reaction forces [381]. This interaction can be modeled using kinematic constraints or a compliant contact model. In the first approach, unilateral kinematic constraints are used to model a perfectly inelastic collision without sliding. Regarding the second approach, the contact geometry must be defined and a constitutive viscoelastic model is applied to estimate the contact forces [382, 390].

In particular, several works have been published to predict the contact forces between the ground and foot for several movements [381, 391–395]. Most of these models represent the foot surface by a set of points [392] or spheres/ellipsoids [382] and apply simple spring/damper elements. However, Shourijeh and McPhee [381] indicate that models based on point contact elements lead to sharp contact forces that do not depict the experimental data, suggesting the use of volumetric models.

4.6 Ligaments

Ligaments are composed of dense fibrous bundles of collagenous fibers, primarily type I collagen, protected by dense irregular connective tissue sheaths. These collagen fibers are extremely stiff and highly aligned in the direction of force transfer [396]. In some cases, ligaments form a sac that surrounds the articulating bones and contains a fluid lubricant, the synovial membrane whereas sometimes fasten around or across bone ends in bands [396].

From a physiological point of view, ligaments are similar to tendons and fasciae as they are all made of connective tissue. Ligaments connect a bone to other bone while tendons connect muscle to bone and fasciae connect muscles to other muscles. The junction between the soft tissue of ligaments and the hard tissue of bones varies greatly among different ligaments as well as between the two ends of the same ligament [397]. Ligaments play a very important role in permitting several degrees of movement, constricting inappropriate movement or guiding joint motion and stabilizing joints even in the absence of muscle and tendon forces [397]. When ligaments no longer ensure joint stability, abnormal kinematics occurs which may lead to damages in the tissues in and around the joint, such as wear of the cartilage or osteoarthritis. In contrast to muscle, ligaments cannot usually regenerate naturally. The mechanical properties of ligaments are related with composition of the collagen fibers and the proteoglycan-rich matrix that surrounds such fibers. Some ligaments are richer in collagenous fibers, which produces more inelastic behavior, whereas others are rich in elastic fibers, which make them quite tough even though they allow elastic movement. Due to their histological similarity with tendons, both tissues have similar mechanical properties.

Likewise tendons, the ligament force–displacement curve behavior is non-linear when subjected to constant strain rates [398]. This occurs due to the progressive recruitment of the collagen fibers during load increases [399].

Moreover, the ligament only responds to traction excitation, therefore, when the ligament length is shorter than the resting length no force is generated, however, small changes in ligaments length can cause large passive forces. Ligaments also present creep, stress relaxation, and hysteresis. However, due to differences in the percentage of collagen molecules, in the content of elastin and in blood supply from insertion sites, ligaments present different behavior in response to loading.

In conclusion, from a mechanical point of view, ligaments are passive elements that present a viscoelastic behavior, i.e., the applied stress results in an instantaneous elastic strain followed by a viscous time dependent strain. Ligaments mainly resist to uniaxial loads, however, they also experience shear and transverse loading in vivo [397]. Moreover, since, in certain joint configurations, ligaments wrap around each other or bones, they are also subjected to compressive contact stresses [397].

4.7 Ligaments Computational Models

Although ligaments play a key role in joint stability they are not commonly used in the modeling of musculoskeletal biomechanical models for human analysis within the framework of multibody systems dynamics, since the purpose of these models is to explain muscle function [213]. However, when included in MSK models, ligaments are usually described by several line elements that correspond to different fiber bundles. Similar to muscles, each ligament requires the definition of the ligament geometry path. For that purpose, a point set composed of an origin, insertion and via points for each ligament is required [400]. The most appropriate stress–strain curve for each ligament must be defined to obtain accurate key ligament properties.

Ligaments have been commonly modeled with elastic nonlinear force-strain relationship [401–404], which means that the force a ligament exerts on bone is only a function of its length. The lack of accurate descriptions of the viscoelastic properties of the ligaments, lead to the representation of the ligaments as elastic springs [402], in which the only variables required are the stiffness and the undeformed length of the spring. However, some authors opted for modelling the ligaments as rigid links to constraint the motion of the articulating anatomical structures. (e.g., shoulder [192], knee [405] and ankle [202]).

More recent models use one-dimensional non-linear spring-damper elements to represent ligaments, which require (i) the ligament zero-load length, i.e., the length when it first becomes tense, (ii) the reference length, i.e., the length at the reference (typically extension) position and (iii) the reference strain, i.e., the strain at that reference position. Despite its low complexity, this model still enables investigators to predict quantities such as joint kinematics [403].

Several studies [401, 402, 406–408] used the force–displacement curve originally presented by Wismans et al. [402] and Blankevoort et al. [401] to obtain the zero-load length of the ligament. In some cases, the ligament reference length and strain value were obtained from previously published studies [401, 409, 410]. Although this approach does

not take subject-specific ligament information into account, it facilitates the modeling of the ligaments due to the difficulty to find data for the actual zero-load length [409]. Optimization techniques can be utilized to overcome the lack of the referred data [408, 409]. Bloemker et al. proposed an alternative approach in which an experimental setup based on cadaveric specimens is used to measure the passive limits of the knee joint, calculate the extent of motion for each ligament bundle and apply a correction factor, to determine its zero-load length [403]. Bersini et al. [404] developed a MBS dynamic model of the lower limb segments that includes ligaments based on MRI from a single Caucasian male and a forward dynamics analysis was performed to obtain the ligaments parameters.

4.8 Application Cases and Discussion

The first aspect that stands out from the literature is the high degree of complexity of the most recent MSK models when compared to the most antique ones. Older models primarily addressed the modeling of simple MSK systems of the most relevant anatomical segments, such as the lower limbs [351, 411], the upper limbs [412], or both [413, 414], while more recently MSK models evolved to represent in high detail those segments. The works of deZee et al. [232], Christophy et al. [415], Raabe and Chaudari [229], Kuai et al.[228] and Bassani et al. [227] concerning the detailed modeling of the lumbar spine; Ignasiak et al. [226] regarding the thoracolumbar spine; Malaquias et al. [59] and Kim and Kipp [416] on the foot; Quental et al. [198] and Nikooyan et al. [412] regarding the shoulder; and Holzbaur et al. [417] and Ma'touq et al. [418] with respect to the hand are representative. Many musculoskeletal models include two specific segments, the patella, and the talus, to define, respectively, quadriceps insertions and subtalar joint axis.

The use of generic or subject-specific MSK models is a relevant topic since in contrast with the first models, nowadays highly detailed subject-specific musculoskeletal models can be implemented. The MSK models were developed based on scaling the muscular parameters obtained from cadaveric specimens [91, 212, 351], which does not consider the inter-individual variability, such as, muscle origin and insertion sites. This issue influence the prediction of muscle force and moment arm, which limits its use for pre-surgical or rehabilitation assessments [101]. Hence, subject-specific models should be used instead, as reported by Martelli et al. [419] and Nejad et al.[420] when comparing the joint contact forces in the hip and knee obtained with generic or subject-specific models.

Traditionally, the implementation of subject-specific models is very time-consuming since the segmentation of the anatomical structures was performed manually, however, developments in medical image processing and visualization have reduced considerably the overall processing time [421].

Thus, a suitable solution to obtain subject-specific models is to register or morph (geometric interpolation technique that is often used to transform one form into another) the medical images of the subject of interest based on previous studies containing muscle–tendon attachment sites and lines-of-action [422], or muscle volumes [422]. For that purpose, statistical shape models (SSM) are a powerful tool to accurately parametrize complex geometries, such as the one provided by an individual's morphology [320]. Consequently, SSM provide a solution to obtain a realistic and personalized description of any subject by combining conventional multivariate statistics and dense sets of homologous landmarks used to depict the underlying structures [423]. The work of Salhi et al. [424] concerning the prediction of subject-specific muscle origin/insertion regions for the shoulder joint and for the lower limb is a demonstrative example of this approach. Nolte et al. [319] used SSM to provide subject-specific bone shapes from surface digitized experimental data.

The SK morphing is very important since the dimension and shape of the model segments have a great impact on force and moment predictions of MSK models. The need of medical images of the subject under analysis, in particular MR images, limits the generalization of SSM.

Another approach that enables the adjustment of the MSK models parameters is based on the comparison between the measured and the estimated kinetic data [425], which, sometimes, present incongruities as a result of inaccurate modelling assumptions (e.g., rigid body), problems with the estimation of segment inertial properties and measurement errors (e.g., soft tissue artifact) [426, 427]. A common approach used to solve this problem is the RRA method [149, 150]. This reduces or eliminates the residual forces and torques estimated by the biomechanical model, which do not actually exist, to comply with the prescribed kinematics and kinetics [375, 428–430]. Usually, these differences are reduced by adjusting the BSIPs of the subject or the kinematics of the movement [431, 432]. Recently, Sturdy et al. [433] proposed a multi-heuristic optimization method to automatically tune the RRA parameters, improving simultaneously the accuracy of the algorithm.

The development and validation of accurate joint models is also relevant for MSK modeling, and most of the studies that estimate muscle and joint forces uses generic joint models [434]. However, the anatomical differences between subjects lead to distinct joint center or axes of rotation, which results in different muscle and joint contact forces that the generic models are not able to reproduce [434, 435]. To address this issue, numerous studies developed subject-specific joint models based on MRI and CT that include detailed representations of the anatomical structures of the joint, such

as: (i) the hip [102, 436–438], (ii) the knee [74, 439–442]; (iii) the ankle [443, 444]; or (iv) the elbow [445, 446].

Musculoskeletal models have been applied in healthy and pathological populations [74, 414, 436] performing distinct movements, such as running at different speeds [414], overground jogging [229], level walking [420], squatting [436] and deep squatting [420], or jumping [447]. Furthermore, the use of these models has not been restricted to a specific technology, since examples of studies using optical motion capture systems [198, 227, 392, 419], inertial motion units and depth sensors [316, 317] can be found.

An important finding is that the use of MSK models is not restricted to researchers able to develop their own computational routines, since commercial and open-source software such as, the AnyBody (AnyBody Technology, Denmark), the Visual3D (C-Motion, Germantown, MD), the SIMM (MotionAnalysis, SantaRosa, USA) or the OpenSim [358] software is available.

Table 4 contains several examples of MSK models, including planar or spatial, generic and subject-specific models depicting different anatomical segments. Furthermore, for each model, the name, author, year of publication, anatomical segments, and software or programming language used in its development are presented.

A final remark worth referring is that although most of the MSK models included in this work are spatial, recently Dumas et al. [43] and Millard et al. [39] proposed full body planar MSK models. Despite their simplicity and limitations, these models provide reliable results under some conditions and are a valuable tool to demonstrate the differences between inter-segmental and contact forces [43].

In summary, MSK models are an important tool to estimate individual muscle forces and their contribution to joint moments. They started by considering generic models and progressively evolved to subject-specific models. Simultaneously, the level of detail of the representation of the anatomical structures, such as joints and muscles increased over time, which led to a more accurate representation of physiological, and anatomical characteristics of an individual. Furthermore, since different technologies and software can be used to obtain the necessary data for MSK models, their use is not restricted to laboratorial environments or limited by financial issues. The main drawback of MSK is neglecting the dynamics of muscle EC coupling, including only the muscle contraction dynamics. To overcome this drawback, NMSK models are a suitable option.

5 Neuromusculoskeletal Models

Neuromusculoskeletal models are representations of an individual's skeletal, muscular, and neural system since they not only include bones, tendons, joints and muscles [429] often represented as Hill-type actuators [356, 449], but also the muscle EC coupling dynamics. Thus, NMSK models are composed of different components, such as the ''neuro", the "musculo" and the "skeletal" that depict the ECC dynamics, the muscle activation dynamics, and the skeletal dynamics, respectively. Therefore, such models overcome some of the limitations of MSK models which make them suitable to identify the relationship between the neurophysiological and muscle levels [118]. The major issues associated with them are the modeling of the EC coupling dynamics which implies a higher computational effort.

5.1 MTU Excitation Contraction Coupling

Humans can produce adaptive movements by skillfully manipulating their MSK system within a temporal and spatial structure [450]. This process is regulated by the CNS that transmits a neural excitation signal to the muscle, which in turn becomes activated and leads to the production of muscle force.

The ECC describes the sequence of occurrences that begins with the propagation of the neural signal from the nervous system on the muscle's surface membrane and leads to the contraction of muscle fibers [451, 452] (see Fig. 4). To produce muscular contraction, the nervous system sends a neural signal or action potential propagated through specialized cells, the motoneurons, which stimulate the muscle fibers. The set formed by these two elements is called a motor unit. Then, the muscle fibers become activated and, therefore, capable of contracting and producing muscle force. The lag activation process describes the time period that occurs between sending a neural signal and the effective muscle fiber contraction [453].

Motoneurons possess structures at their ends called axon terminals, which form a neuromuscular junction to connect the motoneuron to the muscle fiber. A muscle is stimulated when a neural signal arrives at this junction and release a neurotransmitter (acetilcoline or ACh, which is contained within vesicles) into postsynaptic clefts (small gaps located in between the axon terminals and the muscle fiber) causing muscle activation. ACh binds to specialized receptors located at the muscle fiber membrane, which provokes its local depolarization and rapidly propagates to the entire muscle. This alteration in membrane polarization origins the release of calcium ions (Ca^{2+}), which bind to a protein called troponin and take part in muscular contraction occurring at sarcomere level. This occurrence acts as a trigger, causing the actin filaments to bind to myosin filaments (crossbridges), beginning the muscle contraction by the sliding of the two filaments relative to each other, according to the sliding filament theory. When the neural signal ends, the concentration of calcium ions

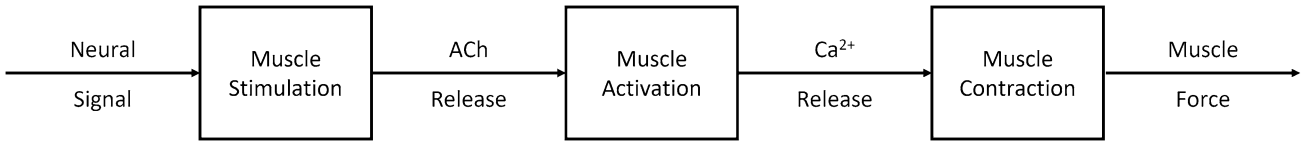

Fig. 4 Processes occurring from neural signal sending until the production of muscle force. When a neural signal arrives to the axons of a motoneuron, it is propagated to the adjacent muscle fibers, provoking muscle stimulation. This occurrence enables ACh to be released in the synaptic cleft, provoking muscle activation. When the muscle is activated, calcium ions are released into the muscle fibers, initiating muscular contraction, which in turn leads to muscle force production

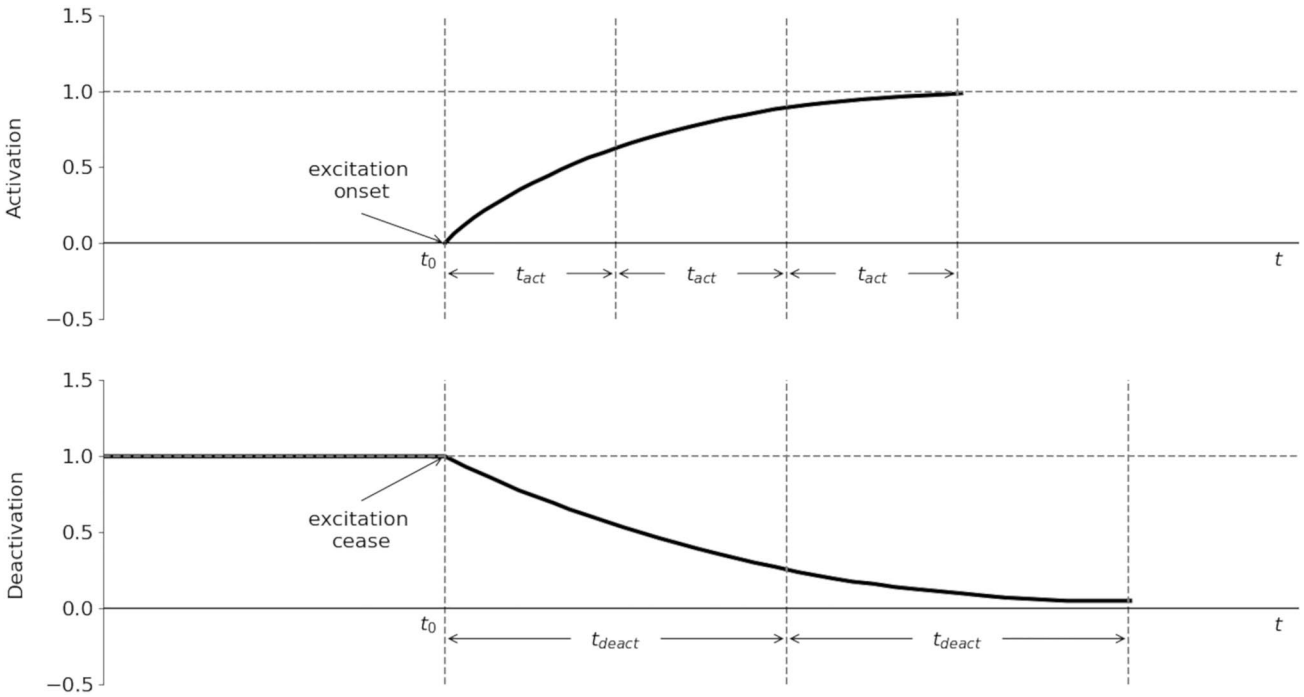

Fig. 5 Representation of the skeletal muscle excitation contraction coupling dynamics

within the muscle fibers is reduced, inhibiting the cross-bridges between the two myofilaments and the muscle relaxes [454, 455].

After the activation, the muscle contracts and produces force, which depends on two physiological processes. The muscular force production may be influenced by the frequency of neural signals or stimuli that arrive at muscle fibers or on the recruitment of additional motor units [456].

The muscle EC coupling dynamics, i.e., the relationship between the neural drive and the muscle activation, is modeled as a first-order process [87]. The following section addresses the computational modeling of the EC coupling dynamics.

5.2 Excitation Contraction Coupling Computational Models

In the last 50 years the knowledge about the ECC coupling process evolved from how an action potential on the muscle surface could initiate contraction within only 1–2 ms to a point in which the major proteins involved in EC coupling were identified, and experiments to define the molecular interactions between the proteins were conducted [457].

Some models of EC coupling distinguish the number of motor units recruited and their firing frequency [343], but, within the framework of MBS dynamics, the more commonly modeling approach assumes that the EC model represents the net effect of both motor neuron recruitment and firing frequency. These EC coupling models include the ones presented by Zajac [87], Winters [458] or Thelen [459], among others [460].

A first-order nonlinear differential equation is used to describe this process [87, 458, 459, 461] which introduces a delay between the neural excitation (i.e., the firing of motor units) and the active state of the muscle (i.e., the concentration of calcium ions within the muscle) [462]. This delay is fundamental to avoid the physiological inaccurate instantaneous MTU activation or relaxation that occurs when the EC coupling modeling is disregarded [463, 464]. The use of a first-order model to represent the activation and deactivation dynamics is a suitable option to model the net result of the EC coupling, however, it is not able to model the underlying complex molecular dynamics [462]. These models relate the activation and deactivation dynamics with two time constants. The activation time constant refers to the delay between the onset of excitation and maximum twitch force, while the deactivation time constant refers to the delay between the neural excitation finish and the decrease in the muscle force production [462]. Several studies provide reference values for these time constants [87, 458, 459, 465].

The inclusion of such features in the EC coupling models allows that the mechanical activation follows the excitation asymptotically and is bounded between 0 (muscle fully relaxed/no excitation) and 1 (muscle fully activated/full excitation). Furthermore, it also guarantees that the muscle force rises faster during excitation than it decays during relaxation, as illustrated in Fig. 5, which is in accordance with experimental evidence [466, 467] and it is explained by the slower rate of calcium diffusion out of the muscle fibers.

Despite their good accuracy, the first-order EC coupling models usually present some drawbacks, namely, the use of similar activation and deactivation time constants throughout the movement trajectory.

From a physiologically perspective, this assumption is inaccurate since it has been shown that these constants are complex functions of muscle fiber length, velocity, and stimulation frequency [462]. The use of similar activation and deactivation time constants for muscles with different fiber composition also undermines the physiological resemblance of these models. These constants should be adjusted according to the selected muscles to increase the accuracy of the EC coupling modeling [468].

5.3 Application Cases and Discussion

This literature review identified a significant body of literature on NMSK modeling, with the first works dating back to the beginning of the 2000s [106, 356, 469, 470]. NMSK models with distinct degrees of complexity were developed almost simultaneously, which contrasts with SK and MSK models since their earlier works started by modeling the major anatomical structures and progressively evolved to more complex models. The full body model by Hase et al. [469], the knee model by Lloyd and Besier [106], the shoulder and elbow model by Buchanan et al. [356], or the elbow model by Koo and Mak [468] are representative of such works.

Table 6 contains several examples of planar or spatial NMSK models, depicting different anatomical segments. Additionally, the approach used to solve the problem is also presented.

Despite their complexity, NMSK have been used in different populations for distinct purposes, namely test the effect of an elbow joint replacement on the NMSK system prior to a surgery [471]; design of lower-limb prosthesis systems [472, 473]; simulate functional tests used in impaired populations [474]; estimate joint moments across a wide range of tasks and contractile conditions [106]; predict normal joint kinematics during single limb support phase of gait [475]; quantify the risk of falling [476], estimate muscle forces [75, 470, 477]; estimate physiologically plausible joint contact forces [107, 478]; or perform predictive gait simulations [479].

The most common NMSK models in the literature are based on the use of EMG data or explore control and optimization algorithms to obtain the optimal solutions. EMG-driven methods can predict physiological muscle forces over a wide range of motor tasks and for different populations with varying age and pathology [485–488]. They also provide a strong correlation with the subject's motion intention. Due to its advantages, EMG has been used by several research groups to obtain dynamic outputs for either isometric or dynamic tasks at different anatomical locations such as the elbow [471, 489], shoulder [55], knee [106], ankle [490], jaw [491], wrist [360] and lower limb [492].

Besides requiring experimental data, EMG-driven methods can present some drawbacks related with experimental and computational conditions that can influence the accuracy of its outcomes, namely: (i) difficulties to incorporate deep muscles for which EMG measurements cannot be made; (ii) muscle cross-talking; (iii) dependence on the quality of EMG signals, which is strongly affected by the sensors placement, the skin condition, the environment and the electric and magnetic noise; (iv) inaccurate prediction of the moments around multiple DoFs; (v) difficulties to attain the true EMG-maxima, since EMG-linear envelopes are normalized to peak values to reflect percentage excitation levels; and (vi) signal alteration due to preprocessing procedures such as the choice of filter type and cut-off frequencies [478].

Optimization- and control-based methods are also utilized to track experimental joint dynamics or to infer muscle excitations of NMSK models [465, 480, 493]. When used to track experimental data, these methods tend to provide results similar to those obtained using EMG [375, 494]. However, several authors have shown that, for the same joint angles and moments, different individuals use

different excitation patterns depending on the control tasks [495–497], pathology [498–500], and training [501, 502].

When used to infer muscle excitations, this approach assumes that human motion is ruled by a set of different performance criteria [503, 504] that may vary according to the task goal. Mathematically, these criteria, which include metrics related with joint kinematics and dynamics, energy, ground-reaction-forces, performance, among other types, are expressed in the form of an objective function that is minimized during the optimization problem, as discussed on Sect. 4.5. An important aspect of the definition of the objective function is its influence on the simulation outcomes, being still an open topic [37, 373, 505].

Numerous optimization techniques have been used within the context of human movement [36]. However, the optimal control formulations stand out, since they not only allow to simulate human motion satisfying all the different equality and inequality constraints imposed on both the system and the motion task, but also to solve the muscle redundancy problem [506]. Optimal control methods have been used for a long time [215, 507, 508]. However, their solution is highly dependent on the algorithm used [507]. More recently, the direct shooting and the direct collocation methods have been successfully used to perform human motion simulation [509]. The direct shooting method requires the parametrization of the muscle excitations that minimize the selected cost function, and the problem is solved sequentially, i.e., the cost function is evaluated in each time frame, which leads to a very high computational cost. Therefore, some studies only address simple problems or use simple control parameterizations that lead to a non-optimal solution to the system of equations [507]. In turn, the direct collocation method solves all time frames simultaneously. Although this approach leads to a non-linear programming problem with a high number of optimization variables (controls and states), the system becomes sparse and more computationally efficient than direct shooting methods. Thus, direct collocation method has been applied to simulate different human movements such as, gait [509], running [510], jump [380] or Olympic track cycling standing start [511], amongst other movements.

A suitable solution to handle with the limitations previously reported to the use EMG-driven and optimization methods are the EMG-informed methods. These combine experimental EMG-driven models and optimization tools to adjust the acquired EMGs and predict the activation patterns of muscles to which no experimental data exists. This approach allows for the computation of the optimal muscle excitations and muscle dynamics that minimize the joint moment tracking errors, while simultaneously calibrate the muscle parameters to the subject and movement in analysis [107, 368, 478, 512]. Furthermore, EMG-informed models also increase the accuracy of subject-specific model parameters and accurate neural commands [513] and allow for the study of co-activation patterns [368, 514].

From a computational point of view, NMSK models are very complex when compared to SK and MSK models, which limits their widely application. Despite their complexity, neuromusculoskeletal computational models play a key role to improve the knowledge on how the human nervous system controls the movement of the limbs during different activities in both unimpaired and impaired subjects. Moreover, their outcomes are fundamental to explain the relations between muscle activity and the kinematics and dynamics of human movement. Additionally, NMSK are also very important to develop solutions that allow impaired people to regain motor function in cases of disability.

6 Conclusion

The human movement requires highly coordinated actions from the neuromusculoskeletal system, and the study of those mechanisms is a challenging topic addressed by numerous researchers. Multibody system dynamics presents an accurate and non-invasive approach to study such mechanisms. This approach is based on the use of biomechanical models, which are mathematical representations of the human SK, MSK or NMSK systems.

Neuromusculoskeletal models are the state of the art in what concerns the biomechanical models, since they provide detailed information about an individual's skeletal, muscular, and neural systems. However, these models present a high computational cost or require some parameters difficult to obtain, which limits its wide use. On the other hand, MSK models are a suitable solution to obtain accurate kinematic and dynamic outcomes of human motion, as well as muscle forces, with a lower level of complexity. MSK and NMSK models present the muscle redundancy problem, which requires the use of optimization-based methods. Finally, SK models are the least complex models, since their outcomes only consist of kinematics and joint moments.

To ensure an appropriate accuracy of biomechanical models' outcomes, several issues must be addressed during the modeling process. In SK models, the selection of the type of body (rigid or flexible) that depict the human segments and corresponding inertial parameters, and the choice of the most accurate joint models and respective axis or center of rotation are the most important issues. In addition to those topics, MSK also requires the MTU modeling, scaling and path definition. Finally, NMSK models also include the neural inputs through the ECC dynamics of the MTU.

In addition, most of the biomechanical model parameter, such as BSIPs, joint centers, segment reference frames, musculotendon and EC coupling parameters, contact models, amongst others, can be tuned using experimental data or by

applying other methods based on geometric relations, optimization, Kalman filtering or optimal control. Therefore, the modelling and analysis procedures are not necessarily independent. The coupling of these two steps enables to obtain more customized models, which better depict the subject in analysis leading to more accurate predictions.

To conclude, the modeling of biomechanical systems for human movement analysis has remarkably evolved during the last decades which allowed to progress from quite simple to very complex models that provide very accurate and realistic representations of the human body. These advances were fundamental to optimize motor performance, treat movement disorders, or to restore motor function in cases of disability. Despite these improvements, the combination of technological progress and human desire for knowledge keeps this field with great interest, namely in the development of complex subject-specific biomechanical models and its application to daily life activities or to simulate human motion using tracking data obtained using innovative approaches such as machine learning techniques.

Acknowledgements The authors would like to thank the Portuguese Foundation for Science and Technology (FCT) for the support given to the Project UIDB/04436/2020 and UIDP/04436/2020, as well as through IDMEC, under LAETA, Project UIDB/50022/2020 and PTDC/CCI-COM/30274/2017. The second author expresses her gratitude to the Portuguese Foundation for Science and Technology through the PhD Grant (2021.04840.BD).

Funding This work has been supported by Portuguese Foundation for Science and Technology, under the national support to R&D units grant, with the reference project UIDB/04436/2020 and UIDP/04436/2020, as well as through IDMEC, under LAETA, Project UIDB/50022/2020 and PTDC/CCI-COM/30274/2017. The second author expresses her gratitude to the Portuguese Foundation for Science and Technology through the PhD Grant (2021.04840.BD).

Declarations

Conflict of interest On behalf of all authors, the corresponding author states that there is no conflict of interest.

References

1. Nigg B, Herzog W (2007) Biomechanics of the musculoskeletal system, 3rd edn. Wiley, Hoboken
2. Xiao T, Fu YF (2016) Biomechanical modeling of human body movement. J Biom Biostat 7:5–8. https://doi.org/10.4172/2155-6180.1000309
3. Machado M, Flores P, Claro JCP et al (2010) Development of a planar multibody model of the human knee joint. Nonlinear Dyn 60:459–478. https://doi.org/10.1007/s11071-009-9608-7
4. Quental C, Folgado J, Ambrósio J (2016) A window moving inverse dynamics optimization for biomechanics of motion. Multibody Syst Dyn 38:157–171. https://doi.org/10.1007/s11044-016-9529-4
5. Ambrósio JAC, Silva MPT (2005) A biomechanical multibody model with a detailed locomotion muscle apparatus. Adv Comput Multibody Syst 2:155–184. https://doi.org/10.1007/1-4020-3393-1_7
6. Castro APG, Completo A, Simões JA, Flores P (2015) Biomechanical behaviour of cancellous bone on patellofemoral arthroplasty with Journey prosthesis: a finite element study. Comput Methods Biomech Biomed Eng 18:1090–1098
7. Quental C, Folgado J, Monteiro J, Sarmento M (2016) Full-thickness tears of the supraspinatus tendon: a three-dimensional finite element analysis. J Biomech 49:3962–3970. https://doi.org/10.1016/j.jbiomech.2016.11.049
8. Quental C, Folgado J, Comenda M et al (2020) Primary stability analysis of stemless shoulder implants. Med Eng Phys 81:22–29. https://doi.org/10.1016/j.medengphy.2020.04.009
9. Nikravesh P (1988) Computer-aided analysis of mechanical systems, 1st edn. Prentice Hall, New Jersey, p 07632
10. De JJG, Avello A, Cuadrado J (1991) An efficient computational method for real-time multibody dynamic simulation in fully cartesian coordinates. Comput Methods Appl Mech Eng 92:377–395. https://doi.org/10.1016/0045-7825(91)90023-y
11. Siciliano B, Khatib O (2008) Springer handbook of robotics, 1st edn. Springer, Phoenix
12. Roupa I, Gonçalves SB, Silva MT (2018) Dynamic analysis of planar multibody systems with fully cartesian coordinates. In: The 5th joint international conference on multibody system dynamics
13. Schiehlen W (1997) Multibody system dynamics: roots and perspectives. Multibody Syst Dyn 1:149–188. https://doi.org/10.1023/A:1009745432698
14. Bauchau O (2011) Flexible multibody dynamics. Springer, New York
15. van den Bogert AJ, Geijtenbeek T, Even-Zohar O et al (2013) A real-time system for biomechanical analysis of human movement and muscle function. Med Biol Eng Comput 51:1069–1077. https://doi.org/10.1007/s11517-013-1076-z
16. Guilbert ML, Raison M, Fortin C, Achiche S (2019) Development of a multibody model to assess efforts along the spine for the rehabilitation of adolescents with idiopathic scoliosis. J Musculoskelet Neuronal Interact 19:4–12
17. Pradhan KK, Chakraverty S (2019) Finite element method. Comput Struct Mech 1:25–28. https://doi.org/10.1016/B978-0-12-815492-2.00010-1
18. Schneider GE (1988) A finite element differential scheme for fluid flow prediction using primitive variables. Computational mechanics '88. Springer, Berlin, pp 2–5
19. Schmidt A, Beyer HR, Hinze M, Vandoros EN (2020) Finite element approach for the solution of first-order differential equations. J Appl Math Phys 08:2072–2090. https://doi.org/10.4236/jamp.2020.810155
20. Reddy JN (2005) An introduction to the finite element method, 3rd edn. McGraw Hill, Singapore
21. Castro APG, Alves JL (2021) Numerical implementation of an osmo-poro-visco-hyperelastic finite element solver: application to the intervertebral disc. Comput Methods Biomech Biomed Engin 24:538–550. https://doi.org/10.1080/10255842.2020.1839059
22. Santos B, Quental C, Folgado J et al (2018) Bone remodelling of the humerus after a resurfacing and a stemless shoulder arthroplasty. Clin Biomech 59:78–84. https://doi.org/10.1016/j.clinbiomech.2018.09.009
23. Comenda M, Quental C, Folgado J et al (2019) Bone adaptation impact of stemless shoulder implants: a computational analysis. J Shoulder Elb Surg 28:1886–1896. https://doi.org/10.1016/j.jse.2019.03.007
24. Hassan CR, Qin YX, Komatsu DE, Uddin SMZ (2019) Utilization of finite element analysis for articular cartilage tissue

engineering. Materials (Basel) 12:1–11. https://doi.org/10.3390/ma12203331
25. Navacchia A, Hume DR, Rullkoetter PJ, Shelburne KB (2019) A computationally efficient strategy to estimate muscle forces in a finite element musculoskeletal model of the lower limb. J Biomech 14:94–102. https://doi.org/10.1016/j.jbiomech.2018.12.020.A
26. Taylor JB, Westbrook AE, Head PL et al (2020) The single-leg vertical hop provides unique asymmetry information in individuals after anterior cruciate ligament reconstruction. Clin Biomech. https://doi.org/10.1016/j.clinbiomech.2020.105107
27. Blache Y, Creveaux T, Dumas R et al (2017) Glenohumeral contact force during flat and topspin tennis forehand drives. Sport Biomech 16:127–142. https://doi.org/10.1080/14763141.2016.1216585
28. Safaeepour Z, Esteki A, Ghomshe FT et al (2014) Quantitative analysis of human ankle characteristics at different gait phases and speeds for utilizing in ankle-foot prosthetic design. Biomed Eng Online 13:19. https://doi.org/10.1186/1475-925X-13-19
29. McDonald AC, Mulla DM, Keir PJ (2019) Muscular and kinematic adaptations to fatiguing repetitive upper extremity work. Appl Ergon 75:250–256. https://doi.org/10.1016/j.apergo.2018.11.001
30. Morooka T, Nakayama H, Okuno M et al (2017) Effect of injury prevention training program on kinematics of drop jump tasks: evaluation with landing error scoring system and three-dimensional kinematic analysis. Arthrosc J Arthrosc Relat Surg 33:e124. https://doi.org/10.1016/j.arthro.2017.08.145
31. Seminati E, Marzari A, Vacondio O, Enrico M (2014) Shoulder injury prevention in volleyball: performance and kinematics analysis of alternative spike techniques. Br J Sport Med 48:659–660
32. Safaeepour Z, Esteki A, Ghomshe FT et al (2014) Quantitative analysis of human ankle characteristics at different gait phases and speeds for utilizing in ankle-foot prosthetic design. Biomed Eng Online 13:1–8. https://doi.org/10.1186/1475-925X-13-19
33. von Lieres und Wilkau HC, Irwin G, Bezodis NE et al (2020) Phase analysis in maximal sprinting: an investigation of step-to-step technical changes between the initial acceleration, transition and maximal velocity phases. Sport Biomech 19:141–156. https://doi.org/10.1080/14763141.2018.1473479
34. Genevois C, Reid M, Creveaux T, Rogowski I (2020) Kinematic differences in upper limb joints between flat and topspin forehand drives in competitive male tennis players. Sport Biomech 19:212–226. https://doi.org/10.1080/14763141.2018.1461915
35. Dallas G, Theodorou AS (2020) The influence of a hurdle target point on the kinematics of the handspring vault approach run during training. Sport Biomech 19:467–482. https://doi.org/10.1080/14763141.2018.1497196
36. Ezati M, Ghannadi B, McPhee J (2019) A review of simulation methods for human movement dynamics with emphasis on gait. Multibody Syst Dyn 47:265–292. https://doi.org/10.1007/s11044-019-09685-1
37. Ackermann M, van den Bogert AJ (2010) Optimality principles for model-based prediction of human gait. J Biomech 43:1055–1060. https://doi.org/10.1016/j.jbiomech.2009.12.012
38. Hof AL, Otten E (2005) Assessment of two-dimensional induced accelerations from measured kinematic and kinetic data. Gait Posture 22:182–188. https://doi.org/10.1016/j.gaitpost.2004.08.007
39. Millard M, Emonds AL, Harant M, Mombaur K (2019) A reduced muscle model and planar musculoskeletal model fit for the simulation of whole-body movements. J Biomech 89:11–20. https://doi.org/10.1016/j.jbiomech.2019.04.004
40. Anderson FC, Pandy MG (2003) Individual muscle contributions to support in normal walking. Gait Posture 17:159–169. https://doi.org/10.1016/S0966-6362(02)00073-5
41. Moissenet F, Chèze L, Dumas R (2014) A 3D lower limb musculoskeletal model for simultaneous estimation of musculo-tendon, joint contact, ligament and bone forces during gait. J Biomech 47:50–58. https://doi.org/10.1016/j.jbiomech.2013.10.015
42. Pereira AF, Silva MT, Martins JM, Carvalho M De (2010) Development of a hill-type muscle model with fatigue for the calculation of the redundant muscle forces using multibody dynamics. In:1st Jt Int Conf Multibody Syst Dyn
43. Dumas R, Barré A, Moissenet F, Aissaoui R (2019) Can a reduction approach predict reliable joint contact and musculo-tendon forces? J Biomech 95:109329. https://doi.org/10.1016/j.jbiomech.2019.109329
44. Rabuffetti M, Crenna P (2004) A modular protocol for the analysis of movement in children. Gait Posture 20:S77–S78. https://doi.org/10.1016/j.gaitpost.2004.06.001
45. Sholukha V, Bonnechere B, Salvia P et al (2013) Model-based approach for human kinematics reconstruction from markerless and marker-based motion analysis systems. J Biomech 46:2363–2371. https://doi.org/10.1016/j.jbiomech.2013.07.037
46. Süptitz F, Catalá MM, Brüggemann G-PP et al (2013) Dynamic stability control during perturbed walking can be assessed by a reduced kinematic model across the adult female lifespan. Hum Mov Sci 32:1404–1414. https://doi.org/10.1016/j.humov.2013.07.008
47. Hingtgen B, Mcguire JR, Wang M, Harris GF (2006) An upper extremity kinematic model for evaluation of hemiparetic stroke. J Biomech 39:681–688. https://doi.org/10.1016/j.jbiomech.2005.01.008
48. Rettig O, Fradet L, Kasten P et al (2009) A new kinematic model of the upper extremity based on functional joint parameter determination for shoulder and elbow. Gait Posture 30:469–476. https://doi.org/10.1016/j.gaitpost.2009.07.111
49. Williams S, Schmidt R, Disselhorst-Klug C, Rau G (2006) An upper body model for the kinematical analysis of the joint chain of the human arm. J Biomech 39:2419–2429. https://doi.org/10.1016/j.jbiomech.2005.07.023
50. Quental C, Folgado J, Ambrósio J, Monteiro J (2012) A multibody biomechanical model of the upper limb including the shoulder girdle. Multibody Syst Dyn 28:83–108. https://doi.org/10.1007/s11044-011-9297-0
51. Quental C, Folgado J, Ambrósio J, Monteiro J (2013) Multibody system of the upper limb including a reverse shoulder prosthesis. J Biomech Eng 135:1–11. https://doi.org/10.1115/1.4025325
52. Kadaba MP, Ramakrishnan HK, Wootten ME (1990) Measurement of lower extremity kinematics during level walking. J Orthop Res 8:383–392. https://doi.org/10.1002/jor.1100080310
53. Leardini A, Benedetti MG, Berti L et al (2007) Rear-foot, mid-foot and fore-foot motion during the stance phase of gait. Gait Posture 25:453–462. https://doi.org/10.1016/j.gaitpost.2006.05.017
54. Nadeau S, McFadyen B, Malouin F (2003) Frontal and sagittal plane analyses of the stair climbing task in healthy adults aged over 40 years: what are the challenges compared to level walking? Clin Biomech 18:950–959. https://doi.org/10.1016/S0268-0033(03)00179-7
55. Nikooyan AA, Veeger HEJJ, Westerhoff P et al (2012) An EMG-driven musculoskeletal model of the shoulder. Hum Mov Sci 31:429–447. https://doi.org/10.1016/j.humov.2011.08.006
56. De Mits S, Segers V, Woodburn J et al (2012) A clinically applicable six-segmented foot model. J Orthop Res 30:655–661. https://doi.org/10.1002/jor.21570
57. Saraswat P, MacWilliams B, Davis RB, D'Astous JL (2013) A multi-segment foot model based on anatomically registered technical coordinate systems: method repeatability and sensitivity in pediatric planovalgus feet. Gait Posture 37:121–125. https://doi.org/10.1016/j.gaitpost.2012.06.023

58. Seo SG, Lee DY, Moon HJ et al (2014) Repeatability of a multi-segment foot model with a 15-marker set in healthy adults. J Foot Ankle Res 7:24. https://doi.org/10.1186/1757-1146-7-24
59. Malaquias TM, Gonçalves SB, da Silva MT (2015) A three-dimensional multibody model of the human ankle-foot complex. Mech Mach Sci 24:445–453. https://doi.org/10.1007/978-3-319-09411-3_47
60. Andersen MS, Benoit DL, Damsgaard M et al (2010) Do kinematic models reduce the effects of soft tissue artefacts in skin marker-based motion analysis? An in vivo study of knee kinematics. J Biomech 43:268–273. https://doi.org/10.1016/j.jbiomech.2009.08.034
61. Stagni R, Fantozzi S, Cappello A, Leardini A (2005) Quantification of soft tissue artefact in motion analysis by combining 3D fluoroscopy and stereophotogrammetry: a study on two subjects. Clin Biomech (Bristol, Avon) 20:320–329. https://doi.org/10.1016/j.clinbiomech.2004.11.012
62. Fuller J, Liu L-J, Murphy MC, Mann RW (1997) A comparison of lower-extremity skeletal kinematics measured using skin- and pin-mounted markers. Hum Mov Sci 16:219–242. https://doi.org/10.1016/S0167-9457(96)00053-X
63. Holden JP, Orsini JA, Siegel KL et al (1997) Surface movement errors in shank kinematics and knee kinetics during gait. Gait Posture 5:217–227
64. Andersen MS, Damsgaard M, MacWilliams B, Rasmussen J (2010) A computationally efficient optimisation-based method for parameter identification of kinematically determinate and over-determinate biomechanical systems. Comput Methods Biomech Biomed Engin 13:171–183. https://doi.org/10.1080/10255840903067080
65. Begon M, Andersen MS, Dumas R (2018) Multibody kinematics optimization for the estimation of upper and lower limb human joint kinematics: a systematized methodological review. J Biomech Eng. https://doi.org/10.1115/1.4038741
66. Al Nazer R, Rantalainen T, Heinonen A et al (2008) Flexible multibody simulation approach in the analysis of tibial strain during walking. J Biomech 41:1036–1043. https://doi.org/10.1016/j.jbiomech.2007.12.002
67. Rao G, Amarantini D, Berton E, Favier D (2006) Influence of body segments' parameters estimation models on inverse dynamics solutions during gait. J Biomech 39:1531–1536. https://doi.org/10.1016/j.jbiomech.2005.04.014
68. Dumas R, Wojtusch J (2017) Handbook of human motion. Springer, New York
69. Dumas R, Chèze L, Verriest J-PP (2007) Adjustments to McConville et al. and Young et al. body segment inertial parameters. J Biomech 40:543–553. https://doi.org/10.1016/j.jbiomech.2006.02.013
70. Silva MPT, Ambrósio JAC (2004) Sensitivity of the results produced by the inverse dynamic analysis of a human stride to perturbed input data. Gait Posture 19:35–49. https://doi.org/10.1016/S0966-6362(03)00013-4
71. Pàmies-Vilà R, Font-Llagunes JM, Cuadrado J, Alonso FJ (2012) Analysis of different uncertainties in the inverse dynamic analysis of human gait. Mech Mach Theory 58:153–164. https://doi.org/10.1016/j.mechmachtheory.2012.07.010
72. Borucka A, Ciszkiewicz A (2019) A planar model of an ankle joint with optimized material parameters and Hertzian contact pairs. Materials (Basel) 12:1–15. https://doi.org/10.3390/ma12162621
73. Yamaguchi GT, Zajac FE (1989) A planar model of the knee joint to characterize the knee extensor mechanism. J Biomech 22:1–10. https://doi.org/10.1016/0021-9290(89)90179-6
74. Peng Y, Zhang Z, Gao Y et al (2018) Concurrent prediction of ground reaction forces and moments and tibiofemoral contact forces during walking using musculoskeletal modelling. Med Eng Phys 52:31–40. https://doi.org/10.1016/j.medengphy.2017.11.008
75. Quental C, Azevedo M, Ambrósio J et al (2018) Influence of the musculotendon dynamics on the muscle force-sharing problem of the shoulder—a fully inverse dynamics approach. J Biomech Eng. https://doi.org/10.1115/1.4039675
76. Rodrigues da Silva M, Marques F, Tavares da Silva M, Flores P (2022) Modelling spherical joints in multibody systems. Mech Mach Sci 110MMS:85–93. https://doi.org/10.1007/978-3-030-88751-3_9
77. Marques F, Roupa I, Silva MT et al (2021) Examination and comparison of different methods to model closed loop kinematic chains using Lagrangian formulation with cut joint, clearance joint constraint and elastic joint approaches. Mech Mach Theory 160:104294. https://doi.org/10.1016/j.mechmachtheory.2021.104294
78. Camomilla V, Cereatti A, Vannozzi G, Cappozzo A (2006) An optimized protocol for hip joint centre determination using the functional method. J Biomech 39:1096–1106. https://doi.org/10.1016/j.jbiomech.2005.02.008
79. Stagni R, Leardini A, Cappozzo A et al (2000) Effects of hip joint centre mislocation on gait analysis results. J Biomech 33:1479–1487. https://doi.org/10.1016/S0021-9290(00)00093-2
80. Lamb PF, Bartlett RM (2018) Assessing movement coordination. Biomech Eval Mov Sport Exerc. https://doi.org/10.4324/9780203095546-3
81. Zatsiorsky V, Prilutsky B (2012) Biomechanics of skeletal muscles, 1st edn. Human Kinetics, Champaign
82. Fukunaga T, Kawakami Y, Kubo K, Kanehisa H (2002) Muscle and tendon interaction during human movements. Exerc Sport Sci Rev 30:106–110. https://doi.org/10.1097/00003677-200207000-00003
83. Huxley AF (1957) Muscle structure and theories of contraction. Prog Biophys Biophys Chem 7:255–318. https://doi.org/10.1016/s0096-4174(18)30128-8
84. Winters JM, Stark L (1987) Muscle models: What is gained and what is lost by varying model complexity. Biol Cybern 55:403–420. https://doi.org/10.1007/BF00318375
85. van Soest AJ, Casius LJR, Lemaire KK (2019) Huxley-type cross-bridge models in largeish-scale musculoskeletal models; an evaluation of computational cost. J Biomech 83:43–48. https://doi.org/10.1016/j.jbiomech.2018.11.021
86. Bhargava LJ, Pandy MG, Anderson FC (2004) A phenomenological model for estimating metabolic energy consumption in muscle contraction. J Biomech 37:81–88. https://doi.org/10.1016/S0021-9290(03)00239-2
87. Zajac FE (1989) Muscle and tendon: properties, models, scaling, and application to biomechanics and motor control. Crit Rev Biomed Eng 17:359–411
88. Zahalak GI, Ma SP (1990) Muscle activation and contraction: Constitutive relations based directly on cross-bridge kinetics. J Biomech Eng 112:52–62. https://doi.org/10.1115/1.2891126
89. Van Den Bogert AJ, Gerritsen KGM, Cole GK (1998) Human muscle modelling from a user's perspective. J Electromyogr Kinesiol 8:119–124. https://doi.org/10.1016/S1050-6411(97)00028-X
90. Bujalski P, Martins J, Stirling L (2018) A Monte Carlo analysis of muscle force estimation sensitivity to muscle-tendon properties using a Hill-based muscle model. J Biomech 79:67–77. https://doi.org/10.1016/j.jbiomech.2018.07.045
91. Delp SL, Loan JP, Hoy MG et al (1990) An interactive graphics-based model of the lower extremity to study orthopaedic surgical procedures. IEEE Trans Biomed Eng 37:757–767. https://doi.org/10.1109/10.102791
92. Blemker SS, Asakawa DS, Gold GE, Delp SL (2007) Image-based musculoskeletal modeling: applications, advances, and

future opportunities. J Magn Reson Imaging 25:441–451. https://doi.org/10.1002/jmri.20805
93. Arnold AS, Salinas S, Asakawa DJ, Delp SL (2000) Accuracy of muscle moment arms estimated from MRI-based musculoskeletal models of the lower extremity. Comput Aided Surg 5:108–119. https://doi.org/10.1002/1097-0150(2000)5:2%3c108::AID-IGS5%3e3.0.CO;2-2
94. Manal K, Buchanan TS (2003) A one-parameter neural activation to muscle activation model: estimating isometric joint moments from electromyograms. J Biomech 36:1197–1202. https://doi.org/10.1016/S0021-9290(03)00152-0
95. Murray WM, Buchanan TS, Delp SL (2000) The isometric functional capacity of muscles that cross the elbow. J Biomech 33:943–952. https://doi.org/10.1016/S0021-9290(00)00051-8
96. Ackland DC, Lin YC, Pandy MG (2012) Sensitivity of model predictions of muscle function to changes in moment arms and muscle-tendon properties: a Monte-Carlo analysis. J Biomech 45:1463–1471. https://doi.org/10.1016/j.jbiomech.2012.02.023
97. Xiao M, Higginson J (2010) Sensitivity of estimated muscle force in forward simulation of normal walking. J Appl Biomech 26:142–149. https://doi.org/10.1123/jab.26.2.142
98. Bayer A, Schmitt S, Günther M, Haeufle DFB (2017) The influence of biophysical muscle properties on simulating fast human arm movements. Comput Methods Biomech Biomed Engin 20:803–821. https://doi.org/10.1080/10255842.2017.1293663
99. Bosmans L, Valente G, Wesseling M et al (2015) Sensitivity of predicted muscle forces during gait to anatomical variability in musculotendon geometry. J Biomech 48:2116–2123. https://doi.org/10.1016/j.jbiomech.2015.02.052
100. Arnold EM, Hamner SR, Seth A et al (2013) How muscle fiber lengths and velocities affect muscle force generation as humans walk and run at different speeds. J Exp Biol 216:2150–2160. https://doi.org/10.1242/jeb.075697
101. Carbone V, van der Krogt MM, Koopman HFJM, Verdonschot N (2012) Sensitivity of subject-specific models to errors in musculo-skeletal geometry. J Biomech 45:2476–2480. https://doi.org/10.1016/j.jbiomech.2012.06.026
102. Wesseling M, De Groote F, Meyer C et al (2016) Subject-specific musculoskeletal modelling in patients before and after total hip arthroplasty*. Comput Methods Biomech Biomed Engin 19:1683–1691. https://doi.org/10.1080/10255842.2016.1181174
103. Hainisch R, Gfoehler M, Zubayer-Ul-Karim M, Pandy MG (2012) Method for determining musculotendon parameters in subject-specific musculoskeletal models of children developed from MRI data. Multibody Syst Dyn 28:143–156. https://doi.org/10.1007/s11044-011-9289-0
104. Winby CR, Lloyd DG, Kirk TB (2008) Evaluation of different analytical methods for subject-specific scaling of musculotendon parameters. J Biomech 41:1682–1688. https://doi.org/10.1016/j.jbiomech.2008.03.008
105. Garner BA, Pandy MG (2003) Estimation of musculotendon properties in the human upper limb. Ann Biomed Eng 31:207–220. https://doi.org/10.1114/1.1540105
106. Lloyd DG, Besier TF (2003) An EMG-driven musculoskeletal model to estimate muscle forces and knee joint moments in vivo. J Biomech 36:765–776. https://doi.org/10.1016/s0021-9290(03)00010-1
107. Pizzolato C, Lloyd DG, Sartori M et al (2015) CEINMS: A toolbox to investigate the influence of different neural control solutions on the prediction of muscle excitation and joint moments during dynamic motor tasks. J Biomech 48:3929–3936. https://doi.org/10.1016/j.jbiomech.2015.09.021
108. Yamaguchi GT (2001) Dynamic modeling of musculoskeletal motion a vectorized approach in three dimensions. Springer, New York
109. Carbone V, Fluit R, Pellikaan P et al (2015) TLEM 2.0—a comprehensive musculoskeletal geometry dataset for subject-specific modeling of lower extremity. J Biomech 48:734–741. https://doi.org/10.1016/j.jbiomech.2014.12.034
110. Garner BA, Pandy MG (2000) The obstacle-set method for representing muscle paths in musculoskeletal models. Comput Methods Biomech Biomed Eng 3:1–30. https://doi.org/10.1080/10255840008915251
111. Gao F, Damsgaard M, Rasmussen J, Tørholm Christensen S (2002) Computational method for muscle-path representation in musculoskeletal models. Biol Cybern 87:199–210. https://doi.org/10.1007/s00422-002-0326-1
112. Stavness I, Sherman M, Delp S (2012) A general approach to muscle wrapping over multiple surfaces. Am Soc Biomech Conf
113. Scholz A, Sherman M, Stavness I et al (2016) A fast multi-obstacle muscle wrapping method using natural geodesic variations. Multibody Syst Dyn 36:195–219. https://doi.org/10.1007/s11044-015-9451-1
114. Hammer M, Günther M, Haeufle DFB, Schmitt S (2019) Tailoring anatomical muscle paths: a sheath-like solution for muscle routing in musculoskeletal computer models. Math Biosci 311:68–81. https://doi.org/10.1016/j.mbs.2019.02.004
115. Crowninshield R, Brand R (1981) A physiologically based criterion of muscle force prediction in locomotion. J Biomech 14:793–801
116. Wen J, Raison M, Achiche S (2018) Using a cost function based on kinematics and electromyographic data to quantify muscle forces. J Biomech 80:151–158. https://doi.org/10.1016/j.jbiomech.2018.09.002
117. Zhang X, Chan FK, Parthasarathy T, Gazzola M (2019) Modeling and simulation of complex dynamic musculoskeletal architectures. Nat Commun 10:1–12. https://doi.org/10.1038/s41467-019-12759-5
118. Bueno DR, Montano L (2017) Neuromusculoskeletal model self-calibration for on-line sequential bayesian moment estimation. J Neural Eng 14:1–31
119. Geyer H, Seyfarth A, Blickhan R (2003) Positive force feedback in bouncing gaits? Proc R Soc B Biol Sci 270:2173–2183. https://doi.org/10.1098/rspb.2003.2454
120. Zajac FE, Neptune RR, Kautz SA (2003) Biomechanics and muscle coordination of human walking: Part II: lessons from dynamical simulations and clinical implications. Gait Posture 17:1–17. https://doi.org/10.1016/S0966-6362(02)00069-3
121. Van Soest AJ, Rozendaal LA (2008) The inverted pendulum model of bipedal standing cannot be stabilized through direct feedback of force and contractile element length and velocity at realistic series elastic element stiffness. Biol Cybern 99:29–41. https://doi.org/10.1007/s00422-008-0240-2
122. Haeufle DFB, Grimmer S, Kalveram KT, Seyfarth A (2012) Integration of intrinsic muscle properties, feed-forward and feedback signals for generating and stabilizing hopping. J R Soc Interface 9:1458–1469. https://doi.org/10.1098/rsif.2011.0694
123. Gonçalves J, Ambrósio J (2002) Advanced modelling of flexible multibody systems using virtual bodies. Comput Assist Mech Eng Sci 9:373–390
124. Geier A, Kebbach M, Soodmand E et al (2019) Neuro-musculoskeletal flexible multibody simulation yields a framework for efficient bone failure risk assessment. Sci Rep 9:1–15. https://doi.org/10.1038/s41598-019-43028-6
125. Amirouche FML, Jia T, Sitki KI (1988) A recursive householder transformation for complex dynamical systems with constraints. J Appl Mech 55:729–734
126. Blajer W (2001) A geometrical interpretation and uniform matrix formulation of multibody system dynamics. ZAMM Zeitschrift fur Angew Math und Mech 81:247–259. https://doi.org/10.

1002/1521-4001(200104)81:4%3c247::AID-ZAMM247%3e3.0.CO;2-D
127. Kim S, Vanderploeg MJ (1986) QR decomposition for state space representation of constrained mechanical dynamic systems. ASME J Mech Transm Autom Des 108:183–188. https://doi.org/10.1115/1.3260800
128. Jalon G, Bayo E (1993) Kinematic and dynamic simulation of multibody systems: the real-time challenge. Springer, New York
129. Wehage RA, Haug EJ (1982) Generalized coordinate partitioning for dimension reduction in analysis of constrained. J Mech Des 104:247–255
130. Camomilla V, Cereatti A, Cutti AG et al (2017) Methodological factors affecting joint moments estimation in clinical gait analysis: a systematic review. Biomed Eng Online 16:1–27. https://doi.org/10.1186/s12938-017-0396-x
131. Amarya S, Kalyani S, Manisha S (2018) Ageing process and physiological changes. In: Grazia D'Onofrio AG (ed) Gerontology. IntechOpen, London, pp 3–24
132. Pain MTG, Challis JH (2001) High resolution determination of body segment inertial parameters and their variation due to soft tissue motion. J Appl Biomech 17:326–334. https://doi.org/10.1123/jab.17.4.326
133. Cizgin P, Kornfeind P, Haßmann M, Baca A (2017) Advancements of methods for fast and accurate estimation of human body segment parameter values. In: icSPORTS 2017—Proc 5th Int Congr Sport Sci Res Technol Support 69–74. https://doi.org/10.5220/0006439400690074
134. Yeadon MR, Morlock M (1989) The appropriate use of regression equations for the estimation of segmental inertia parameters. J Biomech 22:683–689
135. Winter D (2005) Biomechanics and motor control of human movement, third. Waterloo, Ontario
136. Dempster (1955) Space requirements of the seated operator. WADC Tech. Rep. TR-55-159, Wright Air Dev. Center, Wright–Patterson Air Force Base, Dayton, Ohio. 254
137. De Leva P (1996) Adjustments to Zatsiorsky–Seluyanov's segment inertia parameters. J Biomech 29:1223–1230. https://doi.org/10.1016/0021-9290(95)00178-6
138. Zatsiorsky V, VN, Seluyanov V, Chugunova L (1990) Methods of determining mass-inertial characteristics of human body segments. In: Contemporary problems of biomechanics. CRC Press, Massachusetts
139. Clauser CE, McConville JT, Young JW (1969) Weight, Volume, and Center of Mass of Segments of the Human Body. USAF, Tech. Rep. AMRL-TR-69-70, Aerosp. Med. Res. Lab. Wright–Patterson Air Force Base, Dayton, Ohio. 106, Wright-Patterson Air Force Base, Ohio
140. Hatze H (1980) A mathematical model for the computational determination of parameter values of anthropomorphic segments. J Biomech 13:833–843. https://doi.org/10.1016/0021-9290(80)90171-2
141. Baca A (1996) Precise determination of anthropometric dimensions by means of image processing methods for estimating human body segment parameter values. J Biomech 29:563–567. https://doi.org/10.1016/0021-9290(95)00033-X
142. Ori S, Zvi L (1993) A video-based System for the estimation of the inertial propoerties of body segments. J Biomech 26:1011–1016
143. Clarkson S, Choppin S, Hart J, et al (2012) Calculating Body Segment Inertia Parameters from a Single Rapid Scan Using the Microsoft Kinect. In: Proceedings of the 3rd International Conference on 3D Body Scanning Technologies, Lugano, Switzerland, 16–17 October 2012. Hometrica Consulting - Dr. Nicola D'Apuzzo, Ascona, Switzerland, pp 153–163
144. Peyer KE, Morris M, Sellers WI (2015) Subject-specific body segment parameter estimation using 3D photogrammetry with multiple cameras. PeerJ. https://doi.org/10.7717/peerj.831
145. Sheets AL, Corazza S, Andriacchi TP (2010) An automated image-based method of 3D subject-specific body segment parameter estimation for kinetic analyses of rapid movements. J Biomech Eng 132:1–10. https://doi.org/10.1115/1.4000155
146. Venture G, Ayusawa K, Nakamura Y (2008) Motion capture based identification of the human body inertial parameters. In: Proc 30th Annu Int Conf IEEE Eng Med Biol Soc EMBS'08 - "Personalized Healthc through Technol, pp 4575–4578. https://doi.org/10.1109/iembs.2008.4650231
147. Robert T, Leborgne P, Abid M et al (2017) Whole body segment inertia parameters estimation from movement and ground reaction forces: a feasibility study. Comput Methods Biomech Biomed Engin 20:175–176. https://doi.org/10.1080/10255842.2017.1382919
148. Noamani A, Vette AH, Preuss R et al (2018) Optimal estimation of anthropometric parameters for quantifying multisegment trunk kinetics. J Biomech Eng 140:101003
149. Fregly BJ, Reinbolt JA (2004) Estimation of body segment parameters from three-dimensional gait data using optimization. In: International Symposium on 3D Analysis of Human Movement, pp 13–16
150. Vaughan CL, Andrews JG, Hay JG (1982) Selection of body segment parameters by optimization methods. J Biomech Eng 104:38–44. https://doi.org/10.1115/1.3138301
151. Venture G, Ayusawa K, Nakamura Y (2009) Real-time identification and visualization of human segment parameters. In: Proc 31st Annu Int Conf IEEE Eng Med Biol Soc Eng Futur Biomed EMBC 2009 3983–3986. https://doi.org/10.1109/IEMBS.2009.5333619
152. Young J, Chandler RF, Snow CC, et al (1983) Anthropometric and mass distribution characteristics of the adults female. Tech. Rep. FA-AM-83-16, FAA Civ. Aeromed. Institute, Oklaoma City, Oklaoma. 109, FAA Civil Aeromedical Institute, Oklahoma
153. Jovic J, Escande A, Ayusawa K et al (2016) Humanoid and human inertia parameter identification using hierarchical optimization. IEEE Trans Robot 32:726–735. https://doi.org/10.1109/TRO.2016.2558190
154. Escande A, Mansard N, Wieber PB (2014) Hierarchical quadratic programming: fast online humanoid-robot motion generation. Int J Rob Res 33:1006–1028. https://doi.org/10.1177/0278364914521306
155. Hansen C, Venture G, Rezzoug N et al (2014) An individual and dynamic body segment inertial parameter validation method using ground reaction forces. J Biomech 47:1577–1581. https://doi.org/10.1016/j.jbiomech.2014.03.004
156. Martin PE, Mungiole M, Marzke MW, Longhill JM (1989) The use of magnetic resonance imaging for measuring segment inertial properties. J Biomech 22:367–376
157. Mungiole M, Martin PE (1990) Estimating segment inertial properties: comparison of magnetic resonance imaging with existing methods. J Biomech 23:1039–1046. https://doi.org/10.1016/0021-9290(90)90319-X
158. Pearsall DJ, Reid JG, Livingston L (1996) Segmental inertial parameters of the human trunk as determined from computed tomography. Ann Biomed Eng 24:198–210. https://doi.org/10.1007/BF02667349
159. Bauer JJ, Pavol MJ, Snow CM, Hayes WC (2007) MRI-derived body segment parameters of children differ from age-based estimates derived using photogrammetry. J Biomech 40:2904–2910. https://doi.org/10.1016/j.jbiomech.2007.03.006
160. Pearsall JGR Comparison of CT and MRI estimates of inertial properties of the human trunk. p 621

161. Lee MK, Le NS, Fang AC, Koh MTH (2009) Measurement of body segment parameters using dual energy X-ray absorptiometry and three-dimensional geometry: an application in gait analysis. J Biomech 42:217–222. https://doi.org/10.1016/j.jbiomech.2008.10.036
162. Wicke J, Dumas GA, Costigan PA (2009) A comparison between a new model and current models for estimating trunk segment inertial parameters. J Biomech 42:55–60. https://doi.org/10.1016/j.jbiomech.2008.10.003
163. Rossi M, Lyttle A, El-Sallam A et al (2013) Body segment inertial parameters of elite swimmers using DXA and indirect methods. J Sport Sci Med 12:761–775
164. Schneider K, Zernicke RF (1992) Mass, center of mass, and moment of inertia estimates for infant limb segments. J Biomech 25:145–148
165. Sun H, Jensen R (1994) Body segment growth during infancy. J Biomech 27:265–275
166. Jensen RK (1989) Changes in segment inertia proportions between 4 and 20 years. J Biomech 22:529–536. https://doi.org/10.1016/0021-9290(89)90004-3
167. Yokoi T, Shibukawa K, Ae M et al (1986) Body segment parameters of Japanese children. Jpn J Phys Educ 31:53–66
168. Jensen RK, Nassas G (1988) Growth of segment principal moments of inertia between four and twenty years. Med Sci Sport Exerc 20:594–604
169. Chester VL, Jensen RK (2005) Changes in infant segment inertias during the first three months of independent walking. Dyn Med 4:9. https://doi.org/10.1186/1476-5918-4-9
170. van Dam M, Hallemans A, Aerts P (2009) Growth of segment parameters and a morphological classification for children between 15 and 36 months. J Anat 214:79–90. https://doi.org/10.1111/j.1469-7580.2008.01016.x
171. Ackland TR, Blanksby BA, Bloomfield J (1988) Inertial characteristics of adolescent male body segments. J Biomech 21:319–327. https://doi.org/10.1016/0021-9290(88)90261-8
172. Durkin JL (2003) Analysis of body segment parameter differences between four human populations and the estimation errors of four popular mathematical models. J Biomech Eng 125:515. https://doi.org/10.1115/1.1590359
173. Chandler RF, Clauser CEE, McConville JTT, et al (1975) Investigation of inertial properties of the human body. Natl. Highw. Traffic Saf. Adm. Tech. Rep. AMRL-74-137, Aerosp. Med. Res. Lab. Wright–Patterson Air Force Base, Dayton, Ohio. 162
174. McConville JT, Churchill T, Clauser CE, Cuzzi J (1980) Anthropometric Relationships of Body and Body Segment Moments of Inertia. Tech. Rep. AFAMRL-TR-80-119, Aerosp. Med. Res. Lab. Wright–Patterson Air Force Base, Dayton, Ohio. 109, Wright-Patterson AFB
175. Hinrichs RN (1985) Regression equations to predict segmental moments of inertia from anthropometric measurements: an extension of the data of Chandler et al. (1975). J Biomech 18:621–624. https://doi.org/10.1016/0021-9290(85)90016-8
176. Hinrichs RN (1990) Adjustments to the segment center of mass proportions of Clauser et al. (1969). J Biomech 23:949–951
177. Pearsall DJ, Reid JG, Ross R (1994) Inertial properties of the human trunk of males determined from magnetic resonance imaging. Ann Biomed Eng 22:692–706. https://doi.org/10.1007/BF02368294
178. Kingma I, Toussaint HM, De LMP et al (1996) Segment inertial parameter evaluation in two anthropometric models by application of a dynamic linked segment model. J Biomech 29:693–704
179. Cheng CK, Chen HH, Chen CS et al (2000) Segment inertial properties of Chinese adults determined from magnetic resonance imaging. Clin Biomech (Bristol, Avon) 15:559–566
180. Pavol MJ, Owings TM, Grabiner MD (2002) Body segment inertial parameter estimation for the general population of older adults. J Biomech 35:707–712
181. Ganley KJ, Powers CM (2004) Determination of lower extremity anthropometric parameters using dual energy X-ray absorptiometry: the influence on net joint moments during gait. Clin Biomech 19:50–56. https://doi.org/10.1016/j.clinbiomech.2003.08.002
182. Nikolova GS, Toshev YE (2007) Estimation of male and female body segment parameters of the Bulgarian population using a 16-segmental mathematical model. J Biomech 40:3700–3707. https://doi.org/10.1016/j.jbiomech.2007.06.016
183. Challis JH, Winter SL, Kuperavage AJ (2012) Comparison of male and female lower limb segment inertial properties. J Biomech 45:2690–2692. https://doi.org/10.1016/j.jbiomech.2012.07.019
184. Muri J, Winter SL, Challis JH (2007) Changes in segmental inertial properties with age. J Biomech 41:1809–1812. https://doi.org/10.1016/j.jbiomech.2008.03.002
185. Clarys JP, Marfell Jones MJ (1986) Anatomical segmentation in humans and the prediction of segmental masses from l ntrasegmental anthropometry. Hum Biol An Int Rec Res 58:771–782
186. Jensen RK, Fletcher P (1994) Distribution of mass to the segments of elderly. J Biomech 27:89–96
187. Ho Hoang KL, Mombaur K (2015) Adjustments to de Levaanthropometric regression data for the changes in body proportions in elderly humans. J Biomech 48:3732–3736. https://doi.org/10.1016/j.jbiomech.2015.08.018
188. Bernstein N (1967) The co-ordination and regulation of movements. Pergamon Press Ltd., Oxford
189. Duprey S, Naaim A, Moissenet F et al (2017) Kinematic models of the upper limb joints for multibody kinematics optimisation: An overview. J Biomech 62:87–94. https://doi.org/10.1016/j.jbiomech.2016.12.005
190. Asfour S, Eltoukhy M (2012) Development and validation of a three-dimensional biomechanical model of the lower extremity. INTECH 1:38. https://doi.org/10.1016/j.colsurfa.2011.12.014
191. Benedetti M, Manca M, Ferraresi G et al (2008) A new protocol for complete 3D kinematics analysis of the ankle foot complex in stroke patients. J Foot Ankle Res 1:1–2. https://doi.org/10.1186/1757-1146-1-s1-o30
192. Bolsterlee B, Veeger HEJ, van der Helm FCT (2014) Modelling clavicular and scapular kinematics: from measurement to simulation. Med Biol Eng Comput 52:283–291. https://doi.org/10.1007/s11517-013-1065-2
193. Kecskeméthy A, Weinberg A (2005) An improved elasto-kinematic model of the human forearm for biofidelic medical diagnosis. Multibody Syst Dyn 14:1–21. https://doi.org/10.1007/s11044-005-1756-z
194. Wilson DR, Feikes JD, Zavatsky AB, O'Connor JJ (2000) The components of passive knee movement are coupled to flexion angle. J Biomech 33:465–473. https://doi.org/10.1016/S0021-9290(99)00206-7
195. Feikes JD, O'Connor JJ, Zavatsky AB (2003) A constraint-based approach to modelling the mobility of the human knee joint. J Biomech 36:125–129. https://doi.org/10.1016/S0021-9290(02)00276-2
196. Leardini A, Stagni R, O'Connor JJ (2001) Mobility of the subtalar joint in the intact ankle complex. J Biomech 34:805–809. https://doi.org/10.1016/S0021-9290(01)00031-8
197. Leardini A, O'Connor JJ, Catani F, Giannini S (1999) Kinematics of the human ankle complex in passive flexion; a single degree of freedom system. J Biomech 32:111–118. https://doi.org/10.1016/S0021-9290(98)00157-2
198. Quental C, Folgado J, Ambrósio J, Monteiro J (2016) A new shoulder model with a biologically inspired glenohumeral joint.

Med Eng Phys 38:969–977. https://doi.org/10.1016/j.medengphy.2016.06.012
199. Leardini A, O'Connor JJ, Catani F, Giannini S (1999) A geometric model of the human ankle joint. J Biomech 32:585–591. https://doi.org/10.1016/S0021-9290(99)00022-6
200. O'Connor JJ, Shercliff TL, Biden E, Goodfellow JW (1989) The geometry of the knee in the sagittal plane. Proc Inst Mech Eng Part H J Eng Med 203:223–233. https://doi.org/10.1243/PIME_PROC_1989_203_043_01
201. Heller MO, König C, Graichen H et al (2007) A new model to predict in vivo human knee kinematics under physiological-like muscle activation. J Biomech. https://doi.org/10.1016/j.jbiomech.2007.03.005
202. Gregorio R, Parenti-Castelli V, O'Connor JJ, Leardini A (2007) Mathematical models of passive motion at the human ankle joint by equivalent spatial parallel mechanisms. Med Biol Eng Comput 45:305–313. https://doi.org/10.1007/s11517-007-0160-7
203. Barzan M, Modenese L, Carty CP et al (2019) Development and validation of subject-specific pediatric multibody knee kinematic models with ligamentous constraints. J Biomech 93:194–203. https://doi.org/10.1016/j.jbiomech.2019.07.001
204. Brito da Luz S, Modenese L, Sancisi N et al (2017) Feasibility of using MRIs to create subject-specific parallel-mechanism joint models. J Biomech 53:45–55. https://doi.org/10.1016/j.jbiomech.2016.12.018
205. Flores P, Ambrósio J, Pimenta Claro JC, Lankarani HM (2008) Lecture Notes in Applied and Computational Mechanics Volume 34 Series Editors Lecture Notes in Applied and Computational Mechanics
206. Terzini M, Zanetti EM, Audenino AL et al (2017) Multibody modelling of ligamentous and bony stabilizers in the human elbow. Muscles Ligaments Tendons J 7:493–502. https://doi.org/10.32098/mltj.04.2017.03
207. Dzialo CM, Pedersen PH, Simonsen CW et al (2018) Development and validation of a subject-specific moving-axis tibiofemoral joint model using MRI and EOS imaging during a quasi-static lunge. J Biomech 72:71–80. https://doi.org/10.1016/j.jbiomech.2018.02.032
208. Vicon® (2017) Plug-in gait reference guide. Vicon Motion Systems Ltd, Oxford p, p 164
209. Rajagopal A, Dembia CL, DeMers MS et al (2016) Full-body musculoskeletal model for muscle-driven simulation of human gait. IEEE Trans Biomed Eng 63:2068–2079. https://doi.org/10.1109/TBME.2016.2586891
210. Favier CD, Finnegan ME, Quest RA et al (2021) An open-source musculoskeletal model of the lumbar spine and lower limbs: a validation for movements of the lumbar spine. Comput Methods Biomech Biomed Engin 24:1310–1325. https://doi.org/10.1080/10255842.2021.1886284
211. Walker PS, Rovick JS, Robertson DD (1988) The effects of knee brace hinge design and placement on joint mechanics. J Biomech 21:965–974. https://doi.org/10.1016/0021-9290(88)90135-2
212. Arnold EM, Ward SR, Lieber RL, Delp SL (2010) A model of the lower limb for analysis of human movement. Ann Biomed Eng 38:269–279. https://doi.org/10.1007/s10439-009-9852-5
213. Malaquias TM, Silveira C, Aerts W et al (2017) Extended foot-ankle musculoskeletal models for application in movement analysis. Comput Methods Biomech Biomed Engin 20:153–159. https://doi.org/10.1080/10255842.2016.1206533
214. Isman RE, Inman VT (1969) Anthropometric studies of the human foot and ankle. San Francisco
215. Anderson FC, Pandy MG (1999) A dynamic optimization solution for vertical jumping in three dimensions. Comput Methods Biomech Biomed Engin 2:201–231. https://doi.org/10.1080/10255849908907988
216. Leardini A, Caravaggi P, Theologis T, Stebbins J (2019) Multi-segment foot models and their use in clinical populations. Gait Posture 69:50–59. https://doi.org/10.1016/j.gaitpost.2019.01.022
217. Deschamps K, Staes F, Roosen P et al (2011) Body of evidence supporting the clinical use of 3D multisegment foot models: a systematic review. Gait Posture 33:338–349. https://doi.org/10.1016/j.gaitpost.2010.12.018
218. Jameson E, Davids JR, Christopher L et al (2007) The design, development, and initial evaluation of a multisegment foot model for routine clinical gait analysis. Foot Ankle Motion Anal 425:444
219. Oosterwaal M, Carbes S, Telfer S et al (2016) The Glasgow-Maastricht foot model, evaluation of a 26 segment kinematic model of the foot. J Foot Ankle Res 9:1–10. https://doi.org/10.1186/s13047-016-0152-7
220. Sibella F, Galli M, Romei M et al (2003) Biomechanical analysis of sit-to-stand movement in normal and obese subjects. Clin Biomech 18:745–750. https://doi.org/10.1016/S0268-0033(03)00144-X
221. Kubo M, Ulrich B (2006) Coordination of pelvis-HAT (head, arms and trunk) in anterior–posterior and medio-lateral directions during treadmill gait in preadolescents with/without Down syndrome. Gait Posture 23:512–518
222. Menegaldo LL, de Toledo FA, Weber HI (2003) Biomechanical modeling and optimal control of human posture. J Biomech 36:1701–1712
223. Menegoni F, Vismara L, Capodaglio P et al (2008) Kinematics of trunk movements: Protocol design and application in obese females. J Appl Biomater Biomech 6:178–185. https://doi.org/10.1177/228080000800600308
224. Arjmand N, Shirazi-Adl A, Parnianpour M (2007) Trunk biomechanical models based on equilibrium at a single-level violate equilibrium at other levels. Eur Spine J 16:701–709. https://doi.org/10.1007/s00586-006-0263-0
225. Vasavada A, Li S, Delp SL (1998) Influence of muscle morphometry and moment arms on the moment-generating capacity of human neck muscles. Spine (Phila Pa 1976) 23:412–422. https://doi.org/10.1097/00007632-199802150-00002
226. Ignasiak D, Dendorfer S, Ferguson SJ (2016) Thoracolumbar spine model with articulated ribcage for the prediction of dynamic spinal loading. J Biomech 49:959–966. https://doi.org/10.1016/j.jbiomech.2015.10.010
227. Bassani T, Stucovitz E, Qian Z et al (2017) Validation of the AnyBody full body musculoskeletal model in computing lumbar spine loads at L4L5 level. J Biomech 58:89–96. https://doi.org/10.1016/j.jbiomech.2017.04.025
228. Kuai S, Liao Z, Zhou W et al (2017) The effect of lumbar disc herniation on musculoskeletal loadings in the spinal region during level walking and stair climbing. Med Sci Monit 23:3869–3877. https://doi.org/10.12659/MSM.903349
229. Raabe ME, Chaudhari AMW (2016) An investigation of jogging biomechanics using the full-body lumbar spine model: model development and validation. J Biomech 49:1238–1243. https://doi.org/10.1016/j.jbiomech.2016.02.046
230. Hidalgo B, Gilliaux M, Poncin W, Detrembleur C (2012) Reliability and validity of a kinematic spine model during active trunk movement in healthy subjects and patients with chronic non-specific low back pain. J Rehabil Med 44:756–763. https://doi.org/10.2340/16501977-1015
231. Bruno AG, Bouxsein ML, Anderson DE (2015) Development and validation of a musculoskeletal model of the fully articulated thoracolumbar spine and rib cage. J Biomech Eng 137:081003. https://doi.org/10.1115/1.4030408
232. de Zee M, Hansen L, Wong C et al (2007) A generic detailed rigid-body lumbar spine model. J Biomech 40:1219–1227. https://doi.org/10.1016/j.jbiomech.2006.05.030

233. Abedrabbo G, Fisette P, Absil PA, et al (2012) A multibody-based approach to the computation of spine intervertebral motions in scoliotic patients. In: Research into spinal deformities 8. IOS Press, Amsterdam pp 95–98
234. Pearcy MJ, Nikolai B (1988) Instantaneous axes of rotation of the lumbar intervertebral joints. Spine (Phila Pa 1976) 13:1033–1041
235. Moorehead JD, Montgomery SC, Harvey DM (2003) Instant center of rotation estimation using the Reuleaux technique and a lateral extrapolation technique. J Biomech 36:1301–1307. https://doi.org/10.1016/S0021-9290(03)00156-8
236. White AA, Manohar MP (1990) Clinical biomechanics of the spine, 2nd edn. Lippincott Williams & Wikins, Philadelphia
237. Davis RB, Ounpuu S, Tyburski D, Gage JR (1991) A gait analysis data collection and reduction technique. Hum Mov Sci 10:575–587. https://doi.org/10.1016/0167-9457(91)90046-Z
238. Hara R, McGinley J, Briggs C et al (2016) Predicting the location of the hip joint centres, impact of age group and sex. Sci Rep 6:37707. https://doi.org/10.1038/srep37707
239. Harrington ME, Zavatsky AB, Lawson SEM et al (2007) Prediction of the hip joint centre in adults, children, and patients with cerebral palsy based on magnetic resonance imaging. J Biomech 40:595–602. https://doi.org/10.1016/j.jbiomech.2006.02.003
240. Meskers CGM, Van Der Helm FCT, Rozendaal LA, Rozing PM (1997) In vivo estimation of the glenohumeral joint rotation center from scapular bony landmarks by linear regression. J Biomech 31:93–96. https://doi.org/10.1016/S0021-9290(97)00101-2
241. Leardini A, Chiari A, Della Croce U, Cappozzo A (2005) Human movement analysis using stereophotogrammetry Part 3. Soft tissue artifact assessment and compensation. Gait Posture 21:212–225. https://doi.org/10.1016/j.gaitpost.2004.05.002
242. Peters A, Galna B, Sangeux M et al (2010) Quantification of soft tissue artifact in lower limb human motion analysis: a systematic review. Gait Posture 31:1–8. https://doi.org/10.1016/j.gaitpost.2009.09.004
243. Sangeux M (2015) On the implementation of predictive methods to locate the hip joint centres. Gait Posture 42:402–405. https://doi.org/10.1016/j.gaitpost.2015.07.004
244. Andriacchi TP, Andersson GBJ, Fermier RW et al (1980) A study of lower-limb mechanics during stair-climbing. J Bone Jt Surg Ser A 62:749–757. https://doi.org/10.2106/00004623-198062050-00008
245. Bell AL, Brand RA, Pedersen DR (1989) Prediction of hip joint centre location from external landmarks. Hum Mov Sci 8:3–16. https://doi.org/10.1016/0167-9457(89)90020-1
246. Seidel GK, Marchinda DM, Dijkers M, Soutas-Little RW (1995) Hip joint center location from palpable bony landmarks—a cadaver study. J Biomech 28:995–998
247. Shea KM, Lenhoff MW, Otis JC, Backus SI (1997) Validation of a method for location of the Hip Joint Center. Gait Posture 5:157–158. https://doi.org/10.1016/s0966-6362(97)83383-8
248. Hunt MA, Birmingham TB, Jenkyn TR et al (2008) Measures of frontal plane lower limb alignment obtained from static radiographs and dynamic gait analysis. Gait Posture 27:635–640. https://doi.org/10.1016/j.gaitpost.2007.08.011
249. Weinhandl JT, O'Connor KM (2010) Assessment of a greater trochanter-based method of locating the hip joint center. J Biomech 43:2633–2636. https://doi.org/10.1016/j.jbiomech.2010.05.023
250. Campbell AC, Lloyd DG, Alderson JA, Elliott BC (2009) MRI development and validation of two new predictive methods of glenohumeral joint centre location identification and comparison with established techniques. J Biomech 42:1527–1532. https://doi.org/10.1016/j.jbiomech.2009.03.039
251. Lempereur M, Brochard S, Rémy-Néris O (2013) Repeatability assessment of functional methods to estimate the glenohumeral joint centre. Comput Methods Biomech Biomed Eng 16:6–11. https://doi.org/10.1080/10255842.2011.597386
252. Kainz H, Carty CP, Modenese L et al (2015) Estimation of the hip joint centre in human motion analysis: a systematic review. Clin Biomech 30:319–329. https://doi.org/10.1016/j.clinbiomech.2015.02.005
253. Ehrig RM, Taylor WR, Duda GN, Heller MO (2006) A survey of formal methods for determining the centre of rotation of ball joints. J Biomech 39:2798–2809. https://doi.org/10.1016/j.jbiomech.2005.10.002
254. McGibbon C, Fowler J, Chase S et al (2015) Evaluation of anatomical and functional hip joint center methods: the effects of activity type, gender, and proximal reference segment. J Biomech Eng 138:1–7
255. Meng L, Childs C, Buis A (2019) Evaluation of functional methods of joint centre determination for quasi-planar movement. PLoS ONE 14:1–14. https://doi.org/10.1371/journal.pone.0210807
256. Piazza SJ, Okita N, Cavanagh PR (2001) Accuracy of the functional method of hip joint center location: effects of limited motion and varied implementation. J Biomech 34:967–973. https://doi.org/10.1016/S0021-9290(01)00052-5
257. Miller E, Kaufman K (2018) Verification of an improved hip joint center prediction method. Gait Posture 59:174–176
258. Stebbins J, Harrington M, Thompson N et al (2006) Repeatability of a model for measuring multi-segment foot kinematics in children. Gait Posture 23:401–410
259. Siston RA, Delp SL (2006) Evaluation of a new algorithm to determine the hip joint center. J Biomech 39:125–130. https://doi.org/10.1016/j.jbiomech.2004.10.032
260. Cappozzo A (1984) Gait analysis methodology. Hum Mov Sci 3:27–50. https://doi.org/10.1016/0167-9457(84)90004-6
261. Gamage SSHU, Lasenby J (2002) New least squares solutions for estimating the average centre of rotation and the axis of rotation. J Biomech 35:87–93. https://doi.org/10.1016/S0021-9290(01)00160-9
262. Holzreiter SS (1991) Calculation of the instantaneous centre of rotation for a rigid body. J Biomech 24:643–647. https://doi.org/10.1016/0021-9290(91)90297-Z
263. Halvorsen K (2003) Bias compensated least squares estimate of the center of rotation. J Biomech 36:999–1008. https://doi.org/10.1016/S0021-9290(03)00070-8
264. Woltring HJ, Huiskes R, de Lange A, Veldpaus FE (1985) Finite centroid and helical axis estimation from noisy landmark measurements in the study of human joint kinematics. J Biomech 18:379–389. https://doi.org/10.1016/0021-9290(85)90293-3
265. Besier TF, Sturnieks DL, Alderson JA, Lloyd DG (2003) Repeatability of gait data using a functional hip joint centre and a mean helical knee axis. J Biomech 36:1159–1168. https://doi.org/10.1016/S0021-9290(03)00087-3
266. Marin F, Mannel H, Claes L, Darselen L (2003) Accurate determination of a joint rotation center based on the minimal amplitude point method. Comput Aided Surg 8:30–34. https://doi.org/10.3109/10929080309146100
267. Cereatti A, Camomilla V, Cappozzo A (2004) Estimation of the centre of rotation: a methodological contribution. J Biomech 37:413–416. https://doi.org/10.1016/S0021-9290(03)00264-1
268. De Momi E, Lopomo N, Cerveri P et al (2009) In-vitro experimental assessment of a new robust algorithm for hip joint centre estimation. J Biomech 42:989–995. https://doi.org/10.1016/j.jbiomech.2009.02.031
269. Lu TW (2000) On the estimation of hip joint centre position in clinical gait analysis. Biomed Eng 12:89–95
270. Schwartz MH, Rozumalski A (2005) A new method for estimating joint parameters from motion data. J Biomech 38:107–116. https://doi.org/10.1016/j.jbiomech.2004.03.009

271. Sangeux M, Pillet H, Skalli W (2014) Which method of hip joint centre localisation should be used in gait analysis? Gait Posture 40:20–25. https://doi.org/10.1016/j.gaitpost.2014.01.024
272. Lempereur M, Leboeuf F, Brochard S et al (2010) In vivo estimation of the glenohumeral joint centre by functional methods: accuracy and repeatability assessment. J Biomech 43:370–374. https://doi.org/10.1016/j.jbiomech.2009.09.029
273. Wu G, Van Der Helm FCT, Veeger HEJ et al (2005) ISB recommendation on definitions of joint coordinate systems of various joints for the reporting of human joint motion—Part II: shoulder, elbow, wrist and hand. J Biomech 38:981–992. https://doi.org/10.1016/j.jbiomech.2004.05.042
274. Michaud B, Jackson M, Arndt A et al (2016) Determining in vivo sternoclavicular, acromioclavicular and glenohumeral joint centre locations from skin markers, CT-scans and intracortical pins: a comparison study. Med Eng Phys 38:290–296. https://doi.org/10.1016/j.medengphy.2015.12.004
275. Rab G, Petuskey K, Bagley A (2002) A method for determination of upper extremity kinematics. Gait Posture 15:113–119. https://doi.org/10.1016/S0966-6362(01)00155-2
276. Fiorentino NM, Kutschke MJ, Atkins PR et al (2016) Accuracy of functional and predictive methods to calculate the hip joint center in young non-pathologic asymptomatic adults with dual fluoroscopy as a reference standard. Ann Biomed Eng 44:2168–2180. https://doi.org/10.1007/s10439-015-1522-1
277. Baker R, Leboeuf F, Hospitalier C et al (2020) Handbook of human motion. Handb Hum Motion. https://doi.org/10.1007/978-3-319-30808-1
278. Frigo C, Rabuffetti M, Kerrigan DC et al (1998) Functionally oriented and clinically feasible quantitative gait analysis method. Med Biol Eng Comput 36:179–185. https://doi.org/10.1007/BF02510740
279. Begon M, Wieber PB, Yeadon MR (2008) Kinematics estimation of straddled movements on high bar from a limited number of skin markers using a chain model. J Biomech 41:581–586. https://doi.org/10.1016/j.jbiomech.2007.10.005
280. Leardini A, Sawacha Z, Paolini G et al (2007) A new anatomically based protocol for gait analysis in children. Gait Posture 26:560–571. https://doi.org/10.1016/j.gaitpost.2006.12.018
281. Duffell LD, Hope N, McGregor AH (2014) Comparison of kinematic and kinetic parameters calculated using a cluster-based model and Vicon's plug-in gait. Proc Inst Mech Eng H 228:206–210. https://doi.org/10.1177/0954411913518747
282. Armand S, Sangeux M, Baker R (2014) Optimal markers' placement on the thorax for clinical gait analysis. Gait Posture 39:147–153. https://doi.org/10.1016/j.gaitpost.2013.06.016
283. Kiernan D, Malone A, O'Brien T, Simms CK (2014) A 3-dimensional rigid cluster thorax model for kinematic measurements during gait. J Biomech 47:1499–1505. https://doi.org/10.1016/j.jbiomech.2014.02.020
284. Jackson M, Michaud B, Tétreault P, Begon M (2012) Improvements in measuring shoulder joint kinematics. J Biomech 45:2180–2183. https://doi.org/10.1016/j.jbiomech.2012.05.042
285. Haering D, Raison M, Begon M (2014) Measurement and description of three-dimensional shoulder range of motion with degrees of freedom interactions. J Biomech Eng 136:1–6. https://doi.org/10.1115/1.4027665
286. Cerveri P, Pedotti A, Ferrigno G (2005) Kinematical models to reduce the effect of skin artifacts on marker-based human motion estimation. J Biomech 38:2228–2236. https://doi.org/10.1016/j.jbiomech.2004.09.032
287. Metcalf CD, Notley SV, Chappell PH et al (2008) Validation and application of a computational model for wrist and hand movements using surface markers. IEEE Trans Biomed Eng 55:1199–1210. https://doi.org/10.1109/TBME.2007.908087
288. Hwang SJ, Choi HS, Kim YH (2004) Motion analysis based on a multi-segment foot model in normal walking. Conf Proc IEEE Eng Med Biol Soc 7:5104–5106. https://doi.org/10.1109/IEMBS.2004.1404410
289. MacWilliams BA, Cowley M, Nicholson DE (2003) Foot kinematics and kinetics during adolescent gait. Gait Posture 17:214–224. https://doi.org/10.1016/S0966-6362(02)00103-0
290. Simon J, Doederlein L, McIntosh AS et al (2006) The Heidelberg foot measurement method: development, description and assessment. Gait Posture 23:411–424. https://doi.org/10.1016/j.gaitpost.2005.07.003
291. Wu G, Siegler S, Allard P et al (2002) ISB recommendation on definitions of joint coordinate system of various joints for the reporting of human joint motion—part I: ankle, hip, and spine. J Biomech 35:543–548. https://doi.org/10.1016/S0021-9290(01)00222-6
292. Malus J, Skypala J, Silvernail JF et al (2021) Marker placement reliability and objectivity for biomechanical cohort study: Healthy aging in industrial environment (haie—program 4). Sensors 21:1–10. https://doi.org/10.3390/s21051830
293. Caldas R, Mundt M, Potthast W et al (2017) A systematic review of gait analysis methods based on inertial sensors and adaptive algorithms. Gait Posture 57:204–210. https://doi.org/10.1016/j.gaitpost.2017.06.019
294. Nair SP, Gibbs S, Arnold G et al (2010) A method to calculate the centre of the ankle joint: a comparison with the Vicon Plug-in-Gait model. Clin Biomech 25:582–587. https://doi.org/10.1016/j.clinbiomech.2010.03.004
295. Benedetti MG, Catani F, Leardini A et al (1998) Data management in gait analysis for clinical applications. Clin Biomech 13:204–215. https://doi.org/10.1016/S0268-0033(97)00041-7
296. Donati M, Camomilla V, Vannozzi G, Cappozzo A (2008) Anatomical frame identification and reconstruction for repeatable lower limb joint kinematics estimates. J Biomech 41:2219–2226. https://doi.org/10.1016/j.jbiomech.2008.04.018
297. Krosshaug T, Bahr R (2005) A model-based image-matching technique for three-dimensional reconstruction of human motion from uncalibrated video sequences. J Biomech 38:919–929. https://doi.org/10.1016/j.jbiomech.2004.04.033
298. Cerveri P, De Momi E, Marchente M et al (2008) In vivo validation of a realistic kinematic model for the trapezio-metacarpal joint using an optoelectronic system. Ann Biomed Eng 36:1268–1280. https://doi.org/10.1007/s10439-008-9499-7
299. Schmidt R, Disselhorst-Klug C, Silny J, Rau G (1999) A marker-based measurement procedure for unconstrained wrist and elbow motions. J Biomech 32:615–621. https://doi.org/10.1016/S0021-9290(99)00036-6
300. Lloyd DG, Alderson J, Elliott BC (2000) An upper limb kinematic model for the examination of cricket bowling: a case study of Mutiah Muralitharan. J Sports Sci 18:975–982. https://doi.org/10.1080/026404100446775
301. van Andel CJ, Wolterbeek N, Doorenbosch CAM et al (2008) Complete 3D kinematics of upper extremity functional tasks. Gait Posture 27:120–127. https://doi.org/10.1016/j.gaitpost.2007.03.002
302. Fohanno V, Lacouture P, Colloud F (2013) Improvement of upper extremity kinematics estimation using a subject-specific forearm model implemented in a kinematic chain. J Biomech 46:1053–1059. https://doi.org/10.1016/j.jbiomech.2013.01.029
303. Arampatzis A, Klapsing GM, Gert-Peter B (2002) A three-dimensional shank-foot model to determine the foot motion during landings. Med Sci Sport Exerc 34:130–138
304. Kitaoka HB, Crevoisier XM, Hansen D et al (2006) Foot and ankle kinematics and ground reaction forces during ambulation. Foot Ankle Int 27:808–813. https://doi.org/10.1177/107110070602701010

305. Pohl MB, Messenger N, Buckley JG (2007) Forefoot, rearfoot and shank coupling: effect of variations in speed and mode of gait. Gait Posture 25:295–302. https://doi.org/10.1016/j.gaitpost.2006.04.012
306. Jenkyn TR, Nicol AC (2007) A multi-segment kinematic model of the foot with a novel definition of forefoot motion for use in clinical gait analysis during walking. J Biomech 40:3271–3278. https://doi.org/10.1016/j.jbiomech.2007.04.008
307. Rao S, Saltzman C, Yack HJ (2007) Segmental foot mobility in individuals with and without diabetes and neuropathy. Clin Biomech 22:464–471. https://doi.org/10.1016/j.clinbiomech.2006.11.013
308. Cobb SC, Tis LL, Johnson JT et al (2009) The effect of low-mobile foot posture on multi-segment medial foot model gait kinematics. Gait Posture 30:334–339. https://doi.org/10.1016/j.gaitpost.2009.06.005
309. Sawacha Z, Cristoferi G, Guarneri G et al (2009) Characterizing multisegment foot kinematics during gait in diabetic foot patients. J Neuroeng Rehabil 6:1–11. https://doi.org/10.1186/1743-0003-6-37
310. Hyslop E, Woodburn J, McInnes IB et al (2010) A reliability study of biomechanical foot function in psoriatic arthritis based on a novel multi-segmented foot model. Gait Posture 32:619–626. https://doi.org/10.1016/j.gaitpost.2010.09.004
311. Tulchin K, Orendurff M, Karol L (2010) The effects of surface slope on multi-segment foot kinematics in healthy adults. Gait Posture 32:446–450. https://doi.org/10.1016/j.gaitpost.2010.06.008
312. Bruening DA, Cooney KM, Buczek FL (2012) Analysis of a kinetic multi-segment foot model part II: kinetics and clinical implications. Gait Posture 35:535–540. https://doi.org/10.1016/j.gaitpost.2011.11.012
313. Bishop C, Paul G, Thewlis D (2013) The reliability, accuracy and minimal detectable difference of a multi-segment kinematic model of the foot-shoe complex. Gait Posture 37:552–557. https://doi.org/10.1016/j.gaitpost.2012.09.020
314. Chard A, Greene A, Hunt A et al (2013) Effect of thong style flip-flops on children's barefoot walking and jogging kinematics. J Foot Ankle Res. https://doi.org/10.1186/1757-1146-6-8
315. Nester CJ, Jarvis HL, Jones RK et al (2014) Movement of the human foot in 100 pain free individuals aged 18–45: implications for understanding normal foot function. J Foot Ankle Res 7:1–10. https://doi.org/10.1186/s13047-014-0051-8
316. Eltoukhy M, Kuenze C, Andersen MS et al (2017) Prediction of ground reaction forces for Parkinson's disease patients using a kinect-driven musculoskeletal gait analysis model. Med Eng Phys 50:75–82. https://doi.org/10.1016/j.medengphy.2017.10.004
317. Eltoukhy M, Kuenze C, Oh J et al (2018) Concurrent validity of depth sensing cameras for non-contact ACL injury screening during side-cut maneuvers in adolescent athletes: a preliminary study. J Appl Biomech 35:2–10
318. Hidalgo AF, Jalón JG de, Tapia S (2011) High Performance Algorithms and Implementations. In: MULTIBODY DYNAMICS 2011, ECCOMAS Thematic Conference. pp 4–7
319. Nolte D, Ko ST, Bull AMJ, Kedgley AE (2020) Reconstruction of the lower limb bones from digitised anatomical landmarks using statistical shape modelling. Gait Posture 77:269–275. https://doi.org/10.1016/j.gaitpost.2020.02.010
320. Audenaert EA, Pattyn C, Steenackers G et al (2019) Statistical shape modeling of skeletal anatomy for sex discrimination: their training size, sexual dimorphism, and asymmetry. Front Bioeng Biotechnol 7:1–11. https://doi.org/10.3389/fbioe.2019.00302
321. Zajac FE, Neptune RR, Kautz SA (2002) Biomechanics and muscle coordination of human walking: Part I: introduction to concepts, power transfer, dynamics and simulations. Gait Posture 16:215–232. https://doi.org/10.1016/S0966-6362(02)00068-1
322. Banks R (2014) Skeletal muscle. In: Reference module in biomedical sciences. Elsevier, Amsterdam pp 677–682
323. MacIntosh BR, Herzog W, Suter E et al (1993) Human skeletal muscle fibre types and force: velocity properties. Eur J Appl Physiol Occup Physiol 67:499–506. https://doi.org/10.1007/BF00241645
324. Taylor JL, Gandevia SC (2008) A comparison of central aspects of fatigue in submaximal and maximal voluntary contractions. J Appl Physiol 104:542–550. https://doi.org/10.1152/japplphysiol.01053.2007
325. Jones EJ, Bishop PA, Woods AK, Green JM (2008) Cross-sectional area and muscular strength: a brief review. Sport Med 38:987–994. https://doi.org/10.2165/00007256-200838120-00003
326. Fitts RH, McDonald KS, Schluter JM (1991) The determinants of skeletal muscle force and power: their adaptability with changes in activity pattern. J Biomech 24:111–122. https://doi.org/10.1016/0021-9290(91)90382-W
327. Earle TBRW (2008) Essentials of strength training and conditioning, 3rd edn. Human Kinetics, New York
328. Hill AV (1938) The heat of shortening and the dynamic constants of muscle. Proc R Soc Lond Ser B 126:136–195. https://doi.org/10.1098/rspb.1938.0050
329. Kelc R, Naranda J, Kuhta M, Vogrin M (2013) The physiology of sports injuries and repair processes. Curr Issues Sport Exerc Med. https://doi.org/10.5772/54234
330. Kirkendall DT, Garrett WE (1997) Function and biomechanics of tendons. Scand J Med Sci Sport 7:62–66. https://doi.org/10.1111/j.1600-0838.1997.tb00120.x
331. Siebert T, Screen HRCC, Rode C (2021) Computational modelling of muscle, tendon, and ligaments biomechanics, 2nd edn. Elsevier, Amsterdam
332. Finni T, Komi PV, Lukkariniemi J (1998) Achilles tendon loading during walking: application of a novel optic fiber technique. Eur J Appl Physiol Occup Physiol 77:289–291. https://doi.org/10.1007/s004210050335
333. Danion F, Latash ML (2011) Motor control: theories, experiments, and applications. Oxford University Press, Oxford
334. Neptune RR, McGowan CP, Fiandt JM (2009) The influence of muscle physiology and advanced technology on sports performance. Annu Rev Biomed Eng 11:81–107. https://doi.org/10.1146/annurev-bioeng-061008-124941
335. Bobbert MF (2001) Dependence of human squat jump performance on the series elastic compliance of the triceps surae: a simulation study. J Exp Biol 204:533–542
336. Tan T, De Vita R (2015) A structural constitutive model for smooth muscle contraction in biological tissues. Int J Non Linear Mech 75:46–53. https://doi.org/10.1016/j.ijnonlinmec.2015.02.009
337. Hunter PJ, Mcculloch AD, Keurs HEDJ (1998) Modelling the mechanical properties of cardiac muscle. Prog Biophys Mol Biol 69:289–331
338. Romero F, Alonso FJ (2016) A comparison among different Hill-type contraction dynamics formulations for muscle force estimation. Mech Sci 7:19–29. https://doi.org/10.5194/ms-7-19-2016
339. Millard M, Uchida T, Seth A, Delp SL (2013) Flexing computational muscle: modeling and simulation of musculotendon dynamics. J Biomech Eng 135:021005. https://doi.org/10.1115/1.4023390
340. Oliveira AR, Gonçalves SB, de Carvalho M, Silva MT (2016) Development of a musculotendon model within the framework of multibody systems dynamics. Comput Methods Appl Sci 42:213–237. https://doi.org/10.1007/978-3-319-30614-8_10

341. Schultz AB, Faulkner JA, Kadhiresan VA (1991) A simple Hill element-nonlinear spring model of muscle contraction biomechanics. J Appl Physiol 70:803–812. https://doi.org/10.1152/jappl.1991.70.2.803
342. Cheng EJ, Brown IE, Loeb GE (2000) Virtual muscle: a computational approach to understanding the effects of muscle properties on motor control. J Neurosci Methods 101:117–130. https://doi.org/10.1016/S0165-0270(00)00258-2
343. Hatze H (1978) A general myocybernetic control model of skeletal muscle. Biol Cybern 28:143–157. https://doi.org/10.1007/BF00337136
344. Pereira AF, Silva MT, Martins JM, de Carvalho M (2011) Implementation of an efficient muscle fatigue model in the framework of multibody systems dynamics for analysis of human movements. Proc Inst Mech Eng Part K J Multi-body Dyn 225:359–370. https://doi.org/10.1177/1464419311415954
345. Guo J, Huang H, Yu Y et al (2020) Modeling muscle wrapping and mass flow using a mass-variable multibody formulation. Multibody Syst Dyn 49:315–336. https://doi.org/10.1007/s11044-020-09733-1
346. Günther M, Röhrle O, Haeufle DFB, Schmitt S (2012) Spreading out muscle mass within a hill-type model: a computer simulation study. Comput Math Methods Med. https://doi.org/10.1155/2012/848630
347. Pai DK (2010) Muscle mass in musculoskeletal models. J Biomech 43:2093–2098. https://doi.org/10.1016/j.jbiomech.2010.04.004
348. Gerus P, Rao G, Berton E (2015) Ultrasound-based subject-specific parameters improve fascicle behaviour estimation in Hill-type muscle model. Comput Methods Biomech Biomed Engin 18:116–123. https://doi.org/10.1080/10255842.2013.780047
349. Ding Y, Panizzolo FA, Siviy C et al (2016) Effect of timing of hip extension assistance during loaded walking with a soft exosuit. J Neuroeng Rehabil 13:87. https://doi.org/10.1186/s12984-016-0196-8
350. Sartori M, Rubenson J, Lloyd DG, et al (2017) Converging clinical and engineering research on neurorehabilitation II. 15:10–13. https://doi.org/10.1007/978-3-319-46669-9
351. Klein Horsman MD, Koopman HFJM, van der Helm FCT et al (2007) Morphological muscle and joint parameters for musculoskeletal modelling of the lower extremity. Clin Biomech 22:239–247. https://doi.org/10.1016/j.clinbiomech.2006.10.003
352. Delp S (1990) Surgery simulation: a computer-graphics system to analyze and design musculoskeletal reconstructions of the lower limb. Stanford University, Stanford
353. Ward SR, Eng CM, Smallwood LH, Lieber RL (2009) Are current measurements of lower extremity muscle architecture accurate? Clin Orthop Relat Res 467:1074–1082. https://doi.org/10.1007/s11999-008-0594-8
354. Handsfield GG, Meyer CH, Hart JM et al (2014) Relationships of 35 lower limb muscles to height and body mass quantified using MRI. J Biomech 47:631–638. https://doi.org/10.1016/j.jbiomech.2013.12.002
355. Rasmussen J, Damsgaard M, Surma E, et al (2003) AnyBody—a software system for ergonomic optimization. Fifth World Congr Struct Multidiscip Optim May 19–23, 2003, Lido di Jesolo - Venice, Italy 6
356. Buchanan TS, Lloyd DG, Manal K, Besier TF (2004) Neuromusculoskeletal modeling: estimation of muscle forces and joint moments and movements from measurements of neural command. J Appl Biomech 20:367–395. https://doi.org/10.1123/jab.20.4.367
357. Modenese L, Ceseracciu E, Reggiani M, Lloyd DG (2016) Estimation of musculotendon parameters for scaled and subject specific musculoskeletal models using an optimization technique. J Biomech 49:141–148. https://doi.org/10.1016/j.jbiomech.2015.11.006
358. Seth A, Uchida TK et al (2018) OpenSim: simulating musculoskeletal dynamics and neuromuscular control to study human and animal movement. PLOS Comput Biol 14:1–20
359. Manal K, Buchanan TS (2004) Subject-specific estimates of tendon slack length: a numerical method. J Appl Biomech 20:195–203. https://doi.org/10.1123/jab.20.2.195
360. Buchanan TS, Moniz MJ, Dewald JPA, Rymer WZ (1993) Estimation of muscle forces about the wrist joint during isometric tasks using an EMG coefficient method. J Biomech 26:547–560. https://doi.org/10.1016/0021-9290(93)90016-8
361. Tsuang YH, Novak GJ, Schipplein OD et al (1993) Trunk muscle geometry and centroid location when twisting. J Biomech 26:537–546. https://doi.org/10.1016/0021-9290(93)90015-7
362. Zargham A, Afschrift M, De Schutter J et al (2019) Inverse dynamic estimates of muscle recruitment and joint contact forces are more realistic when minimizing muscle activity rather than metabolic energy or contact forces. Gait Posture 74:223–230. https://doi.org/10.1016/j.gaitpost.2019.08.019
363. Rasmussen J, Damsgaard M, Voigt M (2001) Muscle recruitment by the min/max criterion—a comparative numerical study. J Biomech 34:409–415. https://doi.org/10.1016/S0021-9290(00)00191-3
364. Praagman M (2008) Muscle load sharing. An energy-based approach. 168
365. Robertson DGE, Caldwell GE, Hamill J et al (2014) Research methods in biomechanics, 2nd edn. Human Kinetics, New York
366. Marshall RN, Wood GA, Jennings LS (1989) Performance objectives in human movement: a review and application to the stance phase of normal walking. Hum Mov Sci 8:571–594
367. Xiang Y, Arora JS, Abdel-Malek K (2012) Hybrid predictive dynamics: a new approach to simulate human motion. Multibody Syst Dyn 28:199–224. https://doi.org/10.1007/s11044-012-9306-y
368. Hoang HX, Diamond LE, Lloyd DG, Pizzolato C (2019) A calibrated EMG-informed neuromusculoskeletal model can appropriately account for muscle co-contraction in the estimation of hip joint contact forces in people with hip osteoarthritis. J Biomech 83:134–142. https://doi.org/10.1016/j.jbiomech.2018.11.042
369. Wesseling M, Derikx LC, De Groote F et al (2015) Muscle optimization techniques impact the magnitude of calculated hip joint contact forces. J Orthop Res 33:430–438. https://doi.org/10.1002/jor.22769
370. Roelker SA, Caruthers EJ, Hall RK et al (2020) Effects of optimization technique on simulated muscle activations and forces. J Appl Biomech 36:259–278. https://doi.org/10.1123/JAB.2019-0021
371. Heintz S, Gutierrez-Farewik EM (2007) Static optimization of muscle forces during gait in comparison to EMG-to-force processing approach. Gait Posture 26:279–288. https://doi.org/10.1016/j.gaitpost.2006.09.074
372. Edwards WB, Gillette JC, Thomas JM, Derrick TR (2008) Internal femoral forces and moments during running: implications for stress fracture development. Clin Biomech 23:1269–1278. https://doi.org/10.1016/j.clinbiomech.2008.06.011
373. Xiang Y, Arora JS, Abdel-Malek K (2010) Physics-based modeling and simulation of human walking: a review of optimization-based and other approaches. Struct Multidiscip Optim 42:1–23. https://doi.org/10.1007/s00158-010-0496-8
374. Pasciuto I, Ausejo S, Celigüeta JT et al (2014) A comparison between optimization-based human motion prediction methods: data-based, knowledge-based and hybrid approaches. Struct Multidiscip Optim 49:169–183. https://doi.org/10.1007/s00158-013-0960-3

375. Thelen DG, Anderson FC (2006) Using computed muscle control to generate forward dynamic simulations of human walking from experimental data. J Biomech 39:1107–1115. https://doi.org/10.1016/j.jbiomech.2005.02.010
376. Xiang Y, Chung H-J, Kim JH et al (2010) Predictive dynamics: an optimization-based novel approach for human motion simulation. Struct Multidiscip Optim 41:465–479
377. Morrow MM, Rankin JW, Neptune RR, Kaufman KR (2014) A comparison of static and dynamic optimization muscle force predictions during wheelchair propulsion. J Biomech 47:3459–3465. https://doi.org/10.1016/j.jbiomech.2014.09.013
378. Rao A (2010) A survey of numerical mthods for optimal control. Adv Astronaut Sci 135:1–32
379. Umberger BR, Miller RH (2017) Optimal control modeling of human movement. In: Müller B, Wolf SI, Brueggemann G-P et al (eds) Handbook of human motion. Springer, Cham, pp 1–22
380. Porsa S, Lin YC, Pandy MG (2016) Direct methods for predicting movement biomechanics based upon optimal control theory with implementation in OpenSim. Ann Biomed Eng 44:2542–2557. https://doi.org/10.1007/s10439-015-1538-6
381. Shourijeh MS, Mcphee J (2015) Foot—ground contact modeling within human gait simulations : from Kelvin—Voigt to hypervolumetric models. Multibody Syst Dyn. https://doi.org/10.1007/s11044-015-9467-6
382. Lopes DS, Neptune RR, Ambrósio JA, Silva MT (2016) A superellipsoid-plane model for simulating foot-ground contact during human gait. Comput Methods Biomech Biomed Engin 19:954–963. https://doi.org/10.1080/10255842.2015.1081181
383. Dorn TW, Lin Y-C, Pandy MG (2012) Estimates of muscle function in human gait depend on how foot-ground contact is modelled. Comput Methods Biomech Biomed Engin 15:657–668. https://doi.org/10.1080/10255842.2011.554413
384. Silva PC, Silva MT, Martins JM (2010) Evaluation of the contact forces developed in the lower limb/orthosis interface for comfort design. Multibody Syst Dyn 24:367–388. https://doi.org/10.1007/s11044-010-9219-6
385. Mouzo F, Michaud F, Lugris U, Cuadrado J (2020) Leg-orthosis contact force estimation from gait analysis. Mech Mach Theory 148:103800. https://doi.org/10.1016/j.mechmachtheory.2020.103800
386. Mouzo F, Lugris U, Cuadrado J, et al (2018) Calibration and validation of a skeletal multibody model for leg-orthosis contact force estimation. In: International Symposium on Wearable Robotics. pp 257–261
387. Lin CJ, Lin PC, Guo LY, Su FC (2011) Prediction of applied forces in handrim wheelchair propulsion. J Biomech 44:455–460. https://doi.org/10.1016/j.jbiomech.2010.09.029
388. Rankin JW, Kwarciak AM, Richter WM, Neptune RR (2012) The influence of wheelchair propulsion technique on upper extremity muscle demand: a simulation study. Clin Biomech 27:879–886. https://doi.org/10.1016/j.clinbiomech.2012.07.002
389. Slowik JS, Requejo PS, Mulroy SJ, Neptune RR (2016) The influence of wheelchair propulsion hand pattern on upper extremity muscle power and stress. J Biomech 49:1554–1561. https://doi.org/10.1016/j.jbiomech.2016.03.031
390. Bessonnet G, Seguin P, Sardain P (2005) A parametric optimization approach to walking pattern synthesis. Int J Rob Res 24:523–536. https://doi.org/10.1177/0278364905055377
391. Fluit R, Andersen MS, Kolk S et al (2014) Prediction of ground reaction forces and moments during various activities of daily living. J Biomech 47:2321–2329. https://doi.org/10.1016/j.jbiomech.2014.04.030
392. Skals S, Jung MK, Damsgaard M, Andersen MS (2017) Prediction of ground reaction forces and moments during sports-related movements. Multibody Syst Dyn 39:175–195. https://doi.org/10.1007/s11044-016-9537-4
393. Jackson JN, Hass CJ, Fregly BJ (2016) Development of a subject-specific foot-ground contact model for walking. J Biomech Eng 138:9
394. Hamner SR, Seth A, Steele KM, Delp SL (2013) A rolling constraint reproduces ground reaction forces and moments in dynamic simulations of walking, running, and crouch gait. J Biomech 46:1772–1776
395. Neptune R, Wright I, van den Bogert AJ (2000) A method for numerical simulation of single limb ground contact events: application to heel-toe running. Comput Methods Biomech Biomed Engin 3:321–334
396. Neumann DA (2010) Kinesiology of the Musculoskeletal System, 2nd edn. Mosby Elsevier
397. Weiss J (2014) Computational modeling of ligament mechanics computational modeling of ligament mechanics. Crit Rev. https://doi.org/10.1615/CritRevBiomedEng.v29.i3.20
398. Provenzano P, Lakes R, Keenan T, Vanderby R (2001) Nonlinear ligament viscoelasticity. Ann Biomed Eng 29:908–914. https://doi.org/10.1114/1.1408926
399. Viidik A (1972) Simultaneous mechanical and light microscopic studies of collagen fibers. Z Anat Entwicklungsgesch 136:204–212. https://doi.org/10.1007/BF00519178
400. Kelikian AS (2011) Anatomy of the foot and ankle, descriptive, topography, functional, 3rd edn. Lippincott Williams & Wilkins, Chicago
401. Blankevoort L, Kuiper JH, Huiskes R, Grootenboer HJ (1991) Articular contact in a three-dimensional model of the knee. J Biomech 24:1019–1031
402. Wismans J, Veldpaus F, Janssen J et al (1980) A three-dimensional mathematical of the knee-joint. J Biomech 13:677–685. https://doi.org/10.1016/0021-9290(80)90354-1
403. Bloemker KH, Guess TM, Maletsky L, Dodd K (2015) Computational knee ligament modeling using experimentally determined zero-load lengths. Open Biomed Eng J 6:33–41. https://doi.org/10.2174/1874120701206010033
404. Bersini S, Sansone V, Frigo CA (2016) A dynamic multibody model of the physiological knee to predict internal loads during movement in gravitational field. Comput Methods Biomech Biomed Eng 19:571–579. https://doi.org/10.1080/10255842.2015.1051972
405. Nardini F, Belvedere C, Sancisi N et al (2020) An anatomical-based subject-specific model of in-vivo knee joint 3D kinematics from medical imaging. Appl Sci 10:8–12. https://doi.org/10.3390/app10062100
406. Baldwin MA, Laz PJ, Stowe JQ, Rullkoetter PJ (2009) Efficient probabilistic representation of tibiofemoral soft tissue constraint. Comput Methods Biomech Biomed Engin 12:651–659. https://doi.org/10.1080/10255840902822550
407. Qi Y, Song Y (2018) Coupled kinematic and dynamic analysis of parallel mechanism flying in space. Mech Mach Theory 124:104–117. https://doi.org/10.1016/j.mechmachtheory.2018.02.003
408. Li G, Gil J, Kanamori A, Woo SLY (1999) A validated three-dimensional computational model of a human knee joint. J Biomech Eng 121:657–662. https://doi.org/10.1115/1.2800871
409. Blankevoort L, Huiskes R (1996) Validation of a 3D model of the knee. J Biomech 29:955–961
410. Yang NH, Canavan PK, Nayeb-Hashemi H et al (2010) Protocol for constructing subject-specific biomechanical models of knee joint. Comput Methods Biomech Biomed Engin 13:589–603. https://doi.org/10.1080/10255840903389989
411. Modenese L, Phillips ATM, Bull AMJ (2011) An open source lower limb model: hip joint validation. J Biomech 44:2185–2193. https://doi.org/10.1016/j.jbiomech.2011.06.019
412. Nikooyan AA, Veeger HEJ, Chadwick EKJ et al (2011) Development of a comprehensive musculoskeletal model of the shoulder

and elbow. Med Biol Eng Comput 49:1425–1435. https://doi.org/10.1007/s11517-011-0839-7
413. Dorn TW, Schache AG, Pandy MG (2012) Muscular strategy shift in human running: dependence of running speed on hip and ankle muscle performance. J Exp Biol 215:1944–1956. https://doi.org/10.1242/jeb.064527
414. Hamner SR, Seth A, Delp SL (2010) Muscle contributions to propulsion and support during running. J Biomech 43:2709–2716. https://doi.org/10.1016/j.jbiomech.2010.06.025
415. Christophy M, Senan NAF, Lotz JC, O'Reilly OM (2012) A Musculoskeletal model for the lumbar spine. Biomech Model Mechanobiol 11:19–34. https://doi.org/10.1007/s10237-011-0290-6
416. Kim H, Kipp K (2019) Number of segments within musculoskeletal foot models influences ankle kinematics and strains of ligaments and muscles. J Orthop Res 37:2231–2240. https://doi.org/10.1002/jor.24394
417. Holzbaur KRS, Murray WM, Delp SL (2005) A model of the upper extremity for simulating musculoskeletal surgery and analyzing neuromuscular control. Ann Biomed Eng 33:829–840. https://doi.org/10.1007/s10439-005-3320-7
418. Ma'touq J, Hu T, Haddadin S (2019) A validated combined musculotendon path and muscle-joint kinematics model for the human hand. Comput Methods Biomech Biomed Eng 22:727–739. https://doi.org/10.1080/10255842.2019.1588256
419. Martelli S, Kersh ME, Pandy MG (2015) Sensitivity of femoral strain calculations to anatomical scaling errors in musculoskeletal models of movement. J Biomech 48:3606–3615. https://doi.org/10.1016/j.jbiomech.2015.08.001
420. Imani Nejad Z, Khalili K, Hosseini Nasab SH et al (2020) The capacity of generic musculoskeletal simulations to predict knee joint loading using the CAMS-knee datasets. Ann Biomed Eng 48:1430–1440. https://doi.org/10.1007/s10439-020-02465-5
421. Scheys L, Van Campenhout A, Spaepen A et al (2008) Personalized MR-based musculoskeletal models compared to rescaled generic models in the presence of increased femoral anteversion: Effect on hip moment arm lengths. Gait Posture 28:358–365. https://doi.org/10.1016/j.gaitpost.2008.05.002
422. Pellikaan P, van der Krogt MM, Carbone V et al (2014) Evaluation of a morphing based method to estimate muscle attachment sites of the lower extremity. J Biomech 47:1144–1150. https://doi.org/10.1016/j.jbiomech.2013.12.010
423. Heimann T, Meinzer HP (2009) Statistical shape models for 3D medical image segmentation: a review. Med Image Anal 13:543–563. https://doi.org/10.1016/j.media.2009.05.004
424. Salhi A, Burdin V, Mutsvangwa T et al (2017) Subject-specific shoulder muscle attachment region prediction using statistical shape models: a validity study. Proc Annu Int Conf IEEE Eng Med Biol Soc EMBS. https://doi.org/10.1109/EMBC.2017.8037154
425. Kingma I, De Looze MP, Toussaint HM et al (1996) Validation of a full body 3-D dynamic linked segment model. Hum Mov Sci 15:833–860. https://doi.org/10.1016/S0167-9457(96)00034-6
426. Faber H, Van Soest AJ, Kistemaker DA (2018) Inverse dynamics of mechanical multibody systems: an improved algorithm that ensures consistency between kinematics and external forces. PLoS ONE. https://doi.org/10.1371/journal.pone.0204575
427. O'Connor CM, Thorpe SK, O'Malley MJ, Vaughan CL (2007) Automatic detection of gait events using kinematic data. Gait Posture 25:469–474. https://doi.org/10.1016/j.gaitpost.2006.05.016
428. Samaan MA, Weinhandl JT, Bawab SY, Ringleb SI (2016) Determining residual reduction algorithm kinematic tracking weights for a sidestep cut via numerical optimization. Comput Methods Biomech Biomed Engin 19:1721–1729. https://doi.org/10.1080/10255842.2016.1183123
429. Delp SL, Anderson FC, Arnold AS et al (2007) OpenSim: open-source software to create and analyze dynamic simulations of movement. IEEE Trans Biomed Eng 54:1940–1950. https://doi.org/10.1109/TBME.2007.901024
430. De Groote F, De Laet T, Jonkers I, De Schutter J (2008) Kalman smoothing improves the estimation of joint kinematics and kinetics in marker-based human gait analysis. J Biomech 41:3390–3398. https://doi.org/10.1016/j.jbiomech.2008.09.035
431. Kuo AD (1998) A least-squares estimation approach to improving the precision of inverse dynamics computations. J Biomech Eng 120:148–159. https://doi.org/10.1115/1.2834295
432. van den Bogert AJ, Su A (2008) A weighted least squares method for inverse dynamic analysis. Comput Methods Biomech Biomed Engin 11:3–9. https://doi.org/10.1080/10255840701550865
433. Sturdy J, Silverman A, Pickle N (2021) Automated optimization of residual reduction algorithm parameters in OpenSim. bioRxiv
434. Valente G, Pitto L, Stagni R, Taddei F (2015) Effect of lower-limb joint models on subject-specific musculoskeletal models and simulations of daily motor activities. J Biomech 48:4198–4205. https://doi.org/10.1016/j.jbiomech.2015.09.042
435. Dumas R, Moissenet F, Gasparutto X, Cheze L (2012) Influence of joint models on lower-limb musculo-tendon forces and three-dimensional joint reaction forces during gait. Proc Inst Mech Eng Part H J Eng Med 226:146–160. https://doi.org/10.1177/0954411911431396
436. Catelli DS, Wesseling M, Jonkers I, Lamontagne M (2019) A musculoskeletal model customized for squatting task. Comput Methods Biomech Biomed Eng 22:21–24. https://doi.org/10.1080/10255842.2018.1523396
437. Moissenet F, Modenese L, Dumas R (2017) Alterations of musculoskeletal models for a more accurate estimation of lower limb joint contact forces during normal gait: a systematic review. J Biomech 63:8–20. https://doi.org/10.1016/j.jbiomech.2017.08.025
438. Martelli S, Valente G, Viceconti M, Taddei F (2015) Sensitivity of a subject-specific musculoskeletal model to the uncertainties on the joint axes location. Comput Methods Biomech Biomed Eng 18:1555–1563. https://doi.org/10.1080/10255842.2014.930134
439. Correa TA, Pandy MG (2011) A mass-length scaling law for modeling muscle strength in the lower limb. J Biomech 44:2782–2789. https://doi.org/10.1016/j.jbiomech.2011.08.024
440. Sandholm A, Schwartz C, Pronost N et al (2011) Evaluation of a geometry-based knee joint compared to a planar knee joint. Vis Comput 27:161–171. https://doi.org/10.1007/s00371-010-0538-7
441. Taddei F, Martelli S, Valente G et al (2012) Femoral loads during gait in a patient with massive skeletal reconstruction. Clin Biomech 27:273–280. https://doi.org/10.1016/j.clinbiomech.2011.09.006
442. Valente G, Pitto L, Testi D et al (2014) Are subject-specific musculoskeletal models robust to the uncertainties in parameter identification? PLoS ONE. https://doi.org/10.1371/journal.pone.0112625
443. Oosterwaal M, Telfer S, Tørholm S et al (2011) Generation of subject-specific, dynamic, multisegment ankle and foot models to improve orthotic design: a feasibility study. BMC Musculoskelet Disord. https://doi.org/10.1186/1471-2474-12-256
444. Conconi M, Montefiori E (2019) Evaluation of anatomical consistency of three subject-specific ankle joint modelling approaches. 2–3
445. Rahman M, Renani MS, Cil A, Stylianou AP (2018) Musculoskeletal model development of the elbow joint with an experimental evaluation. Bioengineering 5:1–14. https://doi.org/10.3390/bioengineering5020031
446. Fisk JP, Wayne JS (2009) Development and validation of a computational musculoskeletal model of the elbow and

forearm. Ann Biomed Eng 37:803–812. https://doi.org/10.1007/s10439-009-9637-x
447. Kipp K, Kim H (2020) Relative contributions and capacities of lower extremity muscles to accelerate the body's center of mass during countermovement jumps. Comput Methods Biomech Biomed Eng 23:914–921. https://doi.org/10.1080/10255842.2020.1772764
448. Lai AKM, Arnold AS, Wakeling JM et al (2018) Musculoskeletal model for analysing human locomotor tasks. Ann Biomed Eng 45:2762–2774. https://doi.org/10.1007/s10439-017-1920-7.Why
449. Heine R, Manal K, Buchanan TS (2003) Forward dynamic analysis of joint moment. J Mech Med Biol 3:169–186
450. Wickstrom RL (1983) Fundamental motor patterns, 3rd edn. Lea & Febiger
451. Caillé J, Ildefonse M, Rougier O (1985) Excitation-contraction coupling in the skeletal muscle. Prog Biophys Mol Biol 46:185–239. https://doi.org/10.1016/0079-6107(85)90009-4
452. Sandow A (1952) Excitation-contraction coupling in muscular response. Yale J Biol Med 25:176–201
453. Cavanagh PR, Komi PV (1979) Electromechanical delay in human skeletal muscle under concentric and eccentric contractions. Eur J Appl Physiol 42:159–163
454. Sperelakis N (2012) Cell physiology source book: essentials of membrane biophysics, 2nd edn. Elsevier, Amsterdam
455. Oatis CA (2009) The mechanics and pathomechanics of human movement, 2nd edn. Lippincott Williams & Wilkins, Philadelphia
456. Cormie P, McGuigan MR, Newton RU (2011) Developing maximal neuromuscular power: Part 1—biological basis of maximal power production. Sport Med 41:17–38. https://doi.org/10.2165/11537690-000000000-00000
457. Dulhunty AF (2006) Excitation-contraction coupling from the 1950s into the new millennium. Clin Exp Pharmacol Physiol 33:763–772. https://doi.org/10.1111/j.1440-1681.2006.04441.x
458. Winters JM (1995) An improved muscle-reflex actuator for use in large-scale neuromusculoskeletal models. Ann Biomed Eng 23:359–374. https://doi.org/10.1007/BF02584437
459. Thelen DG (2003) Adjustment of muscle mechanics model parameters to simulate dynamic contractions in older adults. J Biomech Eng 125:70. https://doi.org/10.1115/1.1531112
460. Wang M, Sun J, Yang Q (2020) Modeling and simulation of excitation-contraction coupling of fast-twitch skeletal muscle fibers. Technol Heal Care 28:S13–S24. https://doi.org/10.3233/THC-209003
461. Pandy MG (2001) Computer modeling and simulation of human movement. Annu Rev Biomed Eng 3:245–273
462. Neptune RR, Kautz SA (2001) Muscle activation and deactivation dynamics: the governing properties in fast cyclical human movement performance? Exerc Sport Sci Rev 29:76–81. https://doi.org/10.1097/00003677-200104000-00007
463. He J, Levine WS, Loeb GE (1991) Feedback gains for correcting small perturbations to standing posture. IEEE Trans Automat Contr 36:322–332. https://doi.org/10.1109/9.73565
464. Zhang D, Ang WT, Poignet P (2008) A neuromusculoskeletal model exploring peripheral mechanism of tremor. Proc 30th Annu Int Conf IEEE Eng Med Biol Soc EMBS'08 - "Personalized Healthc through Technol 3715–3719. https://doi.org/10.1109/iembs.2008.4650016
465. Anderson FC, Pandy MG (2001) Static and dynamic optimization solutions for gait are practically equivalent. J Biomech 34:153–161. https://doi.org/10.1097/COC.0b013e31817f9e00
466. Gottlieb GL, Agarwal GC (1971) Dynamic relationship between isometric muscle tension and the electromyogram in man. J Appl Physiol 30:345–351. https://doi.org/10.1152/jappl.1971.30.3.345
467. Hill A (1949) The abrupt transition from rest to activity in muscle. Proc R Soc B 136:399–420
468. Koo TKK, Mak AFT (2006) A neuromusculoskeletal model to simulate the constant angular velocity elbow extension test of spasticity. Med Eng Phys 28:60–69. https://doi.org/10.1016/j.medengphy.2005.03.012
469. Hase K, Yamazaki N, Obinata G et al (2002) Computer simulation study of human locomotion with a three-dimensional entire-body neuro-musculo-skeletal model Part I-IV. JSME Int J C 45:1040–1072
470. Koo TKK, Mak AFT (2005) Feasibility of using EMG driven neuromusculoskeletal model for prediction of dynamic movement of the elbow. J Electromyogr Kinesiol 15:12–26. https://doi.org/10.1016/j.jelekin.2004.06.007
471. Doheny EP, Lowery MM, FitzPatrick DP, O'Malley MJ (2007) A neuromusculoskeletal model of the elbow joint for pre-clinical testing of total elbow replacement. Annu Int Conf IEEE Eng Med Biol Proc. https://doi.org/10.1109/IEMBS.2007.4352811
472. Durandau G, Farina D, Asín-Prieto G et al (2019) Voluntary control of wearable robotic exoskeletons by patients with paresis via neuromechanical modeling. J Neuroeng Rehabil 16:1–18. https://doi.org/10.1186/s12984-019-0559-z
473. Kim Y, Tagawa Y, Obinata G, Hase K (2011) Robust control of CPG-based 3D neuromusculoskeletal walking model. Biol Cybern 105:269–282. https://doi.org/10.1007/s00422-011-0464-4
474. Wang R, Ekeberg Ö, Fagergren A et al (2014) A neuromusculoskeletal model to simulate the isokinetic ankle dorsiflexion test of spasticity. J Foot Ankle Res 7:1–2. https://doi.org/10.1186/1757-1146-7-s1-a87
475. Jonkers I, Spaepen A, Papaioannou G, Stewart C (2002) An EMG-based, muscle driven forward simulation of single support phase of gait. J Biomech 35:609–619. https://doi.org/10.1016/S0021-9290(01)00240-8
476. Thangal SNM, Talaty M, Balasubramanian S (2013) Assessment of gait sensitivity norm as a predictor of risk of falling during walking in a neuromusculoskeletal model. Med Eng Phys 35:1483–1489. https://doi.org/10.1016/j.medengphy.2013.03.018
477. Sartori M, Reggiani M, Lloyd DG, Pagello E (2011) A neuromusculoskeletal model of the human lower limb: towards EMG-driven actuation of multiple joints in powered orthoses. IEEE Int Conf Rehabil Robot. https://doi.org/10.1109/ICORR.2011.5975441
478. Sartori M, Farina D, Lloyd DG (2014) Hybrid neuromusculoskeletal modeling to best track joint moments using a balance between muscle excitations derived from electromyograms and optimization. J Biomech 47:3613–3621. https://doi.org/10.1016/j.jbiomech.2014.10.009
479. Rahmati SM, Rostami M, Beigzadeh B (2018) Prediction of human gait trajectories during the SSP using a neuromusculoskeletal modeling: a challenge for parametric optimization. Technol Heal Care 26:889–907. https://doi.org/10.3233/THC-171171
480. Seth A, Pandy MG (2007) A neuromusculoskeletal tracking method for estimating individual muscle forces in human movement. J Biomech 40:356–366. https://doi.org/10.1016/j.jbiomech.2005.12.017
481. Ghafari AS, Meghdari A, Vossoughi G (2009) Feedback control of the neuromusculoskeletal system in a forward dynamics simulation of stair locomotion. Proc Inst Mech Eng Part H 223:663–675. https://doi.org/10.1243/09544119JEIM547
482. Buongiorno D, Barsotti M, Barone F et al (2018) A linear approach to optimize an EMG-driven neuromusculoskeletal model for movement intention detection in myo-control: a case study on shoulder and elbow joints. Front Neurorobot 12:1–12. https://doi.org/10.3389/fnbot.2018.00074
483. Allouch S, Boudaoud S, Younès R et al (2015) Proposition, identification, and experimental evaluation of an inverse dynamic neuromusculoskeletal model for the human finger. Comput Biol

Med 63:64–73. https://doi.org/10.1016/j.compbiomed.2015.04.035
484. Stienen AHA, Schouten AC, Schuurmans J, van der Helm FCT (2007) Analysis of reflex modulation with a biologically realistic neural network. J Comput Neurosci 23:333–348. https://doi.org/10.1007/s10827-007-0037-7
485. Gerus P, Sartori M, Besier TF et al (2013) Subject-specific knee joint geometry improves predictions of medial tibiofemoral contact forces. J Biomech 46:2778–2786. https://doi.org/10.1016/j.jbiomech.2013.09.005
486. Hoang HX, Pizzolato C, Diamond LE, Lloyd DG (2018) Subject-specific calibration of neuromuscular parameters enables neuromusculoskeletal models to estimate physiologically plausible hip joint contact forces in healthy adults. J Biomech 80:111–120. https://doi.org/10.1016/j.jbiomech.2018.08.023
487. Davico G, Pizzolato C, Lloyd DG et al (2020) Increasing level of neuromusculoskeletal model personalisation to investigate joint contact forces in cerebral palsy: a twin case study. Clin Biomech 72:141–149. https://doi.org/10.1016/j.clinbiomech.2019.12.011
488. Veerkamp K, Schallig W, Harlaar J et al (2019) The effects of electromyography-assisted modelling in estimating musculotendon forces during gait in children with cerebral palsy. J Biomech 92:45–53. https://doi.org/10.1016/j.jbiomech.2019.05.026
489. Emer D, Fitzpatrick D, Ma L, Ma O (2006) Validating a neuromusculoskeletal model of the elbow joint. J Biomech 39:47
490. Zhang L, Li Z, Hu Y et al (2021) Ankle joint torque estimation using an EMG-driven neuromusculoskeletal model and an artificial neural network model. IEEE Trans Autom Sci Eng 18:564–573. https://doi.org/10.1109/TASE.2020.3033664
491. Pau JWL, Xie SSQ, Xu WL (2013) Neuromuscular interfacing: a novel approach to EMG-driven multiple DOF physiological models. Proc Annu Int Conf IEEE Eng Med Biol Soc EMBS. https://doi.org/10.1109/EMBC.2013.6611076
492. Sartori M, Reggiani M, Farina D, Lloyd DG (2012) EMG-driven forward-dynamic estimation of muscle force and joint moment about multiple degrees of freedom in the human lower extremity. PLoS ONE. https://doi.org/10.1371/journal.pone.0052618
493. Erdemir A, McLean S, Herzog W, van den Bogert AJ (2007) Model-based estimation of muscle forces exerted during movements. Clin Biomech 22:131–154. https://doi.org/10.1016/j.clinbiomech.2006.09.005
494. Hamner SR, Delp SL (2013) Muscle contributions to fore-aft and vertical body mass center accelerations over a range of running speeds. J Biomech 46:780–787. https://doi.org/10.1016/j.jbiomech.2012.11.024
495. Buchanan TS, Lloyd DG (1995) Muscle activity is different for humans performing static tasks which require force control and position control. Neurosci Lett 194:61–64. https://doi.org/10.1016/0304-3940(95)11727-E
496. Tax AAM, Denier van der Gon JJ, Erkelens CJ (1990) Differences in coordination of elbow flexor muscles in force tasks and in movement tasks. Exp Brain Res 81:567–572. https://doi.org/10.1007/BF02423505
497. De Serres SJ, Milner TE (1991) Wrist muscle activation patterns and stiffness associated with stable and unstable mechanical loads. Exp Brain Res 86:451–458. https://doi.org/10.1007/BF00228972
498. Besier TF, Fredericson M, Gold GE et al (2009) Knee muscle forces during walking and running in patellofemoral pain patients and pain-free controls. J Biomech 42:898–905. https://doi.org/10.1016/j.jbiomech.2009.01.032
499. Fregly BJ, Boninger ML, Reinkensmeyer DJ (2012) Personalized neuromusculoskeletal modeling to improve treatment of mobility impairments: a perspective from European research sites. J Neuroeng Rehabil 9:1–11. https://doi.org/10.1186/1743-0003-9-18
500. Shao Q, Bassett DN, Manal K, Buchanan TS (2009) An EMG-driven model to estimate muscle forces and joint moments in stroke patients. Comput Biol Med 39:1083–1088. https://doi.org/10.1016/j.compbiomed.2009.09.002
501. Menegaldo LL, Oliveira LF (2011) An EMG-driven model to evaluate quadriceps strengthening after an isokinetic training. Procedia IUTAM 2:131–141. https://doi.org/10.1016/j.piutam.2011.04.014
502. Norton JA, Gorassini MA (2006) Changes in cortically related intermuscular coherence accompanying improvements in locomotor skills in incomplete spinal cord injury. J Neurophysiol 95:2580–2589. https://doi.org/10.1152/jn.01289.2005
503. Cerveri P, Rabuffetti M, Pedotti A, Ferrigno G (2003) Real-time human motion estimation using biomechanical models and nonlinear state-space filters. Med Biol Eng Comput 41:109–123
504. Pedotti A, Krishnan VV, Stark L (1978) Optimization of muscle-force sequencing in human locomotion. Math Biosci 38:57–76. https://doi.org/10.1016/0025-5564(78)90018-4
505. Kaphle M, Eriksson A (2008) Optimality in forward dynamics simulations. J Biomech 41:1213–1221. https://doi.org/10.1016/j.jbiomech.2008.01.021
506. Mombaur K (2016) Optimal control for applications in medical and rehabilitation technology: Challenges and solutions
507. Neptune RR (1999) Optimization algorithm performance in determining optimal controls in human movement analyses. J Biomech Eng 121:249–252. https://doi.org/10.1115/1.2835111
508. Pandy MG, Anderson FC, Hull DG (1992) A parameter optimization approach for the optimal control of large-scale musculoskeletal systems. J Biomech Eng 114:450–460. https://doi.org/10.1115/1.2894094
509. De Groote F, Kinney AL, Rao AV, Fregly BJ (2016) Evaluation of direct collocation optimal control problem formulations for solving the muscle redundancy problem. Ann Biomed Eng 44:2922–2936. https://doi.org/10.1007/s10439-016-1591-9
510. Nitschke M, Dorschky E, Heinrich D et al (2020) Efficient trajectory optimization for curved running using a 3D musculoskeletal model with implicit dynamics. Sci Rep 10:1–13. https://doi.org/10.1038/s41598-020-73856-w
511. Jansen C, McPhee J (2020) Predictive dynamic simulation of olympic track cycling standing start using direct collocation optimal control. Multibody Syst Dyn 49:53–70. https://doi.org/10.1007/s11044-020-09723-3
512. Lam SK, Vujaklija I (2021) Joint torque prediction via hybrid neuromusculoskeletal modelling during gait using statistical ground reaction estimates: an exploratory study. Sensors. https://doi.org/10.3390/s21196597
513. Higginson JS, Ramsay JW, Buchanan TS (2012) Hybrid models of the neuromusculoskeletal system improve subject-specificity. In: Proc Inst Mech Eng H. pp 113–119
514. Bennett KJ, Pizzolato C, Martelli S et al (2022) EMG-informed neuromusculoskeletal models accurately predict knee loading measured using instrumented implants. IEEE Trans Biomed Eng. https://doi.org/10.1109/TBME.2022.3141067